ATLANTA REGIONAL MEETING—OCTOBER 31–NOVEMBER 1

JOURNAL
of the
AMERICAN CONCRETE INSTITUTE

(ACI PROCEEDINGS Vol. 51)

Vol. 26 May 1955 No. 9

CONTENTS

Papers and Reports....833-936

Effect of Curing on the Properties Affecting Shrinkage Cracking of Concrete Block.... G. W. WASHA, J. C. SAEMANN, and C. WARREN 833

Performance of Reinforced Concrete and Concrete Masonry in Recent Western United States Earthquakes.... KARL V. STEINBRUGGE and DONALD F. MORAN 853

Behavior of Prestressed Concrete Composite Beams.... R. H. EVANS and A. S. PARKER 861

Ball Test for Field Control of Concrete Consistency.... J. W. KELLY and MILOS POLIVKA 881

Strength of Reinforced Concrete T-Beams Under Combined Direct Shear and Torsion.... EARL I. BROWN, II 889

Air Entrainment in Cement and Silica Pastes.... G. M. BRUERE 905

Eccentric Bending in Two Directions of Rectangular Concrete Columns.... LU-SHIEN HU 921

Letters from Readers....937-948

Permeability Units.... 937

Continuity Splices.... 939

Square Footing Design.... 942

Two-Way Slab Coefficients.... 944

Current Reviews....949-960

News Letter.... 1-30

to provide a comradeship in finding the best ways to do concrete work of all kinds and in spreading that knowledge

ADDRESS: 18263 W. McNICHOLS RD., DETROIT 19, MICH.

$1.50 per copy
Extra copies to ACI Members $1.00

TO KEEP 'EM *Flying*

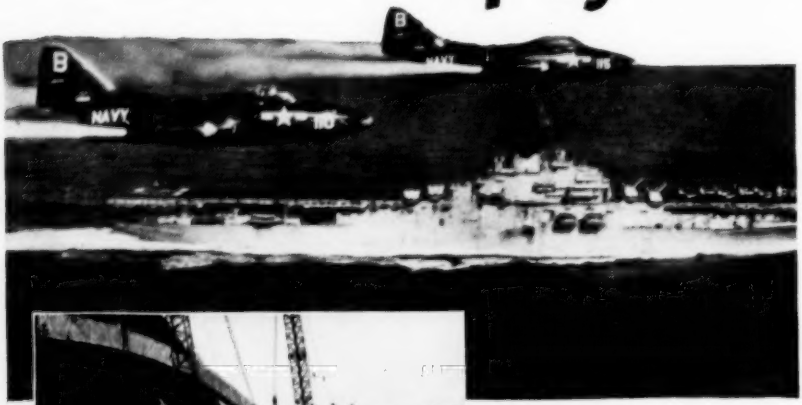

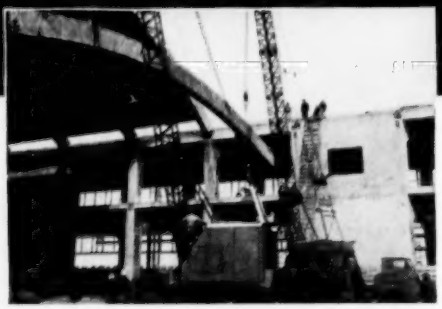

Hollow, Precast Concrete Arch Ribs 164 ft. Long Support Thin-Shell Precast Roof for Navy's Oceana, Va., Aircraft Maintenance Hangar

● Long a pace-setter in precast concrete design, the Navy's new, $2.1-million twin-barreled Aircraft Maintenance Hangar at U. S. Naval Air Station, Oceana, Va., is spanned by hollow, precast concrete arch ribs, each 164 ft. x 3 ft. x 1¾ ft., twelve for each hangar.

Arch ribs were cast at job site in half sections, each weighing 22½ tons. Half arches were hinged at each end, and after full dead load was applied, hinges were welded and concreted to form fixed ends. Arches support a thin-shell concrete roof, consisting of 924 precast panels, each 24 ft. x 4 ft., with ribs 10 in. deep and 1¼ in. shell.

Precise casting and erection schedules resulted in assembly-line speed, in building a hangar which admirably fits its purpose—with over-all economies well worth considering. Lone Star is proud of the privilege of supplying 23,405 bbls. of cement for this project—quality cement, every barrel of it, as reflected in a structure of outstanding character.

LONE STAR CEMENT CORPORATION

Offices: ABILENE, TEX. · ALBANY, N.Y. · BETHLEHEM, PA. · BIRMINGHAM · BOSTON · CHICAGO · DALLAS · HOUSTON
INDIANAPOLIS · KANSAS CITY, MO. · NEW ORLEANS · NEW YORK · NORFOLK · RICHMOND · WASHINGTON, D.C.

LONE STAR CEMENT, WITH ITS SUBSIDIARIES, IS ONE OF THE WORLD'S LARGEST CEMENT PRODUCERS: 18 MODERN MILLS, 141,600,000 SACKS ANNUAL CAPACITY

Vol. 26 – No. 9 May 1955 (Proceedings Vol. 51)

JOURNAL
of the
AMERICAN CONCRETE INSTITUTE

Published by the American Concrete Institute under the authority of its Board of Direction

ACI history and objectives. The Institute was founded 1905, incorporated in the District of Columbia in 1906 as The National Association of Cement Users, the name changed 1913 by charter amendment. It was re-incorporated August 1, 1945 with these objects: "to organize the efforts of its members for a nonprofit public service in gathering, correlating, and disseminating information for the improvement of the design, construction, manufacture, use, and maintenance of concrete products and structures."

Papers, committee reports, and other contributions to the **Proceedings** pages of this Journal, as submitted in furtherance of Institute objectives, are, if published, accepted on the sole responsibility of their authors. Institute authority attaches only to standards adopted as provided in the Bylaws.

Advertising. See statement under "Alphabetical List of Advertisers" final page **News-Letter** section.

Membership dues and Journal subscription rates. Members receive the Journal as one of the considerations of dues payments. Membership grades are: Individual (U. S., its possessions, and North and Central America), $15; Individual (all other foreign countries), $12; Corporation, $50; Contributing, $100; Junior, $7.50; Student, $5. Subscription prices are $12 per year, payable in advance ($15 per year outside North America and U.S. possessions). The Journal is issued monthly, January to June and September to December (the volume year of September to June being completed by title page, contents, indexes, and closing discussion in Part 2 of the subsequent December issue).

Bound volumes 1 to 50 of PROCEEDINGS of the AMERICAN CONCRETE INSTITUTE (1905 to 1954) are for sale as far as available at prices to be had on inquiry of the Secretary-Treasurer. Special prices apply for members ordering bound volumes in addition to the monthly Journal.

Address. American Concrete Institute, 18263 W. McNichols Road, Detroit 19, Michigan. **Copyright, 1955,** American Concrete Institute. Printed in U. S. A. Entered in the Post Office at Detroit, Michigan, as mail of the second class under provisions of the Act of March 3, 1879.

President
CHARLES S. WHITNEY

Vice-Presidents
FRANK KEREKES
WALTER H. PRICE

Secretary-Treasurer
WILLIAM A. MAPLES

Technical Director
PAUL F. RICE

Directors
F. BARONA DE LA O
ARTHUR P. CLARK
HARRY C. DELZELL
PHIL M. FERGUSON
JOSEPH F. JELLEY
JAY E. JELLICK
VERNON P. JENSEN
THOMAS B. KENNEDY
WALTER J. McCOY
DOUGLAS McHENRY
H. C. ROSS
GEORGE W. WASHA

Past Presidents
A. T. GOLDBECK
HENRY L. KENNEDY
C. H. SCHOLER

Advertising Manager
ANDREW M. SMITH

Manager, Publications Sales
ISABELLE DAVIS

Membership Secretary
EVELYN SCHLITZ

This comprehensive guide

now offered in a new expanded edition

pocketsized new easy to read type

durable and handsome binding

ACI MANUAL OF CONCRETE INSPECTION

Third Edition

J. W. Kelly, Author-Chairman,
ACI Committee 611, Inspection of Concrete

A MANUAL THAT TELLS *WHY* AS WELL AS *HOW*

It is more than a handbook. From concrete fundamentals to the latest developments in construction, the manual explains inspection clearly and completely.

A necessity for the inspector, an invaluable aid to anyone responsible for workmanship in concrete construction.

Inspection is insurance for a quality structure. The best materials and design practice cannot be effective unless work is properly done. The ACI Inspection Manual, written and bound for use at the construction site as well as the laboratory and design office, should be a reference for those who must see that any concrete structure is erected as it was intended.

KEY TOOL FOR CONCRETE INSPECTION

(Price $2.50—ACI Members $1.50)

AMERICAN CONCRETE INSTITUTE

18263 W. McNichols Rd., Detroit 19, Michigan

the ACI JOURNAL

is edited by the Secretary of the Technical Activities Committee under the direction of the Committee

BRYANT MATHER
Chairman

CHARLES S. WHITNEY
(ex officio)

WILLIAM A. MAPLES
Secretary

PHIL M. FERGUSON

JAMES A. McCARTHY

W. J. McCOY

DOUGLAS McHENRY

L. H. TUTHILL

I. L. TYLER

WILLIAM A. MAPLES
Editor

ROBERT E. WILDE
Managing Editor

R. G. WIEDYKE
Assistant Editor

BARBARA BURESH
Editorial Secretary

Contributions to the Journal

The ACI JOURNAL technical pages are a medium for reporting what is of current interest in the concrete field; in research, design, construction, maintenance, or manufacturing. Members and readers are urged to "have their say" as a means of sharing knowledge and experience; time and changing interests demand that new names and new ideas take their places beside the old. Contributions describing new materials and techniques or new applications of familiar practices are welcomed by the Institute.

To guide the flow of material the Board of Direction has assigned to the Technical Activities Committee the selection of papers, committee reports, discussions, and other contributions for JOURNAL publication. To assist in their technical appraisal a corps of experts in various segments of the field volunteer their services. From the technical standpoint, acceptable contributions present original material for improvement of design, manufacturing, or construction; confirm, revise, or upset established ideas or practices; or review, digest, or arrange accumulated experience for more ready use.

General considerations by TAC are whether the contribution will be of interest and service, will fit into a well-balanced publications schedule, and can be published at reasonable expense to the Institute.

To expedite appraisal and publication, if accepted, contributors are requested to furnish glossy prints or inked tracings of illustrations accompanying manuscripts submitted for consideration. Further details of form and physical arrangement of contributions begin on p. 14, 1953 *ACI Directory*. Separate prints of the "publications policy" are available free upon request to the Secretary.

Manuscripts of papers, discussions, and reports should be sent in triplicate to:

Secretary, Technical Activities Committee

AMERICAN CONCRETE INSTITUTE

18263 W. McNICHOLS RD., DETROIT 19, MICHIGAN

In ACI Journal next month

In "Structural Model Studies of Concrete Slab Foundations," C. DESMOND PENGELLEY, M. M. LEMCOE, and E. J. DOWER apply the theory of dimensional analysis to the design of reinforced concrete structural models of small home foundation slabs. Methods of fabricating satisfactory models are developed. Static stiffness measurements are reported on six designs of the same cost and size. Two full-scale foundations were tested corresponding to a pair of the model designs and full-scale results are compared.

Specifications for concrete and proportioning and control methods as practiced by the City of Milwaukee for pavement construction are described in "Design and Control of Municipal Paving Concrete," by ROBERT A. BURMEISTER. Compression tests of 3086 cylinders are summarized and 337 air-content tests are reported.

In the research reported in "Tobermorite and Related Phases in the System CaO-SiO_2-H_2O," by GEORGE L. KALOUSEK, the hydrothermal reactions at temperatures of 125 to 175 C between $Ca(OH)_2$ and quartz or silicic acid were studied in detail with regard to the reaction products, particularly in the range of molar compositions of 0.8 CaO:SiO_2. The solid phases were studied by x-ray, DTA, BET nitrogen adsorption, electron microscopy, and chemical analysis.

W. REJMAN offers "Stability of Reinforced Concrete Retaining Walls and Abutments" in which an analytical method is presented whereby minimum width and relative position of the horizontal base can be found for any shape or loading of a cantilever or counterforted retaining wall. The method is particularly applicable to loaded or unorthodox walls as in basements of some industrial buildings, ditch bunkers, and abutments.

"Precast Prestressed Lightweight Concrete Construction," by ARTHUR M. JAMES, describes design, fabrication, and erection of precast, prestressed floor beams, roof beams, and slabs of lightweight expanded shale concrete in two buildings. A discussion is given of the elastic modulus of expanded shale concrete based on measured camber at prestressing, cost data on beams and slabs, and a yard test of one prestressed beam.

Basic principles underlying the behavior of statically indeterminate prestressed concrete structures are investigated in "Strength of Continuous Prestressed Concrete Beams Under Static and Repeated Loads," by T. Y. LIN. Four continuous beams, each 50 ft long, were tested. The cracking and ultimate strengths of these beams were measured and evaluated for static loads as well as for repeated loads up to 5,000,000 cycles. Beam reactions, deflections, and strains were recorded for analysis. The effects of adding nonprestressed mild steel reinforcement were studied.

Effect of Curing on the Properties Affecting Shrinkage Cracking of Concrete Block*

By J. C. SAEMANN,† C. WARREN,‡ and G. W. WASHA§

SYNOPSIS

This investigation attempted to establish relationships between curing procedures and properties that influence shrinkage cracking of concrete block. Shrinkage cracks are influenced by the strength and stiffness properties of the concrete as well as its tendency to shrink because of moisture and temperature changes. In resisting cracking the tensile strength, notably weak for concrete, and the amount of strain accompanying a given stress must be considered. This latter factor is complicated by the fact that concrete tends to deform continuously at a decreasing rate under constant stress. Thus, the ratio of stress to strain is much lower when concrete sustains a load for a long time.

Tests were made to determine modulus of rupture, compressive strength, tensile strength, modulus of elasticity in transverse bending, moisture volume changes, and thermal volume changes. These tests were not intended to provide results that would tell when cracking would occur and when it would not. The objective was to compare the results of tests obtained for block-type concrete made with various aggregates and cured in different ways, and to determine relative immunity to cracking.

INTRODUCTION

A characteristic of all portland cement concrete, including concrete masonry units, is the tendency to decrease in volume with either a decrease in moisture content or a decrease in temperature. This decrease in volume may result in shrinkage cracks when concrete masonry is restrained from shrinking.

A sharp distinction must be made between shrinkage cracks caused by faulty design and those caused by the properties of the building material. Further, a distinction must be made between shrinkage cracks caused by using poor materials for the manufacture of concrete masonry units and shrinkage cracks caused by poor manufacturing procedures. In the past few years many claims have been made as to the relative merits of various manufacturing procedures and their effect on shrinkage cracking. Quite logically it may be expected that the following factors in the manufacture of concrete masonry units influence shrinkage cracking: (1) gradation of aggregate; (2) chemical and physical properties of aggregate; (3) chemical and

*Received by the Institute Nov. 4, 1954. Title No. 51-41 is a part of copyrighted JOURNAL OF THE AMERICAN CONCRETE INSTITUTE, V. 26, No. 9, May 1955, *Proceedings* V. 51. Separate prints are available at 50 cents each. **Discussion** (copies in **triplicate**) should reach the Institute not later than Sept. 1, 1955. Address 18263 W. McNichols Road, Detroit 19, Mich.

†Instructor, Mechanics Department, University of Wisconsin, Madison, Wis.
‡Goodyear Atomic Corp., Portsmouth, Ohio.
§Member American Concrete Institute, Professor of Mechanics, University of Wisconsin, Madison, Wis.

physical properties of portland cement; (4) mix proportions (aggregate and cement); (5) mix consistency (water content); (6) method of curing; and (7) design of unit.

This investigation attempted to establish relationships between curing procedures and properties that influence shrinkage cracking of concrete block. Shrinkage cracks are influenced by the strength and stiffness properties of the concrete as well as its tendency to shrink because of moisture and temperature changes. Of specific importance in resisting cracking is the tensile strength, which is notably weak for concrete. Also the amount of strain accompanying a given stress must be taken into consideration. This latter factor is complicated by the fact that concrete tends to deform continuously at a decreasing rate under constant stress. Thus, the ratio of stress to strain is much lower when concrete sustains a load for a long time.

In this investigation, tests were made to determine modulus of rupture, compressive strength, tensile strength, modulus of elasticity in transverse bending, moisture volume changes, and thermal volume changes. All tests were performed on laboratory specimens 2 x 2 in. in cross section and either 11 or 16 in. long. These tests were not intended to provide results that would tell when cracking would occur and when it would not. The objective was to compare the results of tests obtained for block-type concretes made with various aggregates and cured in different ways and to determine relative immunity to cracking.

MATERIALS

Aggregates

Sand and gravel—from Janesville Sand and Gravel Co., Janesville, Wis. Most material retained on a No. 16 sieve was calcareous in nature and most material passing a No. 16 sieve was siliceous in nature. Waylite—an expanded blast furnace slag from Waylite Co., Chicago, Ill. Haydite—an expanded burned shale manufactured by Western Brick Co., Danville, Ill. Cinders—bituminous coal cinders from Detroit Edison Co., Detroit, Mich. Pumice—from Pumice Aggregate Sales Corp., Albuquerque, N. M.

Before the aggregates were used they were air dryed for a minimum of two days. Moisture tests indicated that the moisture contents after air drying were: sand and gravel 0.15 percent, Waylite 0.08 percent, Haydite 0.20 percent, cinders 0.14 percent, and pumice 0.66 percent. After air drying, the aggregates were sieved into four size fractions, which were then reproportioned by dry compact volume as follows: 25 percent between the No. 4 and $\frac{3}{8}$-in. sieves, 30 percent between the No. 16 and the No. 4 sieves, 30 percent between the No. 50 and the No. 16 sieves, and 15 percent passing the No. 50 sieve.

The percentages by compact volume were converted to percentages by weight so recombination of the various size fractions could be made on a weight basis. Rodding was used for determining the unit weight of the sand and gravel fractions, and jigging was used for the lightweight aggregate

TABLE 1—UNIT WEIGHT OF SIZE FRACTIONS OF AGGREGATE (lb per cu ft)

Aggregate	Size fractions			
	⅜ in.—No. 4	No. 4—No. 16	No. 16—No. 50	No. 50—down
Sand and gravel	102.3	104.0	103.1	103.4
Waylite	33.5	40.0	54.5	61.5
Haydite	57.1	55.8	52.4	78.8
Cinders	56.5	59.4	61.3	75.0
Pumice	27.3	33.3	37.5	50.5

fractions. Unit weights of the size fractions for each aggregate are given in Table 1.

Unit weights of the recombined aggregates are given in Table 2, and the sieve analyses of the recombined aggregate in Table 3. It will be noted that even though all aggregates were recombined in the same volume ratio of size fractions, the fineness moduli varied for the different aggregates. This is due primarily to the difference in the ratios of the unit weights of the various size fractions of the different aggregates. There is also reason to believe that some breakdown occurred in the lighter weight aggregates during the determination of the fineness modulus.

Sieve analyses of the recombined aggregates showed that there was a maximum variation of ± 2 percent from the desired calculated weight proportions of the individual size fractions.

TABLE 2—UNIT WEIGHTS OF RECOMBINED AGGREGATES

Aggregate	Unit weight (lb per cu ft) as determined by		
	Rodding	Jigging	Dry loose volume
Sand and gravel	122.7	125.8	112.6
Waylite	62.4	57.2	51.6
Haydite	70.5	73.3	60.8
Cinders	80.2	79.3	68.2
Pumice	42.0	45.1	36.2

TABLE 3—SIEVE ANALYSES OF RECOMBINED AGGREGATES

Sieve	Percent coarser than sieve				
	Aggregate				
	Sand and gravel	Waylite	Haydite	Cinders	Pumice
⅜ in.	0.0	0.0	0.0	0.0	0.0
No. 4	25.4	17.6	26.0	23.4	20.8
No. 8	42.0	29.8	43.5	40.0	32.6
No. 16	53.6	43.0	53.0	52.2	47.2
No. 30	62.5	64.6	70.0	70.4	68.8
No. 50	87.3	79.6	80.7	82.3	78.2
No. 100	97.9	85.4	85.1	88.8	81.5
No. 200	99.5	91.0	88.9	93.6	85.4
Fineness modulus	3.69	3.20	3.58	3.57	3.29

Cement

A blend of four different commercial brands of Type I portland cement was used. This blend passed all physical requirements for a Type I cement given in ASTM Standard C 150-52.

MANUFACTURE OF SPECIMENS

Mix proportions

The mix proportion used was 1:6 by compact aggregate volume. This volume proportion was converted to a weight proportion so quantities of aggregate and cement for a particular batch could be obtained by weighing For sand and gravel, the ASTM rodded unit weight was used, and for all other aggregates the jigged unit weight was used.

Consistency of mix

The water content used for each mix was such that a thin layer of mortar formed on the bottom of the specimen during the molding process. This consistency represented the maximum water content from the standpoint of molding with the vibrating type mold used, since for wetter mixes difficulty was incurred in stripping the specimens. After determining the proper water content for making concrete with each aggregate, that water content was used in all succeeding batches made with that aggregate. The water-cement ratio by weight for each concrete (based on total water, *i.e.*, free water plus water absorbed by oven-dry aggregate) is given in Table 4.

Mixing procedure

A Lancaster counter-current batch mixer was used. When mixing sand and gravel concrete, the aggregate and cement were mixed dry for 2 min, then water was added, and the batch was mixed for an additional 5 min. For the lightweight aggregate concretes the aggregate and water were mixed for 2 min, then cement was added, and the batch was mixed for an additional 5 min.

Molding procedure

Two 2 x 2 x 11-in. or 2 x 2 x 16-in. specimens were made simultaneously on steel pallets on a vibrating table (Fig. 1). An electric motor with an eccentric weight on its shaft was attached to the center of the underside of the table. The motor had a speed of 3600 rpm and produced an average amplitude of vibration of 0.012 in. After vibrating for 5 sec, a weight producing a pressure of about 2 psi was applied to the top of each specimen and vibration was continued for an additional 10 sec. The specimens were then hand screeded, after which the molds were removed.

TABLE 4—WATER-CEMENT RATIOS OF CONCRETE MIXES

Aggregate	Water-cement ratio
Sand and gravel	0.58
Waylite	0.99
Haydite	0.98
Cinders	0.90
Pumice	1.20

CURING

The molded specimens were subjected to three different procedures as outlined below. After completion of the curing process, specimens were

stored in air at 70 F and 50 percent relative humidity until tested. All specimens were cured at atmospheric pressure; the investigation did not include high pressure steam curing.

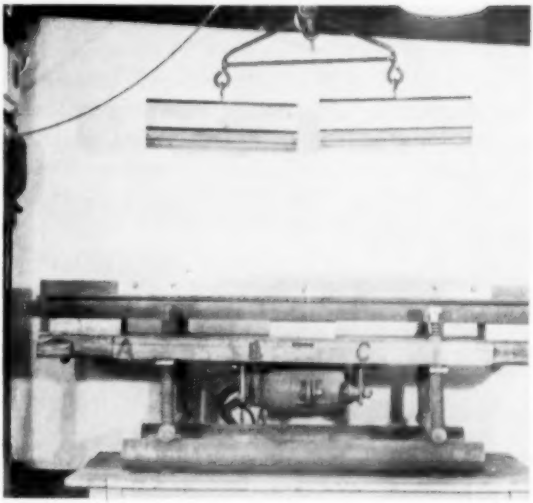

Fig. 1—Vibrating molds used in manufacturing specimens

Method No. 1—Standard moist

The specimens were moist cured for 14 days after manufacture.

Method No. 2—Low pressure steam

Immediately after manufacture the specimens were placed in the steam kiln at approximately 80 F and high relative humidity for a minimum of 2 hr. Low pressure steam was then injected intermittently for 3 hr, during which time the temperature was raised to 170 F at approximately a uniform rate. This temperature was held for 1 hr, and the steam injections were then discontinued. The specimens remained in the steam kiln for a 12-hr soaking period (steam off), during which time the temperature dropped from 170 F to about 125 F.

Method No. 2a—Low pressure steam plus oven drying

This was identical to method No. 2 up to and including the soaking period. The oven drying was done at various temperatures and for various durations, and in most cases followed the soaking period by 1 hr. During the 1-hr interval between the soaking period and oven drying, the specimens were stored in air at 70 F and 50 percent relative humidity. Initial length readings were then taken so that the total percentage change in length in oven drying could be computed. Preliminary tests showed that each specimen reached temperature equilibrium in 1 hr. The drying oven was gas heated and equipped with an automatic temperature control so that combustion took place only in the fractional amount of time necessary to maintain the required temperature. Although there was a metal plate between the drying and combustion chambers, and the drying chamber was adequately vented, the specimens were exposed to the action of the combustion gases. The oven was preheated to the necessary drying temperature before the specimens were admitted. A metal lattice held the specimens 5 in. above the metal plate.

During each drying period, the moisture volume change specimens were taken out of the oven at specific intervals, quickly weighed, and then replaced. Final length readings were taken 24 hr after completion of oven drying,

during which time the specimens were stored in air at 70 F and 50 percent relative humidity. In this period the specimens returned to their temperature prior to oven drying, and thus the measurement of change in length was independent of temperature effect. Final weight readings were also taken at this time so the change in length and the change in weight would be correlated.

TEST METHODS

Modulus of rupture

The 2 x 2 x 16-in. prisms were end-supported in the as-molded position over a 15-in. span and subjected to third-point loading. Five specimens per variable were tested at an age of 28 days.

Compression

The broken beam halves from the modulus of rupture tests were broken as modified cubes. Ten test results per variable were obtained at an age of 28 days.

Tension

The tensile loads were applied to 2 x 2 x 11-in. prisms by means of wire loops which were attached to the prisms by cement caps, as shown in Fig. 2. Five specimens per variable were tested at an age of 28 days.

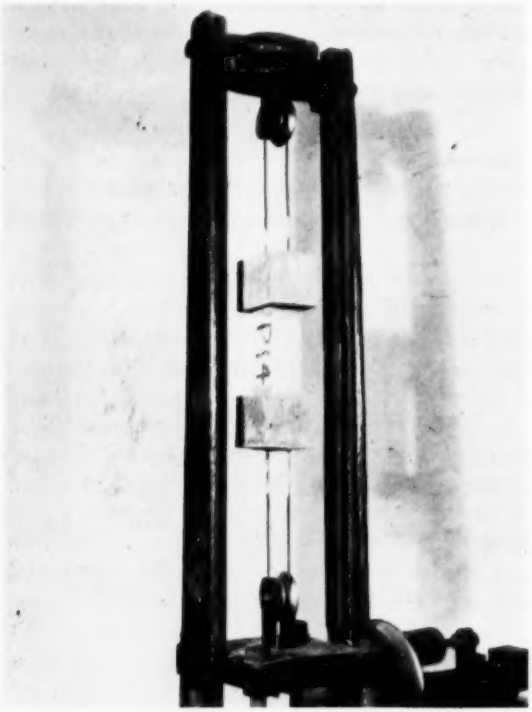

Fig. 2—Tensile test specimen

Modulus of elasticity

These tests were made on 2 x 2 x 16-in. prisms in three different ways.

(*a*) *Dynamic modulus of elasticity*—The prisms were placed on rubber supports and vibrated by an oscillating plunger in contact with the prisms at the middle. By simultaneously varying the frequency of vibration and measuring the amplitude, the resonant frequency was obtained. The dynamic modulus of elasticity was then computed. Five specimens per variable were tested at an age of 28 days.

(*b*) *Static modulus of elasticity*—After the dynamic modulus of elasticity de-

termination, each prism was placed on end supports and loaded to one half of its ultimate through third-point loading, center deflections being taken at regular load intervals. (The half load was taken as one half of the average ultimate load determined from the modulus of rupture tests.) The deflection at half load was used to compute the static modulus of elasticity.

(*c*) *Sustained modulus of elasticity*—After determination of the initial modulus of elasticity, each specimen was placed in a loading frame (Fig. 3) where it could be loaded with one half of its ultimate load through third-point loading. This load was maintained on the specimen and daily deflection readings were taken with a gage bar. After five or six days, the deflection approached a constant value which was used to compute sustained modulus of elasticity.

Moisture volume change

The change in length of the 2 x 2 x 11-in. prisms with end studs was measured in a standard comparator. Three specimens were used per variable.

Stage 1—After completion of curing, the specimens were stored in air at standard conditions (70 F and 50 percent relative humidity). Weekly length and weight determinations were made until constant length was obtained. The total percentage change in length and weight was then computed, using the length and weight after completion of curing as a basis. The initial length and weight values for the moist cured specimens were obtained immediately after removal from the moist closet, and for the low pressure steam cured specimens were obtained 1 hr after they were removed from the steam kiln, during which time they were stored in air at standard conditions. For the specimens subjected to low pressure steam curing plus oven drying, initial length and weight values were obtained 24 hr after they were removed from the drying oven, during which time they were stored in air at standard conditions.

Fig. 3—Loading of specimens for sustained modulus of elasticity tests

Saturation—After completion of Stage 1, the specimens were immersed in water for 24 hr and their lengths and weights in a saturated condition determined. Percentage change in length and weight in saturating was computed, with the length and weight after soaking as a basis.

Stage 2—After saturation, the specimens were stored in air and the Stage 1 procedure was repeated. The percentage change in length and weight was then computed, using the length and weight after saturation as a basis. By comparing the Stage 2 results with the percentage change in length and weight in saturating, it was possible to determine whether the specimens lost all the moisture in Stage 2 that they had gained during saturation.

TABLE 5—PROPERTIES OF SAND AND GRAVEL CONCRETE

Property	Curing method						
			2a				
	1	2	180–5*	120–24	180–24	240–24	240–10D†
Compressive strength, psi	3730	2650	2710	2550	2410	2270	2610
Modulus of rupture, psi	532	467	395	523	435	352	350
Tensile strength, psi	371	298	268	—	—	—	—
Dynamic *E*, 1000 psi	4000	3900	3320	3600	3030	2770	2700
Static *E*, 1000 psi	3900	3520	2800	3100	2480	2190	2180
Sustained *E*, 1000 psi	2560	2620	2760	2310	2020	1720	1930
Absorption, percent	5.0	5.1	5.2	5.1	5.2	5.0	5.1
Absorption, lb per cu ft	6.9	7.0	7.1	7.1	7.2	7.0	7.1
Specific weight (molded), lb per cu ft	141.1	142.0	140.8	140.9	142.7	142.1	142.0
Specific weight, (dry), lb per cu ft	135.5	136.0	134.9	135.2	134.9	135.9	136.1
Thermal coefficient $\times 10^6$ per deg F	5.0	4.9	4.7	—	—	—	—

*Dried at 180 F for 5 hr after steam curing.
†Dried at 240 F for 10 hr at an age of 14 days.

TABLE 6—PROPERTIES OF WAYLITE CONCRETE

Property	Curing method		
	1	2	2a
			180–5
Compressive strength, psi	2115	1740	1675
Modulus of rupture, psi	347	335	326
Tensile strength, psi	246	186	154
Dynamic *E*, 1000 psi	1590	1295	1165
Static *E*, 1000 psi	1340	1115	1095
Sustained *E*, 1000 psi	915	850	845
Absorption, percent	13.0	13.0	13.2
Absorption, lb per cu ft	11.2	11.2	11.5
Specific weight, (molded), lb per cu ft	95.5	95.9	96.6
Specific weight, (dry), lb per cu ft	86.5	86.5	87.2
Thermal coefficient $\times 10^6$ per deg F	4.5	4.3	4.2

Thermal volume change

After completion of Stage 2, the prisms were wrapped in paper and coated with paraffin to prevent moisture change during the test. The thermal coefficient of expansion was computed from the change in length between 0 and 70 F.

DISCUSSION OF RESULTS

Strength properties

A summary of the test results for the concretes made with the various aggregates and subjected to the different curing procedures is given in Tables 5 to 9. These results show that moist curing gave the best compressive strengths and that the low pressure steam cured concrete strengths averaged about 78 percent of the moist cured values. In general, drying after low

TABLE 7—PROPERTIES OF HAYDITE CONCRETE

Property	Curing method						
	1	2	2a				
			180-5	120-24	180-24	240-24	240-10D
Compressive strength, psi	3300	2620	2730	2450	1860	1440	1550
Modulus of rupture, psi	312	424	422	477	350	246	310
Tensile strength, psi	284	308	222	—	—	—	—
Dynamic E, 1000 psi	1770	1630	1450	1620	1300	1150	1180
Static E, 1000 psi	1530	1450	1280	1340	1130	960	1020
Sustained E, 1000 psi	1500	1320	1160	1180	900	870	870
Absorption, percent	16.3	17.2	16.7	17.0	17.0	17.0	17.1
Absorption, lb per cu ft	13.6	14.3	14.2	14.4	14.4	14.4	14.4
Specific weight, (molded), lb per cu ft	92.1	92.4	94.9	94.0	94.5	93.0	94.1
Specific weight, (dry), lb per cu ft	81.4	81.5	83.6	83.0	82.6	81.9	83.0
Thermal coefficient $\times 10^6$ per deg F	3.7	3.5	3.6	—	—	—	—

TABLE 8—PROPERTIES OF CINDER CONCRETE

Property	Curing method		
	1	2	2a
			180-5
Compressive strength, psi	2105	1660	1540
Modulus of rupture, psi	327	288	238
Tensile strength, psi	222	173	152
Dynamic E, 1000 psi	1535	1250	950
Static E, 1000 psi	1245	1060	850
Sustained E, 1000 psi	560	745	775
Absorption, percent	13.7	14.0	13.4
Absorption, lb per cu ft	12.2	12.5	12.1
Specific weight, (molded), lb per cu ft	101.5	101.5	102.4
Specific weight, (dry), lb per cu ft	89.7	89.6	90.4
Thermal coefficient $\times 10^6$ per deg F	2.3	2.1	2.1

TABLE 9—PROPERTIES OF PUMICE CONCRETE

Properties	Curing method						
	1	2	2a				
			180–5	120–24	180–24	240–24	240–10D
Compressive strength, psi	2190	1770	2040	1830	1630	1620	1120
Modulus of rupture, psi	189	293	385	362	289	245	209
Tensile strength, psi	151	187	238	—	—	—	—
Dynamic *E*, 1000 psi	890	750	840	780	580	670	560
Static *E*, 1000 psi	820	710	710	650	470	590	530
Sustained *E*, 1000 psi	380	490	570	520	470	510	420
Absorption, percent	23.2	28.2	23.8	27.2	27.4	28.3	28.5
Absorption, lb per cu ft	14.8	17.6	15.7	17.9	17.9	17.5	17.5
Specific weight, (molded), lb per cu ft	77.3	76.5	80.0	79.4	78.8	75.0	74.8
Specific weight, (dry), lb per cu ft	62.2	61.6	64.7	64.2	63.4	60.2	60.1
Thermal coefficient $\times 10^6$ per deg F	3.8	3.8	3.8	—	—	—	—

pressure steam curing did not cause any significant changes in compressive strength. However, the more severe drying conditions did cause some significant strength decreases for the Haydite and pumice concretes as shown in Tables 7 and 9.

The question of effect of drying on the strength properties of concrete caused considerable concern because of the variability of the results obtained. These variations necessitated a relatively large number of retests before the final values in Tables 5 to 9 could be tabulated. The reason for the low strengths obtained in some cases is difficult to provide in view of the fact that drying of commercial block does not generally produce any great decrease in strength. The results shown in Table 10 obtained for commercially made block subjected to oven drying at an age of 14 days show only slight variations from the results for block that were steam cured but not oven dried.

The data in Table 5 show that the sand and gravel concrete specimens oven dried at an age of 14 days also showed little strength change, but in

TABLE 10—EFFECT OF VARIOUS CURING METHODS ON THE STRENGTH OF COMMERCIALLY MANUFACTURED BLOCK

	Sand and gravel				Waylite				Haydite			
Curing method	2	2a*	2a*	2a*	2	2a*	2a*	2a*	2	2a*	2a*	2a*
Drying oven temperature, deg F		120	180	240		120	180	240		120	180	240
Drying time, hr		10	10	10		10	10	10		10	10	10
Percent change in weight due to curing	−3.5	−4.0	−4.5	−5.1	−5.2	−5.6	−6.5	−7.9	−5.1	−6.7	−7.0	−8.6
Compressive strength (28-day) based on net area, psi	3400	3310	3570	3720	1590	1650	1740	1940	2690	2795	2860	2680

*Oven dried at 14 days, rather than immediately after steam curing.

Table 7 it may be noted that oven drying at 240 F either immediately after or 14 days after low pressure steam curing markedly reduced the compressive strength of the Haydite concrete specimens from that obtained for specimens that were low pressure steam cured but not oven dried. One apparent possible reason for these differences may be the fact that commercially made block dried either in the laboratory or in the manufacturing plant may not be as completely dried by exposure to a given temperature for a given time as the small test specimens because the small test specimens occupied a much smaller portion of the oven than did the block.

A comparison of the compressive strengths of the moist cured concretes shows that the sand and gravel and the Haydite concretes were much the same and that Waylite, cinder, and pumice concretes had lower strengths. The modulus of rupture and tensile strength results are not as consistent as those for compressive strength.

Stiffness properties

The data in Tables 5 to 9 show that the dynamic and static moduli of elasticity show a general tendency to decrease as the oven drying time and/or temperature increases. It is also evident that the sand and gravel concrete is the stiffest and that it is followed in order by Haydite, Waylite, cinders, and pumice concretes.

The ratio of dynamic modulus of elasticity to the static modulus of elasticity was in all cases slightly greater than unity. The consistency of this ratio indicates that the dynamic method for determining modulus of elasticity is a satisfactory way of measuring modulus of elasticity rapidly and without injury to a specimen.

The sustained modulus of elasticity varied between 45 and 100 percent of the initial static modulus and averaged about 80 percent. The greatest difference occurred for the moist cured specimens, with the exception of Haydite. It is believed that the higher moisture content of the moist cured specimens at the time of testing caused them to be relatively more plastic. The inconsistency of the ratio of sustained modulus of elasticity to initial static modulus of elasticity indicates that it is not feasible to attempt to predict sustained E values from known static E values.

Absorption and specific weight

Absorptions and dry specific weights, Tables 5 to 9, were essentially independent of the curing and drying procedures used. The percentage absorptions were least for the sand and gravel concrete, about 5 percent, and increased progressively with Waylite, cinders, Haydite, and pumice concretes. The value for pumice concrete was about 28 percent. The absorptions on a lb-per-cu ft basis were in the same order and varied from about 7.0 for sand and gravel concrete to 18.0 lb per cu ft for the pumice concrete. The sand and gravel concrete had the greatest specific weight and was followed in decreasing order by the cinder, Waylite, Haydite, and pumice concretes.

Thermal volume change properties

The thermal coefficient of linear expansion, Tables 5 to 9, was not much affected by the curing process. The thermal coefficient of linear expansion was greatest for the sand and gravel concrete, with Waylite, pumice, Haydite, and cinders following in that order.

Moisture volume change properties

The percent changes in weight during curing, air drying in Stage 1, saturating after Stage 1, and air drying after saturating are shown in Table 11. The percent changes in weight during the curing process were based on the molded weight, those in Stage 1 drying were based on weight after curing, and those in saturating and in Stage 2 drying were based on weight after saturation.

All moist cured specimens gained weight in the curing process, the amount of gain varying between 1.6 percent for the sand and gravel concrete to 6.6 percent for the pumice concrete. In the steam kiln, however, most specimens showed a slight loss in weight.

The rate of drying for specimens subjected to oven drying, Fig. 4, shows how the weight of sand and gravel, Haydite, and pumice concrete decreased

TABLE 11—CHANGES IN WEIGHT DUE TO CURING, DRYING, AND SATURATING

	Changes in weight, percent, of specimens cured by method						
	1	2	180–5	120–24	180–24	240–24	240–10D
Sand and gravel concrete							
Curing	+ 1.6	− 0.2	− 3.3	− 2.6	− 4.4	− 4.5	− 4.4
Stage 1	− 4.1	− 3.0	− 0.5	− 0.9	+ 0.7	+ 0.7	+ 0.6
Saturating	+ 3.6	+ 4.1	+ 4.4	+ 4.4	+ 4.7	+ 4.8	+ 4.7
Stage 2	− 3.6	− 3.6	− 3.9	− 3.9	− 4.1	− 4.0	− 3.9
Waylite concrete							
Curing	+ 4.6	− 1.6	− 8.7				
Stage 1	−11.6	− 6.8	− 0.8				
Saturating	+ 9.4	+ 9.9	+10.7				
Stage 2	− 8.3	− 8.4	− 9.0				
Haydite concrete							
Curing	+ 6.1	− 0.2	− 9.0	− 6.4	−12.1	−12.7	−12.3
Stage 1	−14.4	−10.0	− 1.9	− 4.0	+ 1.1	+ 1.3	+ 1.1
Saturating	+10.4	+12.5	+12.7	+13.0	+13.5	+14.1	+13.7
Stage 2	− 9.7	−11.6	−11.7	−12.0	−12.1	−12.7	−12.2
Cinder concrete							
Curing	+ 3.8	− 0.8	− 8.7				
Stage 1	−11.6	− 8.5	− 1.0				
Saturating	+ 9.6	+10.4	+10.8				
Stage 2	− 8.8	− 9.2	− 9.5				
Pumice concrete							
Curing	+ 6.6	+ 0.5	−13.4	−11.3	−19.4	−20.3	−19.3
Stage 1	−20.6	−17.2	− 4.7	− 5.6	+ 2.3	+ 3.1	+ 2.8
Saturating	+15.7	+19.6	+17.5	+20.0	+20.6	+21.4	+20.4
Stage 2	−15.0	−18.3	−16.2	−18.9	−19.2	−19.4	−18.6

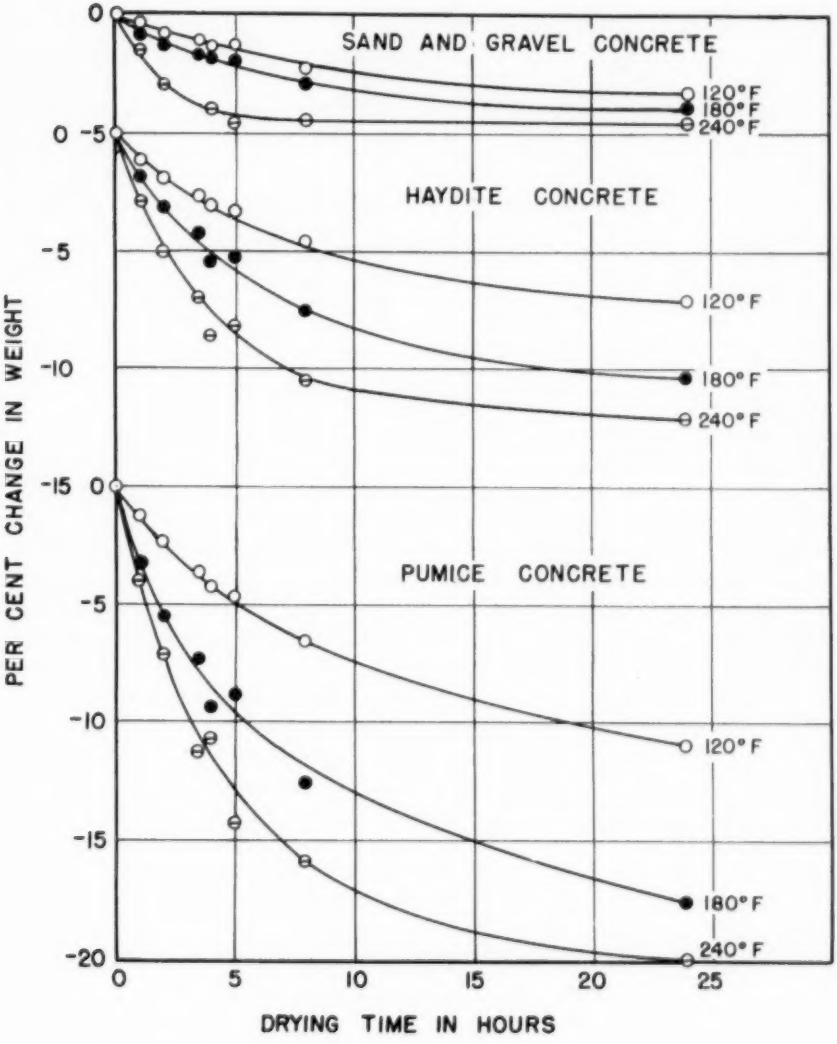

Fig. 4—Change in weight during oven drying at various temperatures

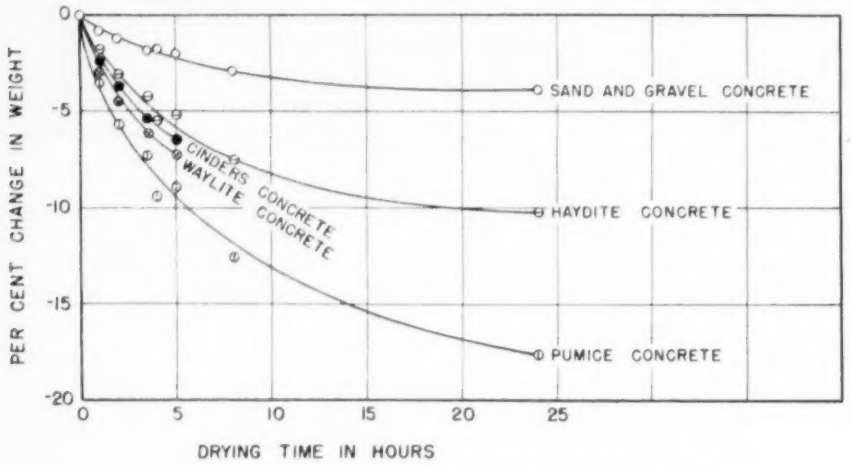

Fig. 5—Change in weight during oven drying at 180 F

with time in the drying oven at various temperatures. Inspection of the curves for pumice concrete indicates that it took about 20 hr to produce a 10 percent decrease in the as-molded weight at a drying temperature of 120 F, while the same percent change in weight was obtained in about 5 hr at 180 F and in about 3 hr at 240 F. Significant information can also be obtained by observing the slope of the curves at various times. For example, the sand and gravel 240 F curve has a slope of almost zero after about 8 hr, which indicates that almost no additional moisture was removed during the latter 16 hr of the 24-hr drying period. Fig. 5 shows the relationship between the rates of drying out at 180 F for the various concretes tested. Pumice concrete had the largest loss in moisture during 5 hrs' oven drying, with Waylite, cinders, Haydite, and sand and gravel following in that order.

The data in Table 11 show that the weight changes were lowest for the sand and gravel concrete and largest for the pumice concrete. Weight changes in Stage 1 drying were lowest for oven dried concrete, but weight changes in saturating after Stage 1 and in Stage 2 drying were slightly higher for oven dried concrete. Since the percent change in weight in saturating was computed on the same basis as the percent change in weight in Stage 2, the two values can be compared. Examination shows that no specimen lost as much weight in its second period of air drying as it gained upon being saturated. It is probable that part of the water absorbed during saturation caused additional hydration.

The percent change in length during air drying and one complete cycle of wetting and drying is shown in Fig. 6, based on results from a separate series of tests. The change in length during initial air drying (Stage 1) followed a rather definite pattern in relation to the curing process. Usually the moist cured specimens underwent the greatest decrease in length, with specimens cured by methods No. 2, 2a (180 F, 5 hr), 2a (120 F, 24 hr), 2a (180 F, 24 hr),

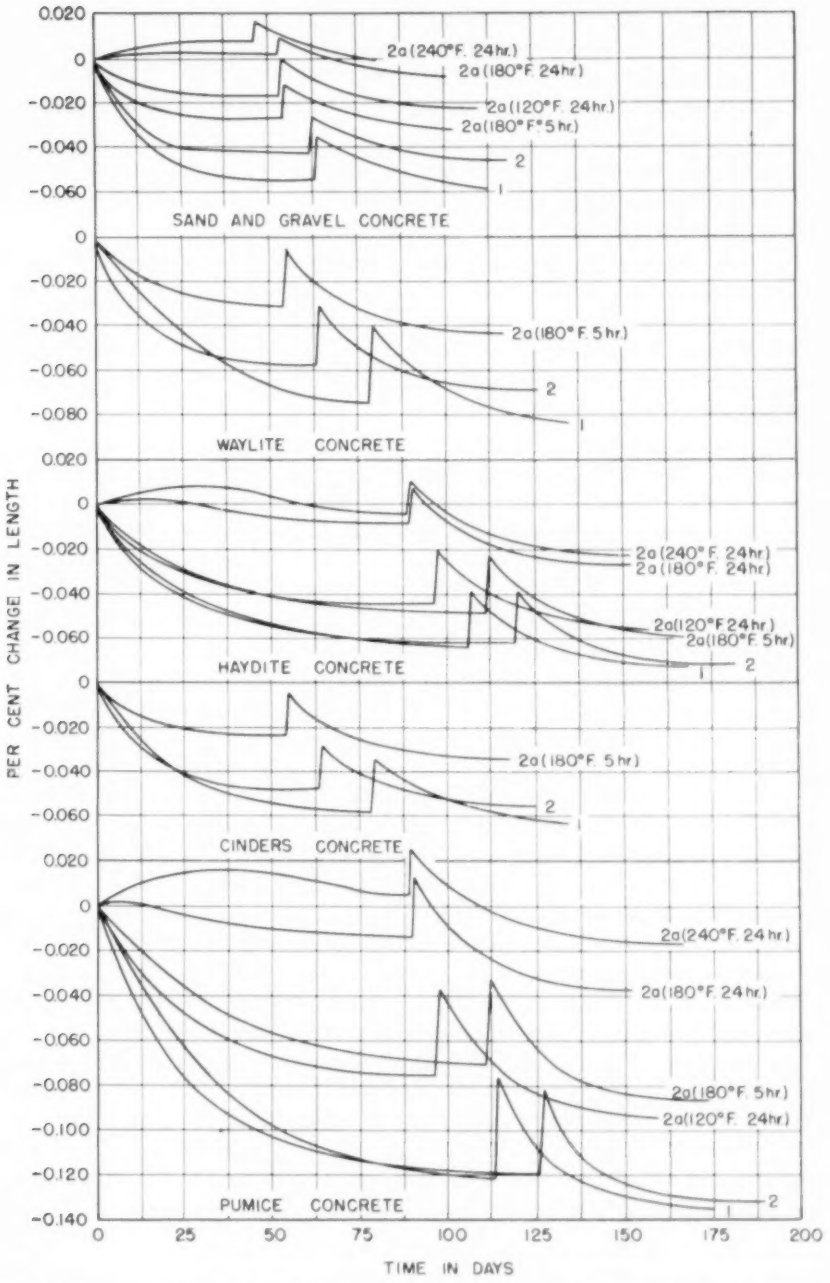

Fig. 6—Change in length during initial air drying and one cycle of wetting and drying of concretes cured by various methods

and 2a (240 F, 24 hr) following in that order. An exception was pumice, where specimens cured by method No. 2a (180 F, 5 hr) changed less in length than specimens cured by method 2a (120 F, 24 hr). The pumice, and sand and gravel specimens dried at 240 F for 24 hr actually increased slightly in length in Stage 1.

The amount of length change due to saturation after the specimens had reached constant length in Stage 1 was much less for the specimens which had been through a more severe drying cycle in curing.

The total percent loss in length during air drying after saturation (Stage 2) was in all instances greater than the percent increase in length during saturation. The total percent change in length in Stage 2 was not greatly dependent upon the curing procedure the concrete had been through. However, in most cases there was slightly less length change in Stage 2 for specimens that had the more severe oven drying.

The total length change in Stage 1 was related to the total weight change, as shown in Fig. 7. (These curves are not to be mistaken for curves indicating rate of drying.) The curves show that the total amount of length change in initial air drying is a function of the amount of moisture left in the concrete after the curing process is completed, and is apparently independent of the curing method. This statement is true only if the drying temperature and drying time are within reasonable limits. The smaller slope of the lower end of the curves indicates that unless a substantial part of the total initial water content is removed during curing there is little gained by removing any moisture. For example, the change in length for pumice concrete is approximately −0.118 percent if it loses 20 percent of its weight during initial air drying, but the change in length is about −0.100 percent if it loses 10 percent of its weight during initial air drying. The effect of a small change in initial moisture content is more drastic if a large percentage of moisture is removed by oven drying. For example, if the initial moisture content of pumice concrete is such that its weight decreases 5 percent during initial air drying, the corresponding length change is likely to be about −0.080 percent, but if the initial moisture content is such that the concrete loses 1 percent of its weight during initial air drying, the corresponding length change is likely to be about −0.050 percent. It is also interesting to note that none of the curves pass through the origin (0–0 point) of the two axes. For example, pumice concrete that has been cured so that it will neither gain nor lose moisture when stored in air at 70 F and 50 percent relative humidity will still change about −0.040 percent in length after the curing process. To have no change in length during initial air drying, the moisture content must be so low as to cause the concrete to absorb moisture from the air after it has been cured.

Interrelationship of the various properties that influence shrinkage cracking

The immunity of a concrete to cracking is influenced by its strength and stiffness properties, its tendency to shrink, and its amount of restraint. The

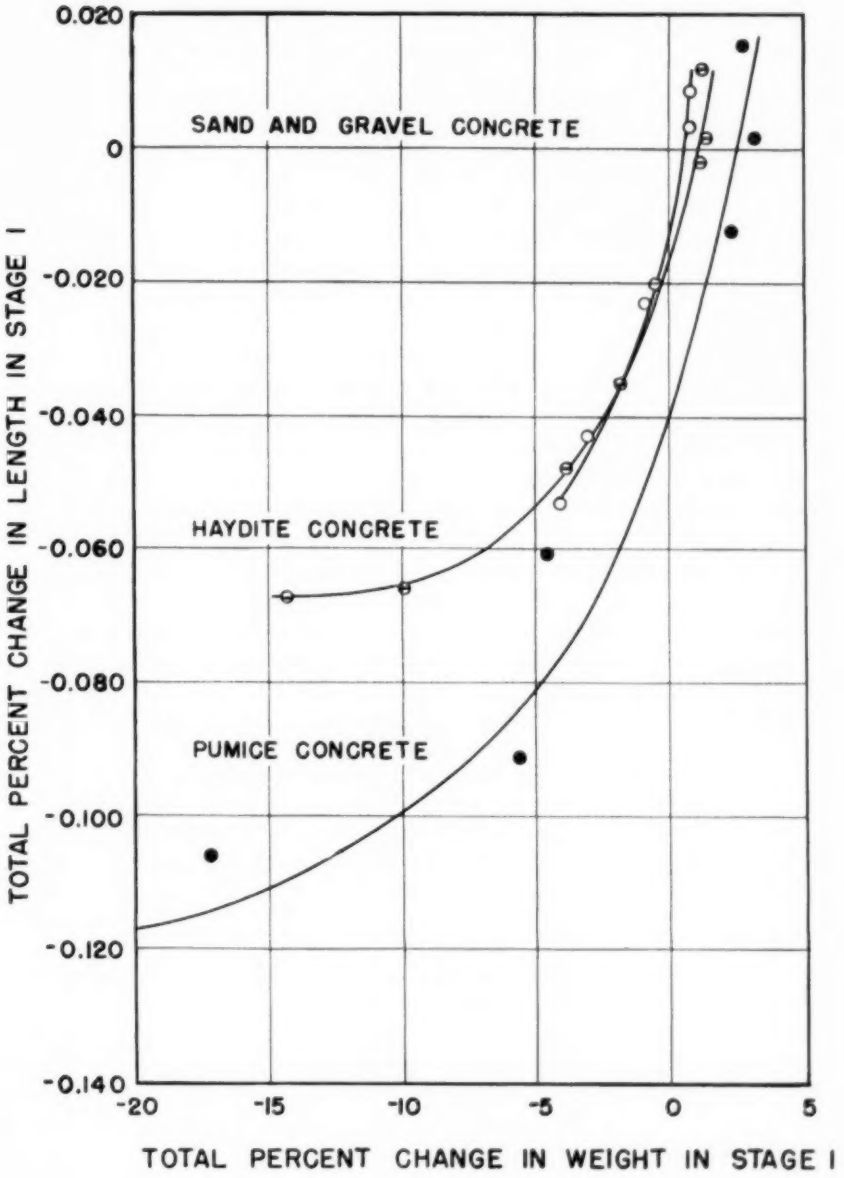

Fig. 7—Relationship between total change in length and total change in weight in Stage 1

relative immunity to cracking can be expressed by the equation

$$R = \frac{F}{(e_s + e_t)\,EI}$$

Where

R = relative immunity to cracking
F = unit tensile strength, psi
e_s = unit free drying shrinkage of the concrete
e_t = unit free temperature shrinkage of the concrete
E = secant modulus of elasticity as determined with the concrete subjected to sustained stress equal to 50 percent of its ultimate strength
I = degree of restraint expressed by the following equation

$$I = \frac{1}{1 + \frac{AE}{A_r E_r}}$$

Where

A = cross-sectional area of restrained concrete measured perpendicular to the direction of stress
A_r = cross-sectional area of restraint measured perpendicular to the direction of stress
E_r = sustained modulus of elasticity of the restraining member

The value of A/A_rE_r varies over a wide range. With A/A_rE_r equal to zero, I equals one, which indicates complete restraint. As the value of A/A_rE_r increases, I becomes smaller, indicating a lesser degree of restraint.

In Table 12, calculated values of relative immunity to cracking are listed for the five concretes cured by methods No. 1, 2, and 2a (180 F, 5 hr). The unit free drying shrinkage from a saturated to an air dry condition (Stage 2) and the unit free temperature shrinkage corresponding to a drop in temperature of 50 F were used. Values of R will vary with different assumptions as to change in moisture content and temperature. The value of R for con-

TABLE 12—RELATIVE IMMUNITY TO CRACKING

Aggregate	Curing method	F, tensile strength, psi	e_s, saturated to air dry condition, in. per in.	e_t, 50 F drop in temperature, in. per in.	E, sustained modulus of elasticity, 1000 psi	Relative immunity to cracking, R		
						$\frac{A}{A_rE_r} = 0$†	$\frac{A}{A_rE_r} = 0.000001$‡	$\frac{A}{A_rE_r} = 0.00001$§
Sand and gravel	1	371	0.00029	0.000250	2560	0.3	0.9	7.1
	2	298	0.00026	0.000245	2620	0.2	0.8	6.1
	2a*	268	0.00026	0.000235	2760	0.2	0.7	5.6
Waylite	1	246	0.00040	0.000225	915	0.4	0.8	4.4
	2	180	0.00036	0.000215	850	0.4	0.7	3.6
	2a*	154	0.00038	0.000210	845	0.3	0.6	2.9
Haydite	1	284	0.00049	0.000185	1500	0.3	0.7	4.5
	2	308	0.00043	0.000175	1320	0.4	0.9	5.5
	2a*	222	0.00047	0.000180	1160	0.3	0.6	3.7
Cinders	1	222	0.00037	0.000115	560	0.8	1.3	5.4
	2	173	0.00035	0.000105	745	0.5	0.9	4.3
	2a*	152	0.00036	0.000105	775	0.4	0.7	3.7
Pumice	1	151	0.00088	0.000190	380	0.4	0.5	1.8
	2	187	0.00074	0.000190	490	0.4	0.6	2.4
	2a*	238	0.00085	0.000190	570	0.4	0.6	2.7

*180 F at 5 hr.
†Complete restraint.
‡Intermediate degree of restraint.
§Low degree of restraint.

cretes with little or no oven drying during curing would be lowered appreciably if the initial shrinkage (Stage 1) were used rather than the Stage 2 shrinkage. It is for this reason, and also because block have a low tensile strength at an early age, that block should not be used in structures too soon after manufacture.

In all calculations for R it was assumed that there was no temperature change in the restraining member. For the usual case where concrete is restrained by reinforcement or footings, allowance for temperature change in the restraining member would increase the relative immunity to cracking of the concrete.

Considering concrete made from any one type aggregate, except pumice, moist curing usually produced the highest relative immunity to cracking. Cinder concrete had the highest values of relative immunity to cracking for relatively high degrees of restraint, and sand and gravel concrete had the highest values of relative immunity to cracking for low degrees of restraint.

It should be noted that the calculated R values represent one method of applying the test information, and they should be considered as being relative rather than absolute in their significance.

CONCLUSIONS

1. The compressive strengths and initial moduli of elasticity of steam cured concrete were smaller than those of moist cured concrete.

2. The dynamic modulus of elasticity was slightly greater than the initial static modulus of elasticity. Consequently dynamic modulus of elasticity may be used to predict the approximate value of the static modulus of elasticity.

3. The sustained modulus of elasticity was less than the initial static modulus of elasticity. Except for Haydite concrete, the largest differences between sustained modulus and initial static modulus of elasticity were obtained for moist cured concrete.

4. All moist cured specimens gained weight in the curing process, but steam cured specimens varied between small losses and small gains.

5. The percent loss in length and weight in oven drying increased as the oven drying temperature or the oven drying time was increased. Pumice concrete underwent the largest changes, and sand and gravel concrete had the smallest changes.

6. Increased oven drying during the curing cycle reduced the change in length obtained in air drying (to constant weight) immediately after curing

7. The absorption of concrete made with a given aggregate was nearly constant for all curing procedures. The percent absorptions varied from 5.0 for sand and gravel concrete to 28.5 for pumice concrete. The absorptions, in lb per cu ft, varied from about 7.0 for sand and gravel concrete to 18.0 for pumice concrete.

8. The increase in length due to saturation following air drying immediately after curing was less for specimens dried at higher temperatures for long periods.

9. The total percent change in length during air drying after saturation was not greatly dependent upon the curing procedure.

10. The thermal coefficient of linear expansion was not much affected by the curing process.

11. Oven drying at a specimen age of 14 days had no apparent advantage over oven drying immediately following steam curing with regard to strength, stiffness, and moisture volume change properties.

12. Relative immunity to cracking for a high degree of restraint was greatest for moist cured cinder concrete.

13. As the degree of restraint decreases, the stronger and stiffer concretes become relatively less susceptible to cracking. Moist cured sand and gravel concrete had the greatest relative immunity to cracking when subjected to a low degree of restraint.

ACKNOWLEDGMENTS

All tests were made in the Materials Testing Laboratory of the University of Wisconsin. The work was done in collaboration with the National Concrete Masonry Assn., and the research program was originally outlined by R. E. Copeland, director of engineering for that organization. Thanks are due to L. M. Basford and L. B. Morgan for their help. The tests were financially supported jointly by the National Concrete Masonry Assn., the University of Wisconsin Engineering Experiment Station, and the research funds of the Mechanics Department of the University of Wisconsin.

Title No. 51-42

Performance of Reinforced Concrete and Concrete Masonry in Recent Western United States Earthquakes*

By KARL V. STEINBRUGGE and DONALD F. MORANt

SYNOPSIS

Recent western United States earthquakes, while not the strongest on record, have given an indication of the effectiveness of modern design methods and construction practices in resisting lateral forces. The examples of damage, although slight in some instances, are keys to weaknesses. The discussion includes cast-in-place reinforced concrete, precast reinforced concrete, and concrete masonry structures. The need for competent field inspection is noted, especially when unusual design or construction features are involved.

INTRODUCTION

There have been three earthquakes in western United States including and since the 1952 earthquakes which have been strong enough to cause structural damage: July 21, 1952, and its aftershocks—Tehachapi, Bakersfield, and southern California; Apr. 25, 1954,—Watsonville and vicinity in northern California; and July 6, 1954,—Fallon-Stillwater in western Nevada.

The Apr. 25, 1954, Watsonville shock did not cause significant damage to reinforced concrete or hollow concrete block structures, save to one relatively new reinforced concrete bridge located on alluvium near the San Andreas Fault. This bridge had broken wing walls after the earthquake.

None of these three earthquakes are among the heaviest to strike the United States; the San Francisco (California, 1906) and the New Madrid (Missouri, 1811 and 1812), among others, were heavier. On the other hand, these recent shocks give the profession an indication of the effectiveness of present design methods.

CAST-IN-PLACE REINFORCED CONCRETE

Relatively few structures are built across or directly in an active fault zone. Active faults are usually in terms of miles apart while their widths may often be expressed in yards. However, surface movement on the White Wolf fault during the main shock of the July 21, 1952, earthquake shattered

*Presented at the ACI Seventh Regional Meeting, Los Angeles, Calif., Oct. 29, 1954. Title No. 51-42 is a part of copyrighted JOURNAL OF THE AMERICAN CONCRETE INSTITUTE, V. 26, No. 9, May 1955, *Proceedings* V. 51. Separate prints are available at 35 cents each. **Discussion** (copies in **triplicate**) should reach the Institute not later than Sept. 1, 1955. Address 18263 W. McNichols Rd., Detroit 19, Mich.

†Members American Concrete Institute, Structural Engineers, Pacific Fire Rating Bureau, San Francisco and Los Angeles, Calif.

Courtesy Southern Pacific Railroad

Fig. 1—Damage to Southern Pacific Railroad tunnel in July 21, 1952, earthquake

all or parts of four reinforced concrete railroad tunnels located in the fault zone (Fig. 1). These tunnels, originally timber lined, were built about 1876, and were later relined with reinforced concrete. Considering the forces involved it is doubtful if any masonry structure located across a fault can successfully resist anything but the slightest fault movement.

On the other hand, structures subjected only to seismic vibratory motions can readily be designed to resist resulting lateral forces. The remainder of this paper is devoted to structures representative of the few which did suffer damage.

Brock's Department Store in Bakersfield, built about 1920, was not specifically designed to resist shock. It has three stories plus mezzanine and basement, and is entirely of reinforced concrete construction (Fig. 2). The Aug. 22, 1952, aftershock caused serious structural damage, principally to the south wall (Fig. 3). The store was closed at this location until May 23 of the following year when major repairs had been completed. Cores taken from this structure tested from 1300 to 2500 psi.

A lateral force analysis revealed that the most rigid element for east-west lateral forces was the south wall and the structure would experience strong rotational forces due to nonsymmetrical resisting elements. Based on an assumed east-west lateral force of 10 percent of the dead load of the structure plus reasonable live loads, a maximum shearing stress of somewhat over 100 psi would result in the piers which failed. Note in Section A-A of Fig. 2 the absence of horizontal ties in these damaged piers.

In Santa Barbara, a six-story office building built in 1923 and not designed to resist shock is an excellent example of repetitive damage when no effective structural repairs are made (Fig. 4). The frame and floors are reinforced concrete, but the exterior walls are hollow tile panels in the concrete frame. Damage has been reported from the following shocks:

June 29, 1925—Damage estimated at 50 percent of building value
Feb. 18, 1926—About $10,000 damage

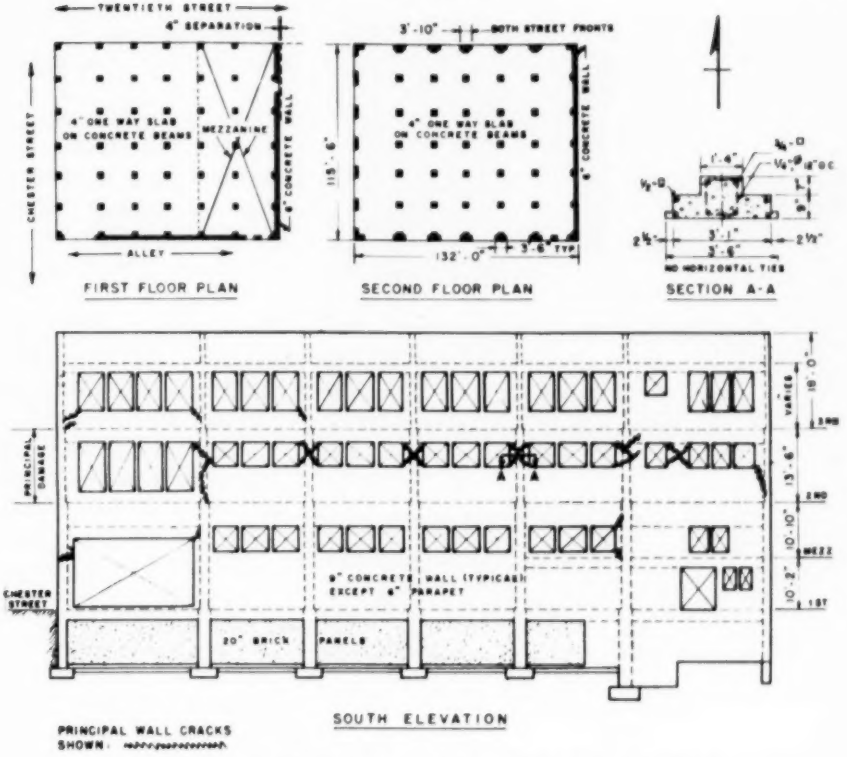

Fig. 2—Plan and elevation of Brock's Department Store, Bakersfield

June 29, 1926—Partition cracking at all floors
June 30, 1941—Repairs estimated at over $50,000
July 21, 1952—Repairs estimated at 22 percent of building value

This structure is typical of other multistory structures having had no effective repairs after previous shocks.

Cummings Valley School, built about 1910, was one story high with concrete walls and wood roof. Several exceedingly poor features were noted after the collapse in the July 21, 1952, earthquake (Fig. 5): reinforcing bars (spaced at approximately 4-ft centers)

Fig. 3—Typical wall crack, Brock's Department Store. Damaged in Aug. 22, 1952, aftershock

Courtesy U. S. C. & G. S.

Fig. 4—Damage to Santa Barbara office building resulting from July 21, 1952, shock

did not lap (Fig. 6), concrete consisted of excessive fines, and construction joints were not cleaned. Prior to the shock, the paint and stucco finishes covered any surface defects and a casual observation might not have revealed any danger points.

Probably the most readily visible evidence of earthquake damage in reinforced concrete structures was "working" at the construction joints. This was noted even where over-all building damage was negligible. Fig. 7 and 8 are typical examples of construction joint movement.

A number of buildings not specifically designed to resist earthquake, yet containing inherent strength, came through undamaged. Two good examples in Tehachapi ("flattened" according to press accounts) were the Beekay Theatre and the two-story Catholic Youth Center. The relatively few wall openings in each instance probably was one of the main reasons for their good performance.

Fig. 5—Cummings Valley School after July 21, 1952, quake

PRECAST REINFORCED CONCRETE

The one notable example of this type which did experience damage was the Lockheed Plant in Bakersfield. Structures at this site were built in 1950-51 and are one story high with precast walls, columns, girders, beams, and roof slabs. Interconnection of these various precast elements was made by welding together metal

plates attached to each member. Since the walls were precast concrete with few openings, the roof was designed as a diaphragm to distribute lateral forces to these exterior walls. Grout was specified for the joint between precast roof panels.

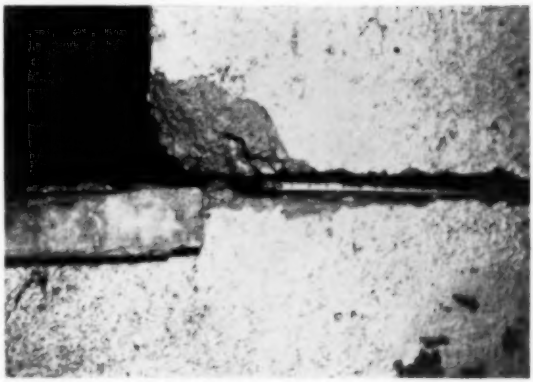

Fig. 6—Detail of construction joint of Cummings Valley School. Note that bars do not lap

During construction, in addition to other deviations such as lengthening one building by 80 ft, mastic was used between roof panels instead of grout (Fig. 9). The excessive horizontal roof deflections in the Aug. 22, 1952, aftershock resulted in one building having a 2 in. permanent set to the east and fracturing interior columns as indicated in Fig. 10.

The Di Giorgio Winery had one structure with precast reinforced concrete roof panels along with some precast roof beams. This structure, also designed to resist shock, received only minor damage during the July 21, 1952, earthquake and its aftershocks. Such damage as did occur was probably the result of high local stresses resulting from different rigidities of bracing elements.

The so-called "tilt-up" construction, having wood roofs and wherein the walls are concreted while horizontal and then lifted into place, were found to have experienced negligible or no damage wherever inspected.

HOLLOW CONCRETE BLOCK

Hollow concrete block buildings in the Bakersfield-Arvin-Tehachapi area are primarily of recent construction and have been laid with cement mortar as well as usually being reinforced with steel. As a result, construction usually had some, if not considerable, earthquake bracing and performed well. Table 1 is a summary of the damage to reinforced and unreinforced masonry

Fig. 7—Movement in construction joint at roof line as a result of July 21, 1952, earthquake

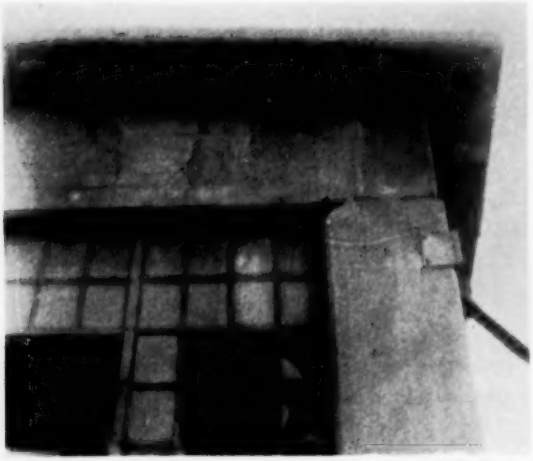

Courtesy V. L. Hanson

Fig. 8—Column moved ¾ in. out at construction joint at top of window. Movement noted at practically all construction joints

structures having wood floors and roofs in Bakersfield. Schools are excluded. As contrasted to the average hollow concrete block, the concrete brick and ordinary brick were usually laid in sand-lime mortar and not reinforced.

One interesting example of damage is that which occurred to a bank in Arvin in the July 21, 1952, earthquake. Earthquake bracing in the front wall was in the form of a reinforced hollow concrete block shear wall (Fig. 11). As noted in this figure, the block was laid in "stack bond" or "jack over jack." Since there was no specific element to resist the vertical shearing stresses which act simultaneously with the horizontal shear, vertical cracks occurred between the block. This cracking could probably have been controlled by adequate horizontal bond beams.

On July 6, 1954, the Fallon-Stillwater earthquake caused as much if not more damage to unreinforced hollow concrete block than to unreinforced brick. Much of the block was 50 years old and of a poor quality. A person could readily break off pieces by hand from the poorest specimens. None of the older block was reinforced and mortar was of a quality which "held apart" the block. The newer concrete block laid in cement mortar but not usually reinforced, performed much better than the older material. However, this was not a strong shock and the use of unreinforced hollow concrete block even with cement mortar is questionable.

Fig. 9—Lockheed plant during construction showing precast roof, beams, and girders. Mastic substituted for grout between panels

CONCLUSIONS

The following conclusions are based on studies made of these and other

earthquakes. The references provide additional examples bearing out these conclusions. Well designed and well placed reinforced concrete is an excellent material for earthquake resistive construction. However, good workmanship, such as the proper cleaning of construction joints, can not be overemphasized.

In precast concrete construction, the "joinery" of the units is critical and qualified field inspection is important.

Hollow concrete block can be made earthquake resistant when properly reinforced. However, since quality depends upon individual workmen more than in other types discussed, inspection again is vital.

Courtesy Lockheed Aircraft

Fig. 10—Damaged column in Lockheed plant due to improperly constructed roof diaphragm

REFERENCES

1. "Kern County, California, Earthquakes of 1952," *Bulletin* No. 171, California Division of Mines, in press 1955.

2. Degenkolb, H. J., "Structural Observations of the Kern County Earthquake," *Proceedings*, ASCE, Separate No. 244.

3. Steinbrugge, K. V., and Moran, D. F., "An Engineering Study of the Southern California Earthquake of July 21, 1952, and Its Aftershocks," *Bulletin of the Seismological Society of America*, V. 44, No. 2B, Apr. 1954.

TABLE 1—SUMMARY OF DAMAGE TO MASONRY STRUCTURES*

Wall	Torn down, percent	Repaired, percent	Repair or demolition undecided, percent	Undamaged, percent	Total area, sq ft
Brick	16	42	20	22	2,717,410
Concrete brick	20	40	36	4	230,950
Concrete	6	12	6	76	1,186,680
Hollow concrete block	2	6	†	92	488,525

*In all cases, the buildings have wood floors (except for first) and wood roofs. Percentages are based on floor areas, and not the number of structures involved.

†Negligible.

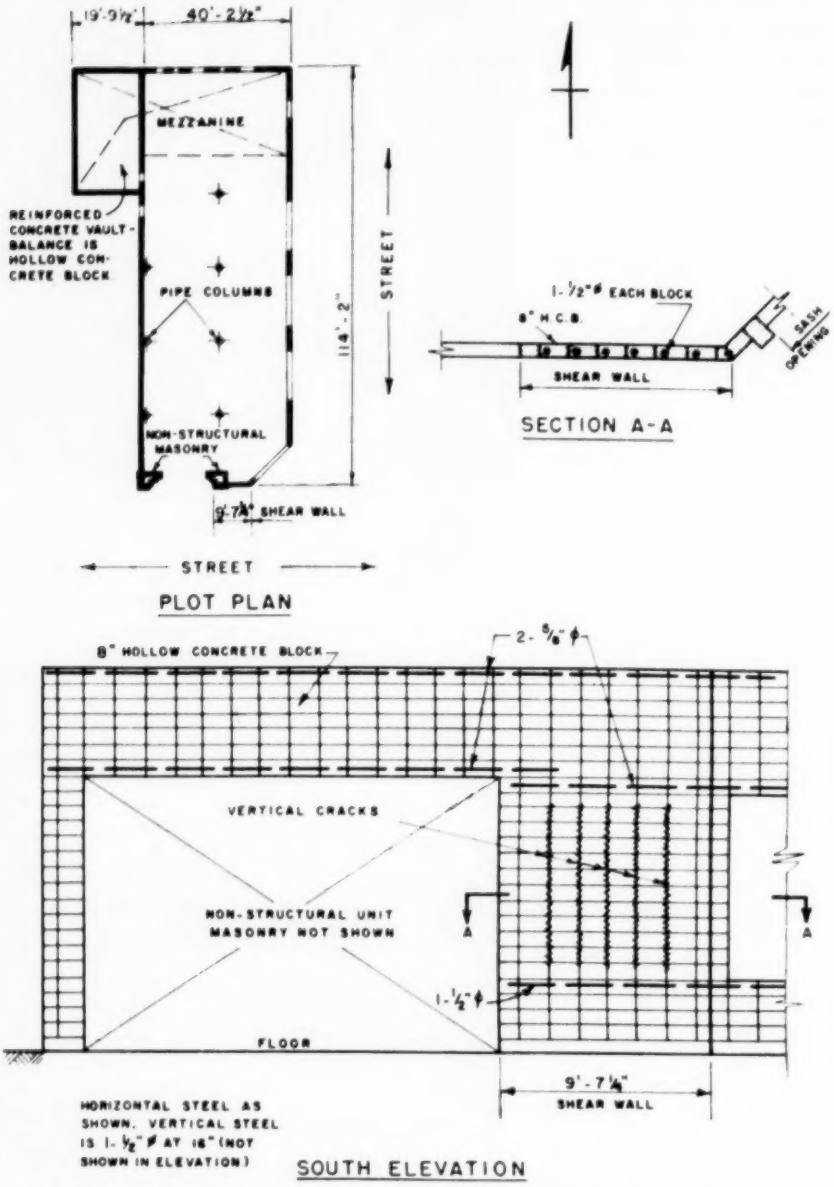

Fig. 11—Plan, elevation, and location of cracks in bank building, Arvin

Title No. 51-43

Behavior of Prestressed Concrete Composite Beams*

By R. H. EVANS† and A. S. PARKER‡

SYNOPSIS

The principal object of the investigation was to determine whether a composite section consisting of in-situ and prestressed concrete acts monolithically with a straight line distribution of strain. Different types of prestressed elements were tested and the quality of bond for varying degrees of roughness of surface was observed. At the same time one set of beams was made specially to investigate the way in which cracks progress across the joint of the two qualities of concrete. Microscopic observations showed that although there is a certain degree of restraint between in-situ and prestressed concrete, the extensibility is unaffected.

In much the same way as shrinkage of concrete in reinforced concrete members produces stresses, differential shrinkage and creep of the two concretes in composite work also have an effect. This was investigated theoretically and the results checked against the observed cracking loads of the beams.

In discussing the significance of the experimental and theoretical results the commercial possibilities of composite construction are considered and various suggestions made with regard to the best type of surface bond, the best relative concrete mixes and times of casting the concrete. The results show that the straight line theory is applicable and stress distributions based on this have been plotted to give examples of good and bad types of combined sections.

INTRODUCTION

Composite construction is an attempt to economize over normal prestressed concrete design and yet retain the advantages of that type of construction. Composite construction, as dealt with in this paper, means any in which ordinary mass or reinforced concrete is cast onto prestressed units to form a new working section, that which is cast on being referred to as in-situ concrete.

The immediate possibilities which follow from this are firstly that the in-situ concrete need not be of the quality necessary for prestressing and may serve the additional function of a wearing surface. Secondly the prestressed units may be used as permanent forms for the in-situ concrete. These then are the basic economies. A natural development such as is used in the Stahlton floor and similar types of construction is to incorporate light precast nonprestressed units to complete the formwork. Composite construction has been used for floors and for decks of fairly short span bridges.

*Received by the Institute Feb. 4, 1954. Title No. 51-43 is a part of copyrighted JOURNAL OF THE AMERICAN CONCRETE INSTITUTE, V. 26, No. 9, May 1955, *Proceedings* V. 51. Separate prints are available at 50 cents each. **Discussion** (copies in **triplicate**) should reach the Institute not later than Sept. 1, 1955. Address 18263 W. McNichols Rd., Detroit 19, Mich.

†Member American Concrete Institute, Professor, Civil Engineering Dept., The University, Leeds, England.
‡The University, Leeds, England.

Design has been based on the assumption that the various elements bond together to a sufficient degree to act monolithically. This investigation was to determine the extent to which this assumption is valid, and the degree of restraint between the concretes. There has been much speculation as to the interaction between the concretes in a combined section. It has been suggested that due to the considerable difference of stress at the jointing plane, there may be a restraining action of the prestressed upon the in-situ concrete. A certain retention of stiffness was observed but it will be shown that the extensibility of the concrete has remained sensibly unaffected. At the same time, the effect of the difference in shrinkage and creep of the two concretes has been considered theoretically and the results checked by observation of cracking loads. The investigation deals only with composite beams although the results will apply qualitatively to other applications of the construction. As little work had been done in this field it was advantageous to vary the type of beam and obtain data covering a wider range of specimens rather than try to eliminate several variables by concentrating upon one specific design.

DESCRIPTION OF BEAMS TESTED

The different types of beams are illustrated in Fig. 1 and the relevent data in Table 1. Two beams were cast using standard British Ministry of Works floor joists as the prestressed element. These joists were not designed for composite construction and as they had been cast in steel molds their surface was very smooth. They were roughened slightly with a chisel before casting the in-situ concrete but even then the quality of bond could be considered as representative of the worst type of condition for a composite member.

The first beam was cast with additional untensioned high tensile wires in the in-situ portion and the second with ordinary mild steel reinforcement

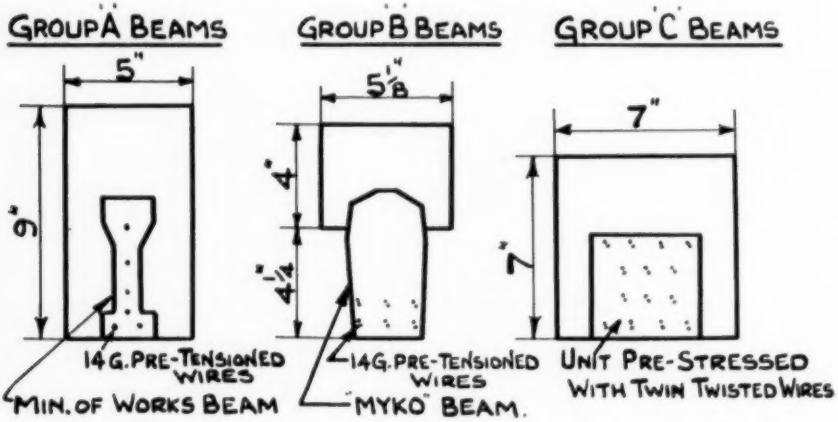

Fig. 1—Types of beams tested

TABLE 1—SUMMARY OF TEST RESULTS

Test No.	Type of prestressed element	Span	Type of loading	B. M. at cracking of prestressed element, in.-tons	B. M. at failure, in.-tons	Type of failure	Remarks
1	Ministry of Works beams (Group A) (Fig. 1)	10 ft 0 in.	Middle third points	32	82	Bond	Untensioned wires used as additional reinforcement
1A		6 ft 10 in.	Central	—	94	Tension	
2		10 ft 0 in.	Middle third points	38	56	Yield of mild steel	Mild steel reinforcement and vertical stirrups
3	Myko beams (Group B) (Fig. 1)	10 ft 0 in.	Middle third points	60	94·8	Tension	
3A		6 ft 0 in.	Central	62	96	Tension	
3B		3 ft 6 in.	Central	—	73	Shear	
4		10 ft 0 in.	Central	54	90	Tension	
4A		4 ft 0 in.	Central	56	85	Shear	
4B		4 ft 0 in.	Central	—	95	Tension	
5		10 ft 0 in.	Central	51	85	Tension	
6	Twin-twisted wire beams (Group C) (Fig. 1)	4 ft 0 in.	Central	45	143	Shear	
7		4 ft 0 in.	Central	46	135	Shear	
8		4 ft 0 in.	Central	—	131	Shear	

and vertical stirrups. Both beams exhibited characteristics of bad permanent set and hysteresis, but there was no tendency at any time for a failure due to horizontal shear along the bonding plane. Cracks were carefully examined and the earliest cracks in the in-situ portion tended to become narrower on approaching the joint. When cracks appeared in the prestressed member they did so always as a continuation of one in the in-situ concrete. On subsequent breaking up of the beams the bond was found to be good. The beam with the untensioned wires gave smaller cracks at shorter intervals than that with the mild steel reinforcement.

Three beams were cast using a special Myko prestressed element specially designed for composite construction.* The bonding surface had been roughened considerably and the recovery of these beams was very good. Strain distributions plotted from extensometer readings at intervals down the sides of the beams were found to be linear both before and after cracking. The only difference which these beams showed from a normal one of similar section was the fact that shrinkage cracks were present in the in-situ topping. This gave slightly decreased stiffness in the early stages of loading and slightly lower cracking loads than those calculated by the normal theory.

The final three beams were cast on columns uniformly prestressed with twin-twisted wires. The design was chosen purely for the investigation of interaction between the in-situ and prestressed concretes during the formation of cracks.

For reference the beams are numbered 1 to 8 in Table 1. Part or half-beam tests are numbered 1A, 1B, etc. The beams employing the British

*Myko beams are essentially pre-tensioned prestressed concrete beams, of nearly rectangular cross section, with some links or stirrups partly projecting from the top of the beam to provide bond with the in-situ concrete.

Ministry of Works joists are group A (beams 1 and 2); those employing the Myko elements are group B (beams 3, 4, and 5); and the final three are group C (beams 6, 7, and 8). The mix used for the in-situ concrete was 1:2:4 with a W/C of 0.5.

DETERMINATION OF CRACKING LOADS

To obtain accurate data upon the effect of composite construction on cracking loads, the sections were measured individually and the theoretical values afterwards calculated. The actual cracking loads were obtained from direct observation by microscope, combined with a method of load cycles and observation of strain readings. As the theoretical cracking load was approached a series of cycles or repeated loadings over small ranges of load was measured by means of mirror extensometers reading to 1×10^{-6} in. on a gage length of 8 in. In this way, the average rate of strain per 0.1 ton range of load was determined for gradually increasing mean loads. When this average rate of strain has increased by 5–10 percent previous experience has shown that a small tension crack is present in the concrete between the extensometer gage points. This method of determining whether or not a tension crack exists in the concrete has always proved to be successful.

It was found that a composite beam, particularly where the in-situ concrete was well below the neutral axis, showed much less marked change of stiffness at cracking than either reinforced or prestressed beams and it was necessary to combine constant observation with the method given above to locate the first cracks at the earliest opportunity. A composite beam will not exhibit sudden changes in strain or deflection as the incidence of cracking is much more gradual than in either reinforced or prestressed concrete beams (Fig. 2-5). Tension cracks, for example, will not appear simultaneously in the in-situ and prestressed concrete sections of the beam.

INTERACTION AND RESTRAINING ACTION OF IN-SITU AND PRESTRESSED CONCRETE

When a plain concrete beam is loaded to cracking, it is possible to find a crack which does not extend across the whole of the soffit. This minute initial crack will however extend right across the beam with a very small further increment of load. With the restraint of reinforcement an initial crack may take a little longer to spread, but experiments have shown that whatever the restraint the extensibility of concrete is unaffected. In some tests on composite beams certain investigators have found that a composite section appears to retain its initial load-deflection slope for a small increase of load beyond that which would normally cause cracking of the in-situ concrete. This suggests that the prestressed member somehow restrains the natural tendency of cracks to spread in the in-situ portion.

Cracks in the group C beams were carefully examined to investigate this phenomenon. Powerful traveling microscopes were used and in the first beam a minute crack was detected before there was any detectable change

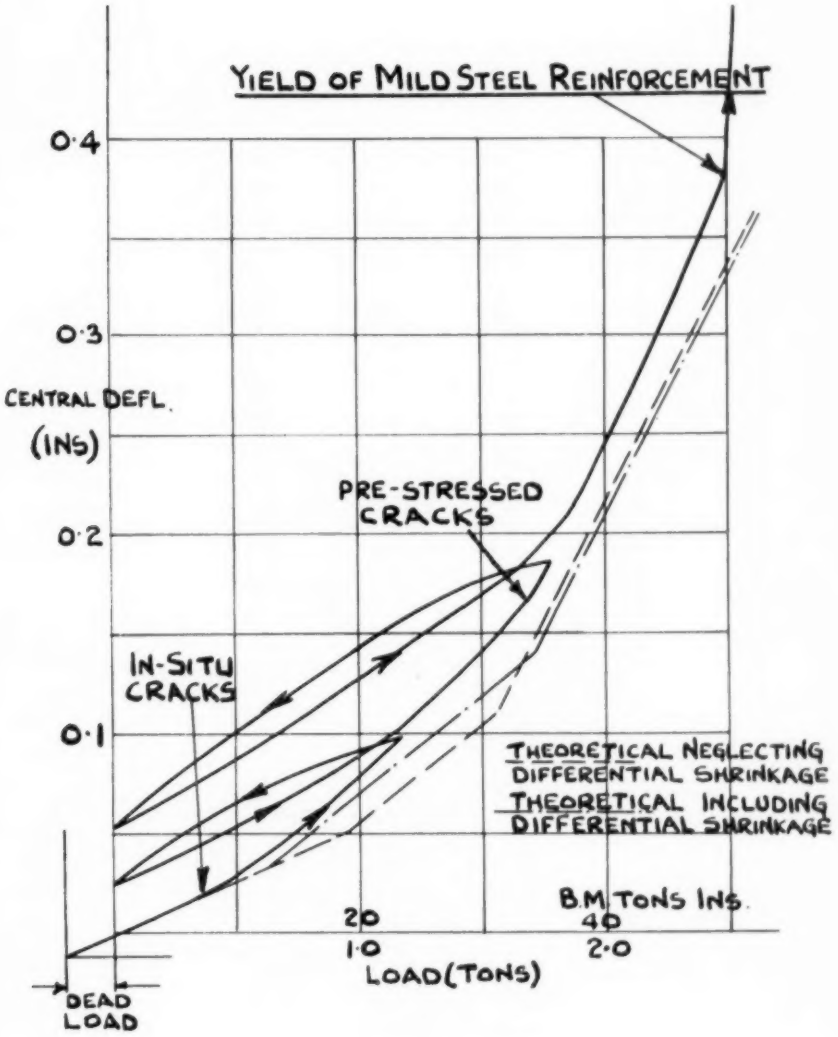

Fig. 2—Loading diagram for beam No. 2

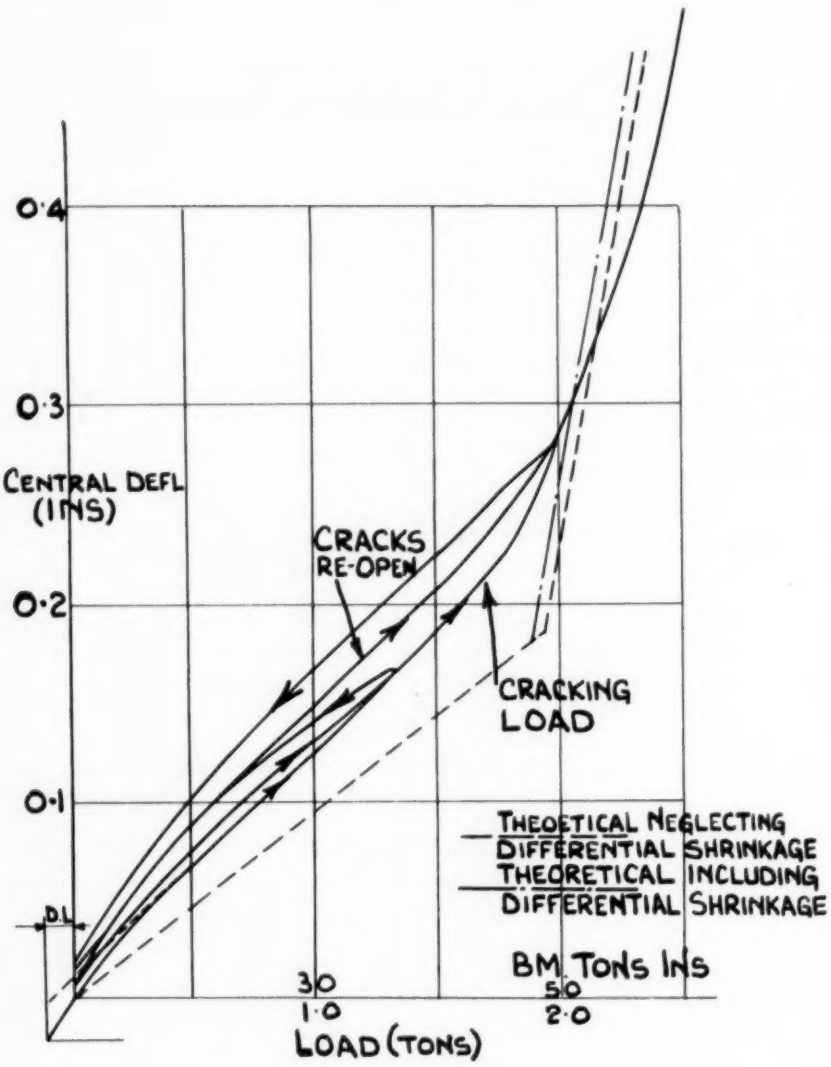

Fig. 3—Loading diagram for beam No. 4

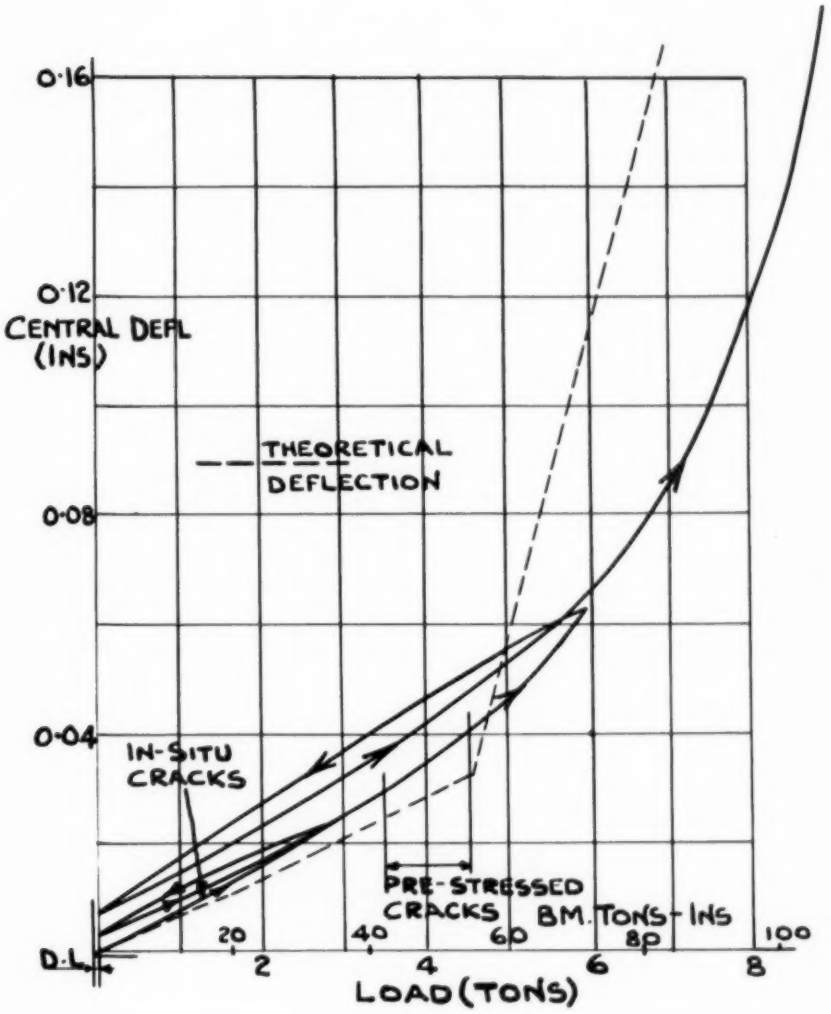

Fig. 4—Loading diagram for beam No. 8

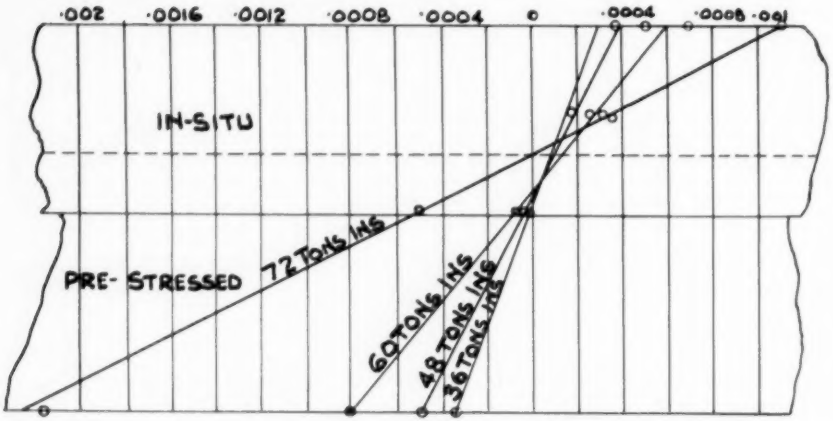

Fig. 5—Strain distribution in group B beams

in stiffness. This crack occurred at a load of 1.7 tons and at the outer edge of the in-situ concrete the width of the crack was 0.0005 in. It was traced toward the prestressed concrete but became continually narrower until it terminated before reaching the joint. With no increase of load it gradually extended as far as the joint where it reached a maximum width of 0.002 in. and at the same time developed minute longitudinal cracks for a short distance along the joint. As load was increased the main crack widened and could be seen to terminate abruptly at the edge of the prestressed member, while the longitudinal cracks showed no further increase in length or width. At a load of 3.5 tons continuation of the original crack into the prestressed element took place but it was not until 4.5 tons that the first crack extended right across the soffit. Until this occurred the stiffness of the beam had not greatly decreased. The remaining cracks on this beam and on the other beams of this group all showed characteristics identical with the first one.

Throughout the investigation there was no evidence that the extensibility of either prestressed or in-situ concrete was sensibly affected by composite construction. Table 3 shows that where there seemed to be an appreciable increase or decrease in a cracking load above or below that obtained by conventional theory, it was in every case shown to be mainly due to differential shrinkage. There is however considerable evidence of restraining action between the concretes. Differential shrinkage between the two kinds of concrete mixes can therefore appreciably affect the cracking load of composite beams but the actual widths of the tension cracks in the in-situ concrete will be greatly restricted by its adhesion to the prestressed concrete. The load-deflection curves show a much more gradual curve than is usual for normal reinforced concrete or prestressed beams (Fig. 2-4). Indeed it is almost impossible to detect any sudden change at cracking loads in some cases.

To appreciate the significance of this behavior, reference is made to a paper* "Extensibility and Modulus of Rupture of Concrete," in which it is stated that cracks were never detected of width less than about 1/13,000 in. in plain concrete beams. The cracks when they occur are usually spaced at least 3 or 4 in. apart and thus the resilience of the uncracked portion is sufficient immediately to open them out to this extent. This present investigation has shown that cracks in the in-situ portion became much smaller toward the joint or common concrete surface. The effect therefore, of a combined construction upon cracks in the in-situ portion is to reduce the influence of the resilience of the uncracked portion and prevent the opening of the concrete crack. In the prestressed concrete part, on the other hand, the evidence is that an in-situ crack induces a stress concentration and is liable to cause early cracking of the prestressed concrete near the joint. These effects can be minimized or obviated by placing all the in-situ concrete in the compression zone, but this cannot always be done in practical design.

THEORY OF DIFFERENTIAL SHRINKAGE AND CREEP APPLIED TO COMPOSITE BEAMS

In reinforced concrete beams the effect of concrete shrinkage is always to put the concrete in tension. In composite beams, however, the three factors: (a) shrinkage of in-situ concrete, (b) shrinkage of prestressed concrete, and (c) creep under prestress of the prestressed concrete, may combine together with the further variables of relative qualities of mix and dates of casting to cause either tension or compression and, in certain conditions, a neutral state. A fairly accurate estimate of the differential movement of the concretes may be obtained from shrinkage and creep samples for a particular beam or else from typical shrinkage and creep/time curves for the mixes used. The following theory predicts the stress distribution in a composite beam due to this movement which, although it involves creep, is thought to be mainly due to shrinkage and will therefore be referred to as differential shrinkage. The assumptions made are:

(a) Perfect bond between the in-situ and prestressed concretes,

(b) Shrinkage is uniform over each section of the composite member, and

(c) No external restraints acting upon the member and complete freedom to bend under the effect of differential shrinkage. (If it is restrained there are additional stresses set up equivalent to bending the member from the position it would normally take up if free.)

The shrinkage of concrete is not strictly uniform over the cross section of a beam but decreases from the outside fibers toward the center of the beam. The shrinkage coefficient, however, is measured in the laboratory from a specimen of similar cross section to the beam so that little error arises from the above second assumption. Creep in concrete is proportional to stress up to stresses equal to about one-third of the crushing strength so that the effect of creep is to diminish the effective value of the modulus of elasticity

*Evans, R. H., *The Structural Engineer* V. 24, No. 12, 1946.

of the concrete and to reduce the stresses induced by differential shrinkage of the concrete.

The appropriate values for E_1 and E_2 in these calculations have been ascertained from tests on columns or cubes of identical mixes. In the case of prestressed beams, of high quality concrete, the value of E_2 does not vary much and a value of 4.5–5.5 $\times$ 10^6 psi would be satisfactory.

Notation

x = Differential shrinkage coefficient
i.e., x = (Free shrinkage strain of in-situ concrete) − (Free creep plus free shrinkage strain of prestressed concrete)
σ_1 and σ_2 = Strain at the centers of gravity of the in-situ and prestressed sections, respectively
σ' = $x - (\sigma_1 + \sigma_2)$
n and y = Distance from center of gravity to top and bottom fibers, respectively
e = Distance between centers of gravity of in-situ and prestressed sections
e_1 and e_2 = Distance from line of action of mutual force to centers of gravity of in-situ and prestressed sections, respectively
c_1 = Compressive strain in top of in-situ section
t_1 = Tensile strain in bottom of in-situ section
c_2 = Compressive strain in top of prestressed section
t_2 = Tensile strain in bottom of prestressed section
A = Area
E = Young's modulus
I = Moment of inertia
δ = Central deflection
R = Radius to which beam bends
D = Total depth of beam
l = Length of simply supported span
Subscript 1 refers to the in-situ section
Subscript 2 refers to the prestressed section

All values used are measured from the date of casting the in-situ to the date at which the stress distribution is required.

Consider a typical composite section as in Fig. 6. Assuming perfect bond between the sections, the strain distribution must be linear and for equilibrium the following conditions must be satisfied:

(a) The resultant tension in the in-situ concrete must equal the resultant compression in the prestressed concrete (or vice versa).

(b) The resultant tension and compression cannot form a couple as there is no external bending moment. They must therefore act in the same line. The mutual force between the concretes due to differential shrinkage therefore acts as an eccentric load on each section, the respective eccentricities being e_1 and e_2.

From (a)

$$\sigma_1 E_1 A_1 = \sigma_2 E_2 A_2 \quad \ldots\ldots (1)$$

From the strain diagrams and eccentric force we have

$$\sigma' E_1 = \frac{\sigma_1 E_1 A_1 e e_1}{I_1}$$

$$\therefore \quad \sigma' = \frac{\sigma_1 A_1 e e_1}{I_1}$$

$$\text{Also } \sigma' E_2 = \frac{\sigma_1 E_1 A_1 e e_2}{I_2}$$

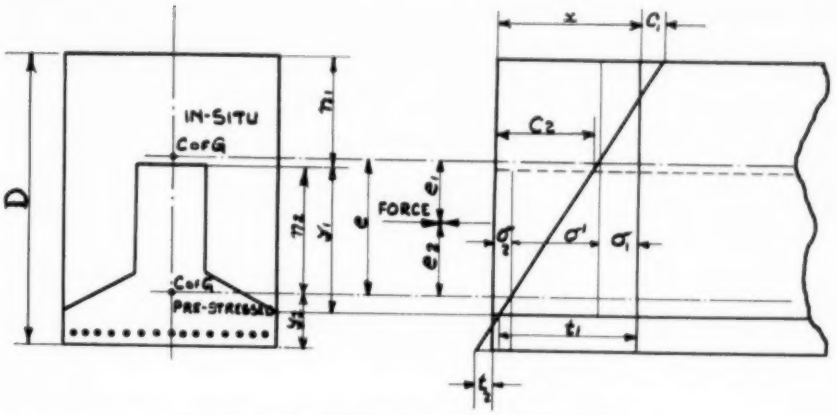

Fig. 6—Typical section for differential shrinkage theory

$$\therefore \quad \sigma' = \frac{\sigma_1 A_1 e e_2}{I_2} \frac{E_1}{E_2}$$

$$\therefore \frac{e_1}{e_2} = \frac{E_1 I_1}{E_2 I_2} \qquad (2)$$

$$\text{Now } \frac{\sigma_1 A_1 e e_1}{I_1} = \sigma' = x - (\sigma_1 + \sigma_2) \qquad (3)$$

$$\text{But } e_1 = e_2 \left(\frac{E_1 I_1}{E_2 I_2}\right) \text{ and } e = e_1 + e_2$$

$$\therefore e = e_2 \left(1 + \frac{E_1 I_1}{E_2 I_2}\right) = e_1 \left(1 + \frac{E_2 I_2}{E_1 I_1}\right)$$

$$\therefore e_1 = \frac{e}{1 + \dfrac{E_2 I_2}{E_1 I_1}}$$

$$\text{Also } \sigma_2 = \frac{\sigma_1 A_1 E_1}{A_2 E_2} \text{ from Eq. (1)}$$

Therefore, substituting in Eq. (3) we have

$$\frac{\sigma_1 A_1 e^2}{I_1 \left(1 + \dfrac{E_2 I_2}{E_1 I_1}\right)} = x - \sigma_1 \left(1 + \frac{A_1 E_1}{A_2 E_2}\right) \qquad (4)$$

By symmetry

$$\frac{\sigma_2 A_2 e^2}{I_2 \left(1 + \dfrac{E_1 I_1}{E_2 I_2}\right)} = x - \sigma_2 \left(1 + \frac{A_2 E_2}{A_1 E_1}\right) \qquad (5)$$

Thus if x is known these equations can be solved for σ_1, σ_2, and σ' and from the diagram the following stresses can be estimated:

(1) Compressive stress in top of in-situ $= E_1 C_1$

Where

$$\frac{c_1 + \sigma_1}{n_1} = \frac{\sigma'}{e} \text{ or } C_1 = \left(\frac{n_1 \sigma'}{e}\right) - \sigma_1$$

(2) Tensile stress in bottom of in-situ concrete

$$= E_1\left(\frac{y_1\sigma'}{e} + \sigma_1\right)$$

(3) Tensile stress in bottom of prestressed concrete

$$= E_2\left(\frac{y_2\sigma'}{e} - \sigma_2\right)$$

(4) Compressive stress in top of prestressed concrete

$$= E_2\left(\frac{n_2\sigma'}{e} + \sigma_2\right)$$

A negative coefficient reverses these stresses. Also if C_1 is negative and C_1E_1 is numerically greater than the modulus of rupture of the in-situ concrete then shrinkage cracks will occur at the top fibers of the beam and the stress distribution will be relieved.

The axes about which I_1 and I_2 are calculated must be perpendicular to the line joining the centroids of the two elements. If this condition is observed the theory holds for nonsymmetrical sections provided that n_1, n_2, y_1, and y_2 also conform to the correct axes.

Deflection due to differential shrinkage

Consider the effect of shortening of the upper fibers and lengthening of the lower fibers in Fig. 6.

$$\frac{R}{l(1 - x - C_1)} = \frac{R + D}{l(1 + t_2)}$$

$$\therefore R = D\frac{(1 - x - C_1)}{(t_2 + x - C_1)}$$

Central deflection $\delta = l^2/8R$ neglecting second order small quantities

$$= \frac{l^2(t_2 + x + C_1)}{8D(1 - x - C_1)}$$

A close approximation, because x and C_1 are small compared with unity, is

$$\delta = \frac{l^2(t_2 + x + C_1)}{8D}$$

A positive value for δ indicates that the beam is sagging.

BOND AND MONOLITHIC ACTION

The three groups of beams tested represent three distinct grades of roughness of the prestressed element. The surface of the Ministry of Works joists in group A was very smooth and the top parts of the Myko beams of group B were very rough. For this latter purpose two extra pre-tensioned wires were placed near the top of the beam and when the concrete had hardened these two wires were ripped out tearing an outer layer of concrete away and leaving a jagged rough surface. The surface of the group C prestressed elements was roughened by hand while the concrete was fresh and the result represented a mean between groups A and B.

The beams of group A showed considerable hysteresis and permanent set which might well have been due to bad bonding of the wires. Beam

No. 1 failed in bond but there was slight movement between the concretes during loading. When the load was removed the few wires, namely six, were unable to pull the section back into its original state. It is thought that this movement is too small to have broken down the actual bond. In studies of bond upon mild steel reinforcement it has been shown that an elastic bond may allow the steel to take up small movements relative to the concrete, to establish a bond stress distribution, without necessarily breaking down the adhesion of the concrete. It is thought that a similar phenomenon was present between the concretes of these beams, although in some relatively small areas near the soffit it is almost certain that adhesion had been broken. It must be borne in mind, however, that a good composite design does not use in-situ concrete at the lower fibers.

The group C beams showed greatly reduced hysteresis and permanent set over group A but slightly greater than group B. The microscopic observation of cracks showed conclusively, by the presence of minute longitudinal cracks, that the bond was actually broken at certain areas near the soffit.

Only the beams of group B appeared to give complete monolithic action. Here the roughness was at its greatest and in addition the in-situ concrete was confined almost entirely to the compression zone. Under the influence of repeated load and vibration, however, there would be a much greater tendency to failure by bond, and therefore the following suggestions for establishing the best possible bond are made. If these are carried out, complete monolithic action should be obtained and a linear strain distribution may be assumed. The suggestions are:

1. Roughness should be at least as great as the size of the largest aggregate.
2. The line of the joint in cross section should be as long as possible.
3. There should be as much jointing surface in a vertical plane as in the horizontal.
4. The roughness should preferably be made after the concrete has hardened.
5. The roughened surface should extend over the whole of the jointing planes.

STRAIN AND STRESS DISTRIBUTION

It follows that if the beam is bonded sufficiently to act monolithically then all the normal theories of strain and stress distribution apply. All the beams tested have shown approximately linear strain distributions and small deviations of groups A and C from pure monolithic behavior have already been discussed.

Deviations from the straight line in all cases have been of the order which would be expected in a normal reinforced or prestressed concrete beam. Particularly will it be applicable when the various bond precautions listed above are made.

DESIGN CONSIDERATIONS

Referring to Fig. 7, 8, 9, and 10 which show stress distribution for the three groups of beams using the classical theory, it is apparent that groups A and C are of poor design. In Fig. 7 the whole of the lower portion of the

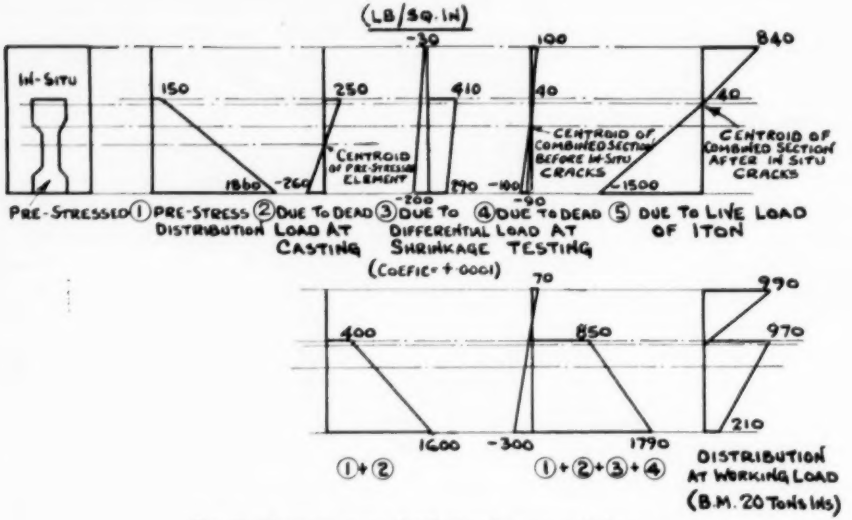
(LB/SQ.IN)
IN-SITU
PRE-STRESSED
CENTROID OF PRE-STRESSED ELEMENT
CENTROID OF COMBINED SECTION BEFORE IN-SITU CRACKS
CENTROID OF COMBINED SECTION AFTER IN-SITU CRACKS
① PRE-STRESS DISTRIBUTION
② DUE TO DEAD LOAD AT CASTING
③ DUE TO DIFFERENTIAL SHRINKAGE
④ DUE TO DEAD LOAD AT TESTING
⑤ DUE TO LIVE LOAD OF 1TON
(COEFIC=+·0001)
① + ②
① + ② + ③ + ④
DISTRIBUTION AT WORKING LOAD
(B.M. 20 TONS INS)

Fig. 7—Concrete stress distribution for group A beams

in-situ concrete has been wasted at working load. The distribution across the prestressed member is quite good but much better capacity could have been obtained by giving a greater compressive prestress at the bottom fibers. One or two wires placed at the top are quite sufficient to prevent rupture due to prestress during handling. Fig. 8 and 9 do not show an ideal design, but there has been great improvement by giving a greater compressive prestress. The resulting tensile prestress at the upper fibers is clearly no dis-

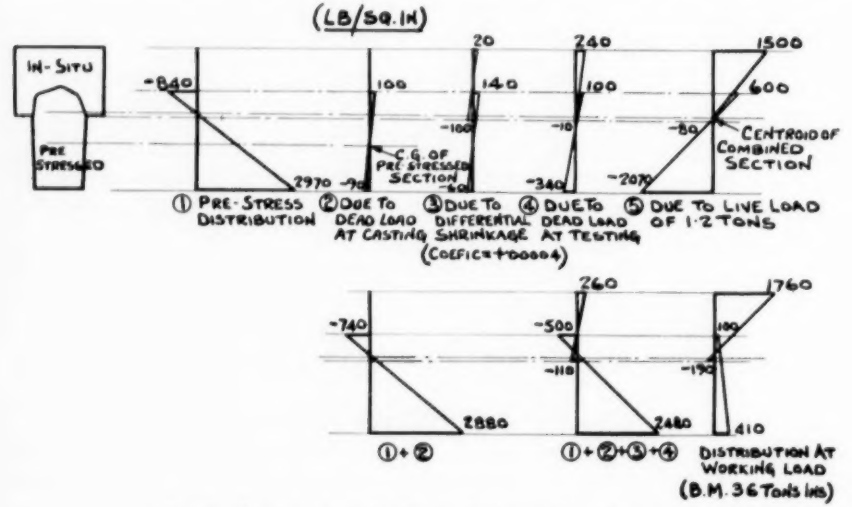
(LB/SQ.IN)
IN-SITU
PRE STRESSED
C.G. OF PRE-STRESSED SECTION
CENTROID OF COMBINED SECTION
① PRE-STRESS DISTRIBUTION
② DUE TO DEAD LOAD AT CASTING
③ DUE TO DIFFERENTIAL SHRINKAGE
④ DUE TO DEAD LOAD AT TESTING
⑤ DUE TO LIVE LOAD OF 1·2 TONS
(COEFIC=+0·0004)
① + ②
① + ② + ③ + ④
DISTRIBUTION AT WORKING LOAD
(B.M. 36 TONS INS)

Fig. 8—Concrete stress distribution for beam No. 4 (group B)

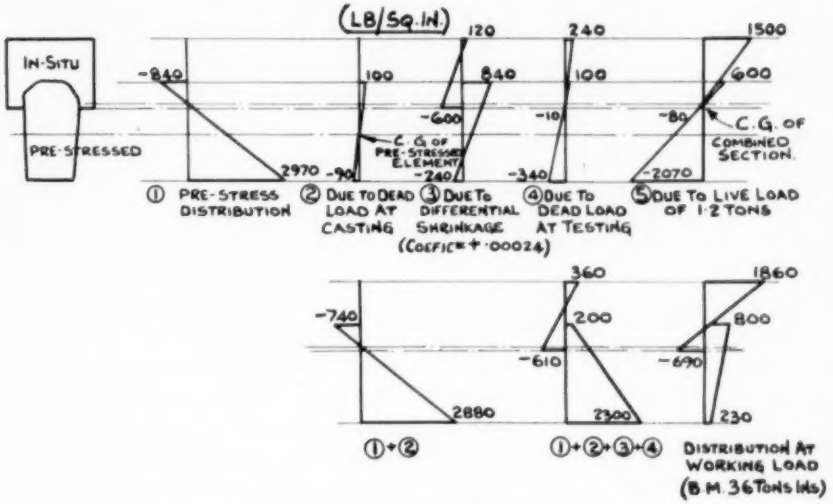

Fig. 9—Concrete stress distribution in beam No. 5 (group B)

advantage because even if it reaches a value of 1000 psi or more when cracks may be present, the combined dead load of prestressed and in-situ portions will close the cracks before any live load is applied. Improvement has also been made in these beams by leaving out the lower in-situ concrete. The working load has brought the strains in the prestressed section back to very low values and the in-situ concrete is taken to a reasonably high stress.

Fig. 10 shows again a waste of in-situ concrete and a complete waste of initial compressive stress in the upper fibers of the prestressed portion. This type of beam, as already stated, was not designed to have a good working

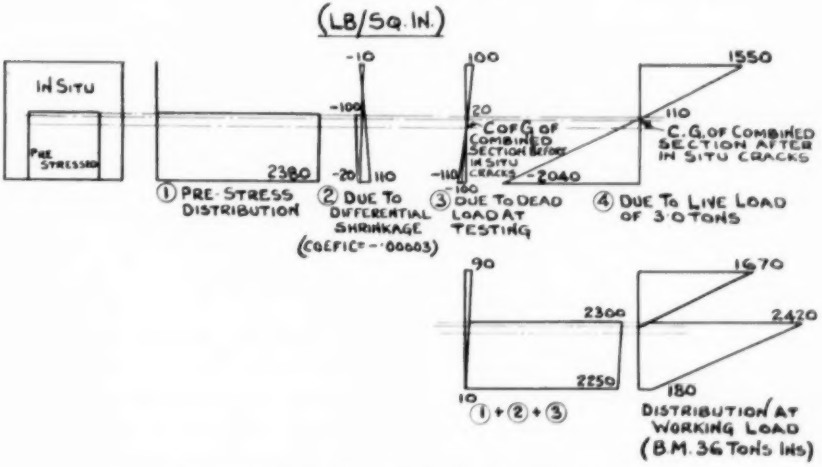

Fig. 10—Concrete stress distribution for group C beams

section, but it does serve to illustrate how prestress may be wasted by bad design. Neglecting for the time being the effect of differential shrinkage the following recommendations for composite design are made.

Assuming that the bond conditions already given are followed as far as possible, a good composite design is one in which at working load the stress in the prestressed section is as low as possible in tension, and that in the in-situ section as highly compressive as working stresses allow. Clearly, when in-situ topping is added to a prestressed section to form a composite member, the centroid of the section is raised, and after the concrete is set, all applied loads will give stresses about this new axis as long as no cracks occur. To achieve approximately zero stress in the prestressed concrete at working load, this new axis should, as nearly as possible, coincide with the axis of zero stress of the prestressed section. If the whole of the dead load is carried by the prestressed member, its neutral axis will rise from the initial value at stressing and unless the initial prestress is such that a reasonable tension is present at the upper fibers, the axis may easily move outside the prestressed section. This is undesirable since some of the lower in-situ concrete necessary for bonding will probably be cracked at cracking load and will have lost its bending resistance.

A study of Fig. 7, 8, 9, and 10 shows that group B beams are superior to those in group A or C in spite of the fact that the soffit of the in-situ concrete in group B beams is under tension at working loads. The distribution of stress in group B beams is better with a smaller volume of concrete. The final stress distribution in Fig. 9 indicates that it is advantageous to place the in-situ concrete as much as possible in the compression zone. In the case of a T-beam this will not be so important because only a small proportion of the in-situ concrete will be in the web. It is recommended therefore that a large eccentric prestress be given to the prestressed member and that, if possible, the relative sizes of in-situ and prestressed sections be such that excessive cracking of the in-situ concrete is avoided. It is, of course, impossible to make conditions for all types of composite construction as the possibilities are too numerous. For instance, the Stahlton floor type of construction employs planks which are given an approximately uniform prestress. The in-situ topping then raises the centroid well above the planks and, at working load, cracks which must form in the lower portion of the in-situ concrete are protected by the planks.

DIFFERENTIAL SHRINKAGE

The stress diagrams in Fig. 7, 8, 9, and 10, and the differential shrinkage coefficients and cracking loads in Tables 2 and 3 show that the effect of this differential shrinkage may vary from a negligible to an appreciable amount. It has also been demonstrated that the sign of the coefficient x may be either positive or negative. There are in fact four extreme cases which will serve to simplify the possibilities arising from this variable factor. In all cases it

TABLE 2—ESTIMATED DIFFERENTIAL SHRINKAGE COEFFICIENTS

Test No.	Time between prestressed cast and in-situ cast, days	Time between in-situ cast and test, days	Prestress at C. of G. of prestressed section, psi	Estimated strains between date of in-situ cast and date of testing			Differential shrinkage coefficient, x
				Creep of prestressed concrete	Shrinkage of prestressed concrete	Shrinkage of in-situ concrete	
1	21	21	1000	0.00011	0.0001	0.00024	+0.00003
2	41	21	1000	0.00005	0.00009	0.00024	+0.0001
3	28	25	1160	0.00011	0.00012	0.00026	+0.00003
3A	28	29	1160	0.00012	0.00013	0.00028	+0.00003
4	32	28	1160	0.00011	0.00013	0.00028	+0.00004
4A	32	32	1160	0.00012	0.00014	0.0003	+0.00004
5	140	27	1160	0.00002	0.00002	0.00028	+0.00024
6	24	25	2865	0.00016	0.00012	0.00026	−0.00002
7	24	32	2865	0.00018	0.00015	0.0003	−0.00003
8	38	25	2865	0.0001	0.00012	0.00025	+0.00004

will be assumed that the prestressed concrete is of a rich quality, such as a 1:1:2 or 1:1½:3 mix.

The four possible extreme cases are:

1. If the in-situ concrete is cast soon after the concrete that is prestressed and is of a similar quality, the resulting differential shrinkage coefficient after a fairly long time will probably be small because the initial shrinkage of the prestressed concrete before casting the in-situ will be approximately compensated by creep under prestress.

2. With the same conditions as in (1) but with a weaker mix for the in-situ, say 1:2:4, the coefficient will be negative and of the order of 0.0001, because the weaker concrete mix will shrink less.

3. If the in-situ concrete is cast a long time after the prestressed concrete then almost the whole of the in-situ shrinkage will be effective and if a rich mix is used the coefficient may reach a value of the order of 0.0004 after some time.

4. As in case (3) but with a weaker mix for the in-situ, the figure will be lower, probably about 0.0002.

These examples are an over-simplification but they do show the limits to which differential shrinkage can be effective, and with careful varying of dates of casting and quality of mix it is possible either to approximate a coefficient of zero or else to achieve a stress distribution which may be made use of in design. In most cases it will be desirable to cause the bottom fibers of the prestressed member to gain in compression. It will be found that, for a normal design where most of the in-situ concrete is in the compression zone, this will be achieved by a negative differential shrinkage coefficient, and for this the in-situ mix should be weaker than that of the prestressed

TABLE 3—ACTUAL AND THEORETICAL CRACKING LOADS

Test No.	In-situ			Prestressed		
	Actual cracking load, tons	Theoretical, neglecting differential shrinkage, tons	Theoretical, including differential shrinkage, tons	Actual cracking load, tons	Theoretical, neglecting differential shrinkage, tons	Theoretical, including differential shrinkage, tons
1	0.5	0.595	0.52	1.4	1.3	1.36
2	0.4	0.93	0.61	1.7	1.5	1.69
3	——	——	——	2.8	2.97	2.90
3A	——	——	——	3.4	3.34	3.3
4	——	——	——	1.7	1.92	1.84
4A	——	——	——	4.8	5.05	4.9
5	——	——	——	1.6	1.9	1.67
6	1.7	1.48	1.64	4.5	4.45	4.43
7	1.8	1.48	1.71	4.4	4.45	4.41
8	1.3	1.72	1.41	4.7	4.62	4.67

element and should be cast as soon as possible. From the point of view of bond, the tests have shown that there is no need to take any steps to ensure that the concretes are of the same type or mix. It is more economical to use a fairly weak mix for the in-situ topping. If this is to be used as a wearing surface the stresses can be kept low by building up a high modulus of section or deeper beam and the possibility of shrinkage causing a loss of compression in the prestressed member is minimized.

This applies mainly to cases where dead load is low compared with live load. In cases of the opposite type, such as long span bridges, it may be a disadvantage to build up a heavy section and in-situ concrete of a quality similar to the prestressed may be necessary.

CONCLUSIONS

1. Good bond between prestressed and in-situ concretes can be obtained if the jointing surface is sufficiently roughened. It is thought that complete monolithic action will be exhibited by a beam bonded in this way. That is, the "bond length" of the prestressed member may be considered negligible. Bond may be assisted by leaving stirrups protruding from the prestressed concrete, but this is only necessary when the jointing surface is not sufficiently rough in itself, and in that case the bond may still fail in between the stirrups.

If the surface of the prestressed member is left smooth then the nature of the bond appears to be like that of concrete to steel, except that beams bonded in this way tend to exhibit undue hysteresis and permanent set.

2. Composite construction does not affect the extensibility of either prestressed or in-situ concrete.

The action of the prestressed member upon the in-situ concrete is that of restraint after cracking. Cracks in the in-situ concrete of a composite beam open more slowly than those in either reinforced concrete or normal prestressed beams.

The effect of cracks in the in-situ concrete upon the prestressed member is to cause stress concentrations which may cause early cracking at the edge of the prestressed member. Both these effects can be eliminated if the whole of the in-situ concrete is placed in the compressive zone at cracking load.

3. The differential shrinkage between the two elements may affect cracking loads either to advantage or adversely and the magnitude of the effect may be as much as 20 percent in normal design.

4. The relative qualities of concrete in a composite design do not affect bond. If the relative strengths are taken into consideration in the normal way, then the only additional effect peculiar to this type of construction is that of differential shrinkage.

5. Any of the plastic theories of failure may be applied to composite beams in the same way as they are applied to normal prestressed beams.

Title No. 51-44

Ball Test for Field Control of Concrete Consistency*

By J. W. KELLY and MILOS POLIVKA†

SYNOPSIS

A simple field test is described for determining the consistency of fresh concrete in terms of the penetration of a 6-in. 30-lb ball. Experiences of users are given, and comparisons with slump are made. Considerations in the practical use of the ball are discussed.

INTRODUCTION

The penetration principle for gaging the placeability of fresh concrete has long been applied in the form of drawing a shovel heavily across the surface, and in the early days by observing the depth to which workmen sank in the mass. The ball-penetration test described here makes use of a constant gravity force to displace a volume of concrete in a manner comparable to construction operations. It is in wide and growing use as a simple means of uniform control of consistency.

Briefly, the apparatus (Fig. 1) consists of a 30-lb weight with a 6-in. hemispherical tip, equipped with a sliding reference stirrup and a handle graduated in inches. The test is made by lowering the "ball" gently onto a leveled-off surface of concrete and observing its depth of penetration with respect to the stirrup, which rests on the surface. The concrete may be in a container, hopper, wheelbarrow, cart, or form, so long as the depth is at least 6 in. and the least horizontal dimension 12 in. It is recommended that the "eyeball" average of three tests, to the nearest 0.1 in., be taken as the value of penetration. Details are given in the appendix.

DEVELOPMENT

The test was developed in the Engineering Materials Laboratory of the University of California at Berkeley as an outgrowth of an attempt to devise a simple test for *workability* of concrete. Workability is an elusive property, and early trials with various balls showed little correlation with the more elaborate tests in laboratory use. However, it was observed that static ball penetration correlated rather well with slump and it became apparent that the penetration test measured some property similar to slump — a property which had been termed "consistency" but which is now called

*Presented at the ACI Seventh Regional Meeting, Los Angeles, Calif., Oct. 28, 1954. Title No. 51-44 is a part of copyrighted JOURNAL OF THE AMERICAN CONCRETE INSTITUTE, V. 26, No. 9, May 1955, *Proceedings* V. 51. Separate prints are available at 35 cents each. Discussion (copies in triplicate) should reach the Institute not later than Sept. 1, 1955. Address 18263 W. McNichols Rd., Detroit 19, Mich.

†Members American Concrete Institute, Professor and Assistant Professor of Civil Engineering, respectively, University of California, Berkeley, Calif.

Fig. 1—Penetration of the 6-in. 30-lb "ball" into fresh concrete is read on the graduated riser rod at the top edge of the sliding stirrup which rests on the surface of the concrete

merely "slump" in ASTM C 143. It is the significant property which is measurable in the field for practical purposes.

A 6-in. ball was considered to be the smallest that would integrate the resistance to penetration over several pieces of aggregate, and a 30-lb weight was found to be the lightest that would penetrate reproducibly the stiffest mixes of plastic concrete. This combination of area (or displaced volume) and force has been found applicable even to harsh concrete containing 2½-in. aggregate and having a nominal slump when wet-screened of 1½ in. The apparatus has also been used on mass concrete containing 0 to 6-in. crushed aggregate by making the penetration test only on areas which had been found by probing to be free from the larger pieces of aggregate. A 20-lb weight on a 6-in. ball has sometimes been used for lightweight concrete.

Penetration tests have been developed independently in other countries. A static test used in Spain employs a weight on a spherical tip and having a flared edge so that the plunger will not sink too deep into wet concretes. The German Committee on Reinforced Concrete has adopted an impact test suitable for stiff mixes or mixes of low cement content; it consists in dropping a 33-lb plunger having a 4-in. hemispherical tip 8 in. onto the surface. In England, the Wigmore consistometer employs a metal ball set on the surface of a concrete sample which is vibrated on a table.

The authors are engaged in investigations to develop a dynamic form of penetration test which it is hoped will measure workability and will be suitable for laboratory use. One handicap for laboratory purposes is that relatively large batches of concrete are required—at least 70 lb—whereas 35 lb is sufficient for the slump test or the Powers remolding test. However, the principle is believed to be sound and is essentially that employed in the remolding test and the English and German tests. Herein the discussion is confined to the static ball test for field use.

FIELD USE

The static ball test was introduced to field use by E. L. Howard, testing engineer, Pacific Coast Aggregates, Inc., San Francisco. His experience with the variety of mixes used in ready-mixed concrete was so successful that it encouraged the authors to report the test to ASTM Committee C9 at its

San Francisco meeting in 1949.[1] Mr. Howard has continued to contribute to its field development, and is convinced that it will eventually replace the slump test[2,3] (see Fig. 2).

Many other organizations have adopted the ball test, and hundreds of balls are in use throughout the country. The California Division of Highways has adopted it as a standard for field use on pavement construction (Fig. 3). At least two other state highway departments—North Carolina and Colorado[4]—are using it extensively (see Fig. 4). The Waterways Experiment Station, Concrete Division, U. S. Army Corps of Engineers, has adopted it as an alternative standard CRD-C 46-53. There are four known manufacturers of the apparatus.

Fig. 2—Ball-penetration test for plant control of lightweight concrete for building job in San Francisco

COMPARISON WITH SLUMP

Since the ball test is essentially an alternative or supplement to the slump test, two questions are pertinent: (1) What are the relationships between measured slumps and penetrations? (2) Assuming that both tests are satisfactory, what are the advantages and disadvantages of each?

One factor in the selection of the 6-in. 30-lb ball size was that, roughly, twice the penetration was equal to the slump; and this relation is often used for rough mental comparisons or conversions. However, it has been observed that the ratio of penetration to slump, though fairly constant under a given set of mix conditions, varies somewhat with conditions (Fig. 5 and 6); and it is recommended that any

Fig. 3—Standard field test employed by California Division of Highways

Fig. 4—Comparison of slump and ball tests by Colorado State Highway Department

relationship, when desired, be established by comparative tests on the particular type of concrete.

Precise correlation is not to be expected, in view of the variability of the slump test itself. To illustrate this variability, in an extensive series of tests on truck mixers conducted by the National Ready Mixed Concrete Assn.,[5] hundreds of slump tests and ball tests were made on the same batches. The over-all average ratio of slump to penetration was 1.66. A striking fact was that, for some 250 pairs of slump tests on the same test *samples* (not merely batches), the average discrepancy between duplicate slumps was ½ in., even though the tests were carefully made by experienced technicians. Variation in *single* ball tests was about ¼ in., which is of the same order of magnitude, but in practice ball-penetration uses an average of three readings.

In another extensive series of comparative tests by the Concrete Division, Waterways Experiment Station, U. S. Army Corps of Engineers, Jackson, Miss., slumps were measured to ¼ in. and penetrations to ⅛ in. The average ratio of slump to penetration was found to be 1.79 for the range of slump covered—2.0 to 3.5 in. If this value of 1.79 were taken as a conversion factor for predicting the slumps from the penetrations, 63 percent of the slumps

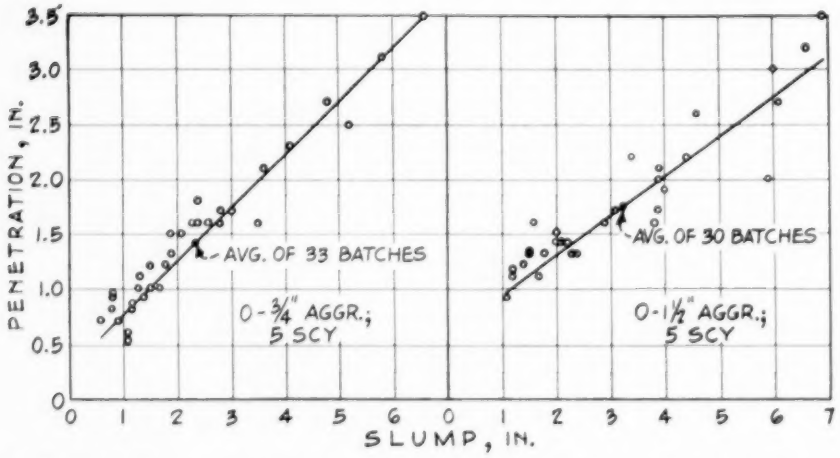

Fig. 5—Penetration varies consistently with slump under given conditions, but the ratio is not necessarily constant. (Laboratory tests by authors)

could have been predicted correctly within ¼ in. and 87 percent within ½ in.

In the field, discrepancies between slump and penetration can only be evaluated by the practical tests of visual observation and actual placing. Mr. Howard[3] has found that the ball is sensitive to changes in consistency not always detected by the slump test, particularly for lightweight concretes.

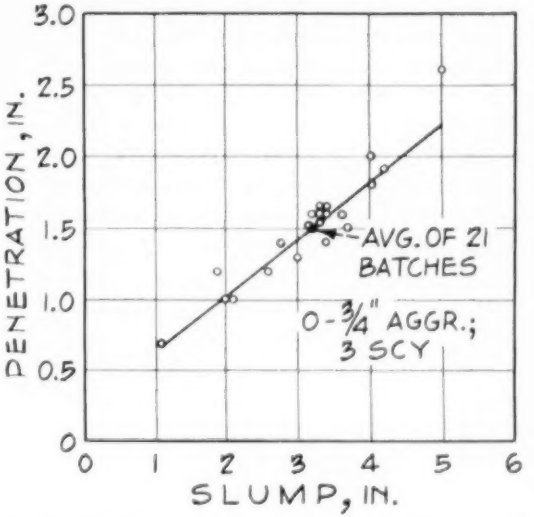

Fig. 6—Relation between penetration and slump for lean air-entrained concrete containing pozzolanic admixture. (Laboratory tests by authors)

Justification for the ball test lies not so much in precision, which is perhaps somewhat higher than that of the slump test, as in the advantages of speed, less likelihood of personal error, and adaptability to use on undisturbed samples of concrete in the handling devices and the forms. A ball test requires seconds to perform whereas a slump test requires minutes; thus it is reasonable to expect that more ball tests will be made and closer control will be secured.

The slump test is subject to personal differences in sampling, rigidity and smoothness of base, dampening the apparatus, filling the cone, rodding, raising the cone, freedom from jarring, and selection of point to which the slump is measured. The principal possible source of error in the ball test—the rate of releasing the ball—can be quickly detected in case of dispute if the opposing observer also makes the test, lowering the ball gently as recommended. With reasonable care in observing, error in reading the scale to the desired precision (0.1 in.) is negligible.

It is often desirable to test the concrete en route to or in the forms. With the ball, tests can be made at the mixer, in the receiving hopper, in wheelbarrows or carts, and in the forms; thus segregation and/or stiffening can be traced. Quoting Mr. Howard,[3] "The Kelly ball seems to be the best to find the troublesome spots where segregation occurs . . . by variation in consistency measurements." On a pavement job in the state of Washington, premature stiffening was traced by ball-testing the concrete at intervals during and after the finishing operations, whereas use of the slump test would have required "disturbed" samples in which the stiffening would be lost.

PROCEDURE OF TEST

Detailed instructions for making the ball test are given in the appendix. Some explanatory comments follow.

Apparatus

The essential features are a 30-lb weight on a 6-in. hemispherical surface and means for measuring the penetration. The feet of the stirrup are at least 9 in. apart to avoid any "bulge" of concrete around the ball. The zero reading can be checked quickly on any flat rigid surface and can be adjusted if necessary. The apparatus is not patented and can be made in any machine shop, but would probably be cheaper and more satisfactory if obtained commercially. It is easily cleaned. A wood carrying case is recommended for transportation in automobiles.

Sample

The ball needs plenty of depth in which to operate to avoid riding on piled-up stones beneath. The clearance under the ball after penetration should be at least twice the maximum size of aggregate; greater clearance is desirable. Side clearance should be great enough to avoid restriction of the displaced concrete. The surface should be struck off level, but not overworked. During the test, the concrete must be kept free from jarring, which would tend to work the ball down.

Procedure

The ball is lowered gradually onto the concrete, and the penetration is read immediately on the graduated handle. Readings to 0.1 in. (by estimation) are recommended, although readings to $\frac{1}{4}$ in. are probably precise enough for field control purposes and are equivalent to slump observations to $\frac{1}{2}$ in. Mental averaging of three tests and discarding of obviously bad values is recommended to avoid the effect of local soft or hard spots not representative of the general run. If the stirrup feet settle through a surface layer of mortar, it is evident that the ball would penetrate an equal distance before meeting resistance, hence no correction is made. In an extremely wet mix any stirrup settlement beyond the thickness of a normal surface layer should be compensated by common-sense adjustment. For concrete containing aggregate of maximum size larger than $2\frac{1}{2}$ in., the ball should be placed on a portion free from pieces larger than $2\frac{1}{2}$ in. as determined by probing.

APPLICATIONS

At its present stage of development, the ball test is considered useful for controlling a given concrete mix on a job to the consistency established as desirable by those in authority, that consistency being expressed either in the customary terms of slump or by penetration readings from actual batches which have been pronounced satisfactory. For a slump-conscious industry, penetration is not now recommended as a basis for general specifications; eventually it may be.

One valuable result of the field use of the ball test to date has been a definite tendency toward closer control and toward the avoidance of the extremely wet mixes which are one of the industry's greatest headaches. Slump tests are often "estimated;" ball tests are actually made. When the ball sinks

into concrete, that concrete is just too wet even for heavily reinforced thin members or for house foundations.

ACKNOWLEDGMENTS

In the early stages of development, tests were made in the Engineering Materials Laboratory of the University of California by Gordon F. Lammiman and Clifford A. Misener, senior students in civil engineering. Subsequently, Norman E. Haavik and George R. Hayler, engineers on the laboratory staff, participated in laboratory development. E. L. Howard and his associates in Pacific Coast Aggregates, Inc., were instrumental in field development. Many others have contributed helpful experiences and suggestions.

REFERENCES

1. Kelly, J. W., and Haavik, Norman E., "A Simple Field Test for Consistency of Concrete," *ASTM Bulletin*, No. 163, Jan. 1950, pp. 70-74 (discussion: No. 169, Oct. 1950, pp. 50-51).

2. Howard, E. L., and Leavitt, George, "Kelly Ball vs. Slump Cone—Comparative Tests of Samples Taken at Travis Air Base," ACI JOURNAL, Dec. 1951, *Proc.* V. 48, pp. 353-356.

3. Howard, E. L., "Is the Slump Cone on Its Way Out?" *Western Construction*, V. 28, No. 7, July 1953, pp. 81-82.

4. Haynes, Ben F., "Using the Kelly Ball to Test Concrete," *Western Construction*, V. 29, No. 6, June 1954, pp. 77-78.

5. Walker, Stanton, and Bloem, D. L., "Tests of Concrete Truck Mixers," *Publication* No. 50, National Ready Mixed Concrete Assn., Jan. 1954, 35 pp.

APPENDIX—INSTRUCTIONS FOR BALL TEST FOR PENETRATION OF FRESH CONCRETE

Scope

This method of test covers a procedure to be used both in the laboratory and in the field for determining consistency of portland cement concrete.

Apparatus

(a) The ball-penetration apparatus shall consist essentially of a 30-lb weight which can be applied on a hemispherical surface 6 in. in diameter, a graduated handle, and a sliding stirrup which serves as a reference to measure the depth of penetration. The dimensions and arrangement of the apparatus, if made of steel, shall be as shown in Fig. 7.

Note—Other metals or forms may be used, provided the basic requirement of a 30-lb weight on a 6-in. hemispherical surface is maintained.

(b) Each foot of the stirrup shall be approximately 1½ in. square, and the clear distance between the feet shall be 9 in.

(c) The top edge of the stirrup shall read zero on the graduated handle when the apparatus is set on a flat solid surface.

Sample

(a) The concrete may be tested either in a container (such as a can, hopper, or wheelbarrow) or in place in the forms. The minimum depth shall be such that the clearance under the ball after penetration is at least twice the maximum size of aggregate, but in no case shall the depth of concrete be less than 6 in. The minimum horizontal dimension of the concrete under test shall be 12 in., except that concrete tested in place may have a minimum dimension, in one direction only, of 8 in.

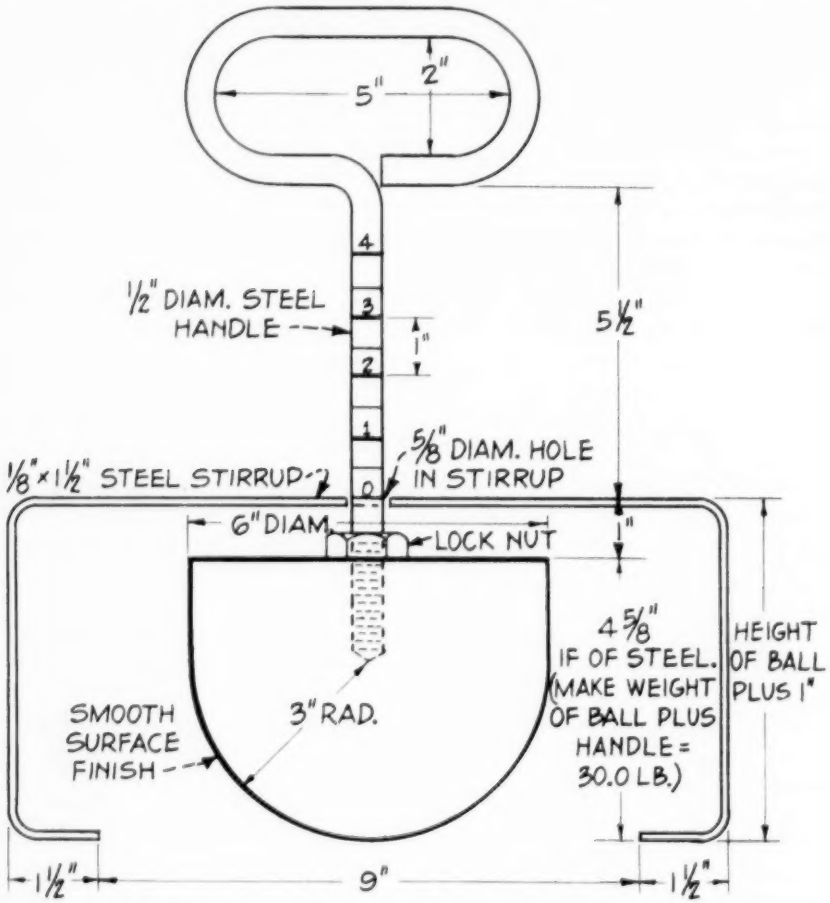

Fig. 7—Details of simple form of ball-penetration apparatus. (All dimensions are approximate except 3-in. radius of ball and ½-in. graduations on handle)

(b) The surface of the concrete shall be smooth and level. Working of the surface shall be a minimum to avoid the formation of a relatively soft layer.

(c) During the test, the concrete shall be kept free from agitation or jarring.

Procedure

The ball shall be set carefully on the concrete, with the handle erect and with the stirrup resting on the concrete and being free to slide on the handle. The penetration shall be read immediately, on the graduated handle, to the nearest 0.1 in. by estimation. Readings shall be taken at three locations, and a representative value chosen.

Note 1—If one reading differs markedly from the others, it shall be discarded and another reading taken.

Note 2—No correction shall be applied for any slight settlement of the stirrup feet, as such settlement automatically corrects for the existence of a similar soft surface layer at the ball.

The consistency shall be recorded in terms of inches of subsidence of the ball with respect to the stirrup, which shall be known as the penetration.

Title No. 51-45

Strength of Reinforced Concrete T-Beams Under Combined Direct Shear and Torsion*

By EARL I. BROWN, II†

SYNOPSIS

Tests on longitudinally reinforced concrete sections without web reinforcement are reported. The strength of reinforced concrete T-beams in combined direct shear and torsion are compared to the strength of similar sections in direct shear alone. Theoretical torsion strengths, based upon a plastic theory, are in fair agreement with experimental results at first diagonal cracking but are on the safe side.

INTRODUCTION

Several commonly used textbooks give typical examples illustrating design of reinforced concrete sections subjected to combined direct shear and torsion. The term direct shear, as used here, refers to the beam shear that is commonly considered in reinforced concrete design. Torsion produces an additional shear that acts on the same planes. The textbook calculations are based upon the elastic distribution of stresses. Such an analysis of existing spandrel or marginal beams often indicates that torsion stresses, when calculated by the elastic method, increase the total diagonal tension to several times that calculated from direct shear alone. Since torsion stresses are often completely omitted in design, this raises the question of why there are not more recorded failures of marginal beams attributed to diagonal tension.

This paper reports a study of the combined effect of direct shear and torsion on the strength of reinforced concrete T-beams without web reinforcing. The strength under this combination of loading is compared to the strength of a similar section in direct shear alone.

TEST SPECIMENS

Twenty-six small size beams without web reinforcing were tested. Although diagonal tension strength may be a function of beam size, combined strength is here compared as a relative value to strength in direct shear alone, and it is assumed that size affects each case similarly. Cylinder strength and modulus of rupture serve, as usual, as a check of the relative strength of the concrete used.

*Presented at the ACI 51st annual convention, Milwaukee, Wis., Feb. 23, 1955. Title No. 51-45 is a part of copyrighted JOURNAL OF THE AMERICAN CONCRETE INSTITUTE, V. 26, No. 9, May 1955, *Proceedings* V. 51. Separate prints are available at 50 cents each. **Discussion** (copies in **triplicate**) should reach the Institute not later than Sept. 1, 1955. Address 18263 W. McNichols Rd., Detroit 19, Mich.

†Member American Concrete Institute, Head, Professor, Department of Civil Engineering, Alabama Polytechnic Institute, Auburn, Ala.

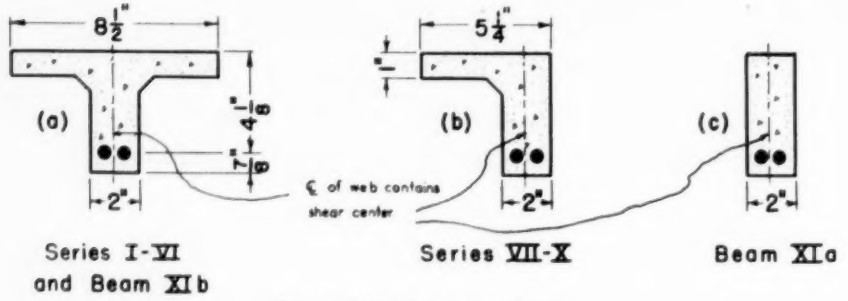

Fig. 1—Sections of test specimens

For a particular cross section, the only intended variable was the eccentricity of loading. During each test, deflection and rotation were measured, and each test was completed to failure.

Each test group was composed of two beams, three or four compression cylinders, and two modulus of rupture beams cast at the same time. One beam from each test group was loaded eccentrically about the shear center and the companion beam was loaded concentrically. The shear center of any section was assumed to be contained in the longitudinal plane of the vertical centerlines of the web. Eight groups with symmetrical T-sections, four with unsymmetrical T- or L-sections, and one with a rectangular section were tested. Fig. 1 and 2 show diagrams of the test beams. Fillets were all ½ in.

The concrete was made with Type III (high-early) portland cement and with a maximum size aggregate of ¼ in. The W/C ratio was 7.7 gal. per sack and the average slump, ⅞ in. It was vibrated into place. Specimens were kept damp in their forms for 18 hr, then removed and placed in a moist room for 48 hr. They were then placed in the laboratory to air dry until tested at 8 days. Cylinder and modulus of rupture beams were cured in the same way.

The longitudinal steel in all test specimens was two #4 bars having yield point stress of approximately 60,000 psi. Anchor plates were welded to the ends of the reinforcing bars to forestall the possibility of slippage as well as to act as a spacer to locate the reinforcing bars properly in the forms.

The test specimens were cast with three diaphragms or stiffeners, at the ends and the center of the beam. These were to distribute the torsion over the entire cross section and to provide adequate end supports. Typical stiffeners are shown in the loading diagram, Fig. 2, and in Fig. 3.

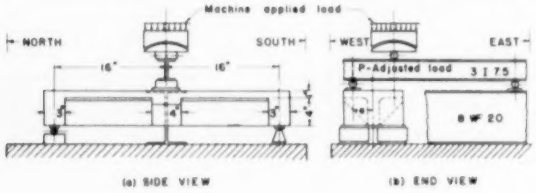

Fig. 2—Loading arrangement

TESTING APPARATUS

Beam specimens were tested to failure in a hydraulic testing machine with a loading table 30 in. square (Fig. 3). It was necessary to place the beams diagonally across the table with little latitude for adjustment of the beam under the loading head. The longitudinal axis of the beam was always placed parallel to the north-south diagonal of the loading table. The center of the beam span was always on the east-west diagonal. A lever system was adopted to place the load at a variable eccentricity from the web of the test specimen. Eccentric loads were applied at a point to the west of the web, and failure behavior is described in terms of the east and west face of the web.

No standard increments of load were used in the tests. An attempt was made to apply loads in increments such as to obtain an approximate average time of 30 min for loading from zero to failure. Beams were frequently examined for cracks, and deflection readings were taken after each increment of load was applied.

Six deflection gage reference points on the test beam consisted of six small metal squares set in plaster of paris. Two points were located at each end over the supports, on a line drawn normal to the axis of the beam. The other two points were located on a line normal to the axis of the beam and 2 in. from the centerline of the beam span. The location of these deflection reference points varied in distance from the longitudinal axis because of various arrangements necessary for locating the lever system to apply the eccentric loads. For more detailed information see reference 7.

A frame for mounting dial gages was rigged after the specimen was in testing position. Ames 0.0001-in. dial gages with 0.3-in. range were mounted

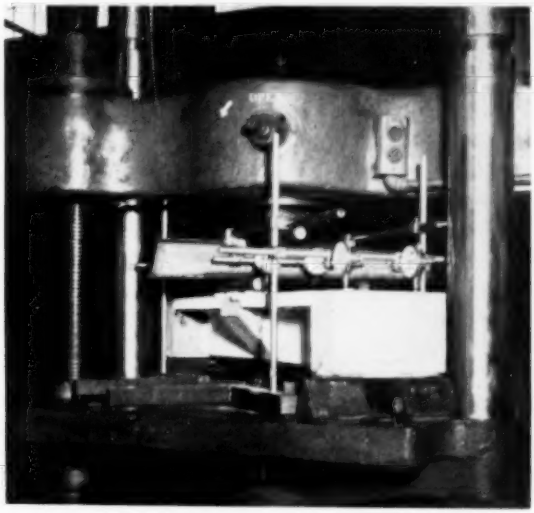

Fig. 3—Beam IIIa in testing machine

at the six deflection reference points. Dial gages and frame may be seen in position in Fig. 3.

Plain concrete 6 x 12-in. cylinders were tested to determine the compressive strength of the concrete. They were vibrated in their forms, and were tested air dry. Curing conditions were the same as those for the test beams and the modulus of rupture beams. The average cylinder strength was 4335 psi ± 25 percent.

Modulus of rupture test beams were standard 6 x 6 x 36 in. The length permitted each beam to be subjected to two fracture tests in an 18-in. simple span, third-point loading type beam tester. The average modulus of rupture was 477 psi ± 13 percent.

FAILURE BEHAVIOR

Every test group included a companion beam, *i.e.*, a beam that was loaded with the load line of action in the vertical longitudinal plane of the web center ($e = 0$). In all but test group I, the other beam of the test group was loaded in combined direct shear and torsion by applying the load eccentrically or outside this plane.

Both beams of test group I were tested in direct shear alone to compare the action of the small beams to that of a series of larger beams of similar sections.[1] The deflection characteristics and failure behavior of the small beams were found to be similar to those of the larger beams, but the ultimate strength was found to be approximately ⅓ higher.

All companion beams ($e = 0$) failed by diagonal cracks which crossed the neutral axis about halfway between the load and the reaction. Small diagonal cracks would first appear and then, with increase in load, one would suddenly increase in width and length. T-beams IIIb, IIId, and IVd ruptured at one end of the beam only. T-beams IIb, Vb, VIb, and XIb and L-beams VIIb, VIIIb, and Xb seriously cracked at one end, took further load, and finally ruptured at the other end. Diagonal tension strength of all these beams was calculated from the ultimate load applied. T-beams Ia, Ib, and IVb and L-beam IXb cracked at both ends and then seemed to act as a tied arch. For these four beams, the load applied when the second large crack appeared was taken as that measuring the diagonal tension strength (column 5, Table 1).

Eccentrically loaded test beams never regained ultimate load capacity after one diagonal crack penetrated the web, but the beginning of failure was somewhat similar to that of the concentrically loaded companion beams. Diagonal cracks opened across the neutral axis about halfway between the center and the end stiffeners. Cracks always appeared first on the west face of the web. This was expected as the diagonal tension stresses resulting from direct shear and from torsion were additive on that face.

Failure cracks were steeper on the west face of the web than on the east face. Cracks on both faces of the web ran diagonally upward toward the center stiffener in all beams except Va and VIa. These two T-beams experienced final failure similar to that of other beams, but the cracks appearing

(a) East face of web

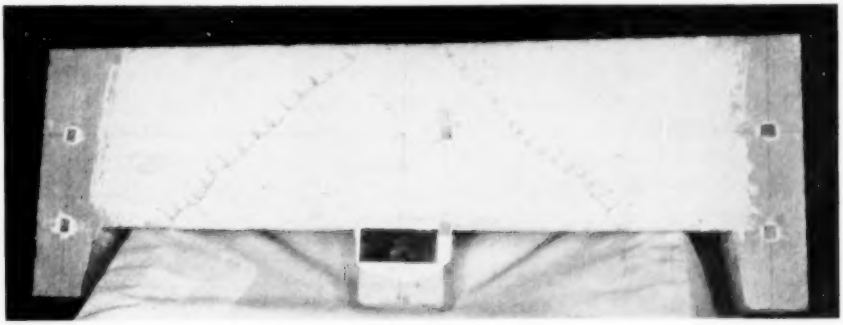

(b) Top of flange

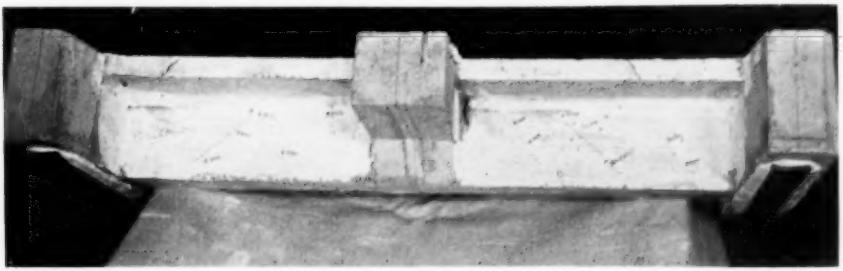

(c) West face of beam

Fig. 4—Failure pattern, T-beam Va

first on the east face of the web ran diagonally upward from the lower portion of the web near the center of the beam to upper regions of the web toward the ends (Fig. 4). This failure pattern is that which would be expected in the case of pure torsion.

It was expected that tensile bending stresses below the neutral axis would affect the slope of this failure plane, but it can be seen in Fig. 4a that the slope of these cracks in beam Va changes little over their entire length. This was also observed to be the case in beam VIa.

TABLE 1—RESULTS OF TORSION AND DIRECT SHEAR TESTS

Beam	e, in.	f_c', psi	Mod. of rupture, psi	Selected strength, V', lb	First diagonal crack		Maximum	
					Shear, lb	Torque, in.-lb	Shear, lb	Torque, in.-lb
1	2	3	4	5	6	7	8	9
Tee								
Ia	0	4260	477	2280*	1900	0	2740	0
Ib	0	4260	477	2270*	1900	0	2615	0
IIa	1.5	4960	515		1630	2400	2080	3080
IIb	0	4960	515	2425	1830	0	2425	0
IIIa	2.5	4650	487		1190	2900	1970	4850
IIIb	0	4650	487	2340	1845	0	2340	0
IIIc	2.5	3780	460		1155	2812	1848	4546
IIId	0	3780	460	2030†	1630	0	1900	0
IVa	3.75	3310	420		712	2560	1139	4161
IVb	0	3310	420	1955*	1830	0	2505	0
IVc	3.75	5320	501		822	2972	1450	5372
IVd	0	5320	501	2395	2030	0	2395	0
Va	5.00	4170	475		730	3500	1110	5400
Vb	0	4170	475	2240	1830	0	2240	0
VIa	6.25	4290	479		590	3500	948	5740
VIb	0	4290	479	2330	2030	0	2330	0
Ell								
VIIa	1.5	5180	539		1280	1875	1955	2887
VIIb	0	5180	539	2405	2080	0	2405	0
VIIIa	3.0	3720	460		880	2550	1127	3290
VIIIb	0	3720	460	2165	1957	0	2165	0
IXa	5.0	3710	430		630	3000	820	3950
IXb	0	3710	430	2044*	1915	0	2390	0
Xa	7.0	5310	535		480	3150	680	4550
Xb	0	5310	535	2390	2055	0	2390	0
Rectangular								
XIa	2.5	3690	448		830	2000	1190	2900
Tee								
XIb	0	3690	448	2030	1930	0	2030	0

*Beams appeared to arch and went higher as noted in column 8 (See discussion under Failure Behavior).
†Because of apparent weakness of beam IIId, diagonal tension strength of this group taken as that of beam XIb.
Note: $V' = (P + 60)/2$, where 60 lb = weight of beam considered for shear.
$T = Pe/2$ (P not shown in table).

TEST RESULTS

Test results are given in Table 1. The cylinder strength and modulus of rupture shown for each test group are average values. The unit shear stress v of the companion beam is used as a measure of the ultimate tensile strength (column 3, Table 3) of each test group where

$$v = \frac{V'}{b'jd}$$

V' = shear strength of companion beam ($e = 0$), including a portion of the weight of the beam (column 5, Table 1), *i.e.*,

$$V' = (P + 60)/2$$

$j = \frac{7}{8}$

Torque, as given in Table 1, is one-half the product of the load applied to the test specimen times the eccentricity, *i.e.*, $Pe/2$.

Beams IIId and XIb showed air pockets in the surface. T-beam IIId, in particular, contained very poor concrete in the web. The result of the direct shear test on beam IIId indicated an exceptional weakness and the result is rejected as not being a true indication of the diagonal tension strength of that test group. The diagonal tension strength of that group is assumed to

be that of T-beam XIb because of the close similarity of the cylinder strength and modulus of rupture of the two groups.

Earlier investigators with plain concrete sections found that torsion failure was sudden and often without warning; they also found torsion moment at first crack was maximum for plain sections. The load-deflection curves (Fig. 5) and the torque-rotation curves (Fig. 6) of the eccentrically loaded test beams show a tendency to creep after cracks have been observed. These tests are of relatively short time loading and it is believed that the creep would be greatly accentuated under long time loading. After cracking has occurred, present theoretical analyses of torsion are not applicable. For these reasons, in the tests on eccentrically loaded beams the load applied when the first diagonal cracks appeared is considered as the critical load. The surface of the specimens and the load-deflection characteristics were carefully watched to detect diagonal cracks as they appeared.

All beams loaded in combined shear and torsion carried a maximum load much larger than the cracking load, or critical load as defined above. The average maximum load was 150 percent of the average load causing diagonal cracks. This strength is unaccounted for by present theoretical analyses.

It is acknowledged that an extremely conservative assumption is made when it is assumed that the usable strength is limited by the appearance of diagonal cracks, but there are so many "unknown" factors involved that the assumption seems to be warranted. Further discussion of strength greater than cracking loads is included under "Maximum Strength of Test Beams," p. 898.

CONCRETE AS A PLASTIC MATERIAL

Prevailing practice in the design of reinforced concrete structures in the United States is based upon the maximum stress criterion of failure. It is generally assumed that reinforced concrete acts elastically, but an exception is made in the design of columns where plastic behavior is acknowledged.

The theory of elasticity is highly idealized in its basic concepts. The classical theory of plasticity is also highly idealized. To apply the theory to a given material, the following assumptions are made of that material:

1. It does not exhibit work hardening, but flows plastically under constant stress.
2. For sufficiently small values of strain, the material behaves elastically, but once the stress reaches a critical value, the material flows plastically under that stress.

In the case of the theory of plastic torsion, it is also assumed that all elements of a cross section have been stressed to a critical stress value.

A review of the study of torsion reveals that a material must be assumed in most cases to be either in the elastic state or in the plastic state to obtain a mathematical solution of its torsion characteristics. To apply theory to experimental data, one or the other conditions must be assumed.

Turner and Davies[2] and also Marshall and Tembe[3] considered the possibility of a partially elastic, partially plastic behavior of plain concrete, but their method of solution involved an empirical variation to the torsion strength calculated elastically.

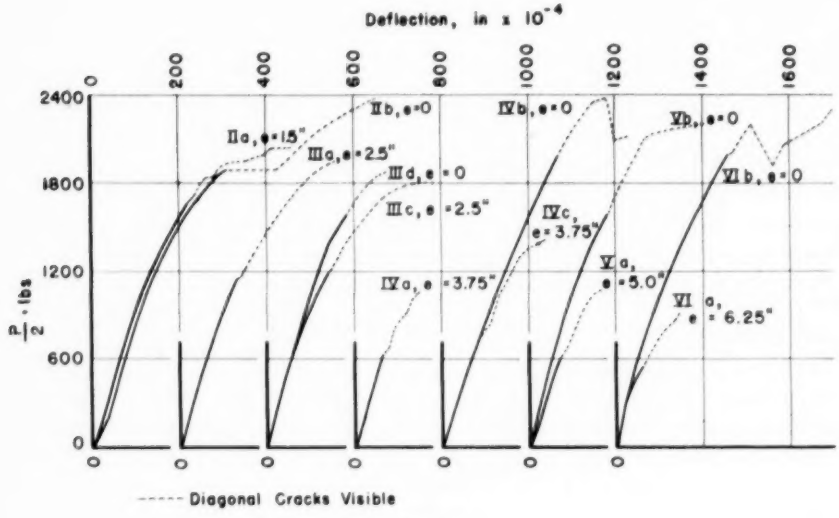

(a) T-sections

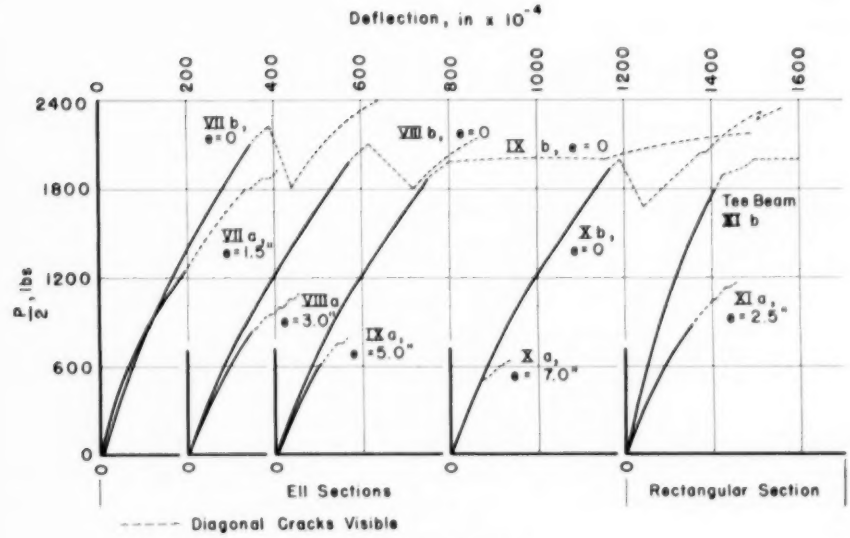

(b) L- and rectangular sections

Fig. 5—Load-deflection ratio

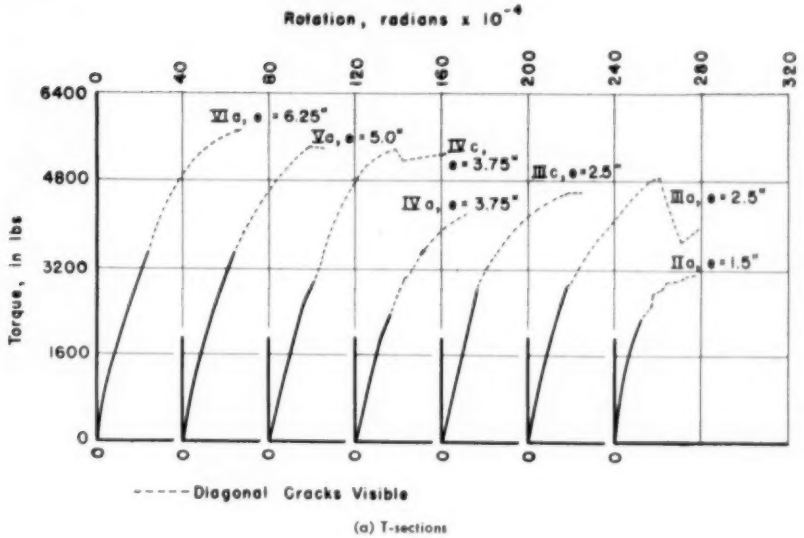

(a) T-sections

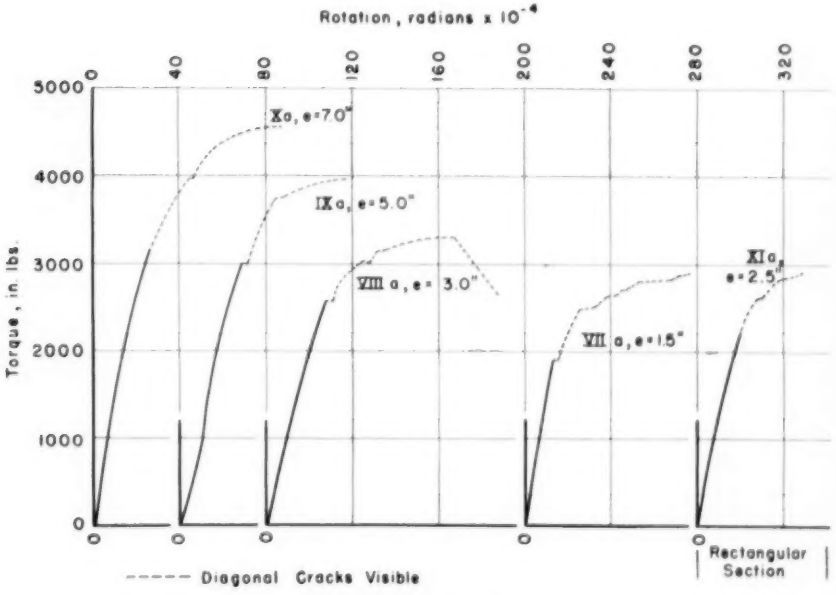

(b) L- and rectangular sections

Fig. 6—Torque-rotation ratio

TABLE 2—RATIO OF ELASTIC TO PLASTIC TORSIONAL SHEAR STRESSES

SHAPE					
CALC. ELASTIC SHEAR* / CALC. PLASTIC SHEAR*	1.3	1.6	1.7	1.8	1.9

*SHEAR STRESS CALCULATED FOR SAME TORQUE IN EACH CASE

Marshall[4] later showed that agreement between the results of a wide range of experiments involving concrete in torsion could be obtained if the concrete was treated as a plastic material. Nylander[5] and Cowan and Armstrong[6] later confirmed this by experiment.

The plastic behavior of concrete explains some increase in the strength of a specimen over that calculated elastically, but the amount depends upon the limit of the plastic behavior and upon the shape of the cross section. Assuming the same material is used in all cases, it is not valid to determine by experiment the ratio of increased strength for one particular section and then assume this ratio to apply to all sections. The ratio varies according to the shape of the cross section (Table 2). The T- and L-section illustrated in Table 2 are the sections used in these tests.

COMBINED STRESS

Nylander's[5] report is in Swedish but there is a summary in English, and many subtitles and explanations of diagrams and tables are in English. One section of his report deals with combined direct shear and torsion on longitudinally reinforced rectangular sections. The English summary does not say what condition was assumed to be critical but loads indicated as failure loads give close agreement with the present tests at first diagonal cracks, here assumed to be critical. Nylander's results and the results of these tests are given in Table 3. Direct shear has been calculated by V/bjd and torsional shear has been calculated by the equations of plastic action in torsion (Table 4). The torsional rigidity constants have been derived from the "sand-heap analogy."[8]

The test results show that the diagonal tension strength at cracking loads of the test beams in torsion (assuming plastic action in torsion of the reinforced concrete) is greater than the ultimate diagonal tension strength in direct shear, but generally there is good agreement between the theory and the test results (Fig. 7).

MAXIMUM STRENGTH OF TEST BEAMS

The average ultimate load of the eccentrically loaded beams is calculated to be 150 percent of the average cracking load, but the average deflection at ultimate load is 215 percent of the average deflection at cracking load; also the average rotation at ultimate load is 316 percent the average rotation at cracking load (Fig. 8).

TABLE 3—CALCULATED UNIT SHEAR STRESSES
(Torsion stresses based upon plastic assumptions)

Beam	e, in.	Ultimate tensile strength psi	At first diagonal crack		Calculated unit shear stresses at first diagonal crack			Ratio of Col. 8/Col. 3, percent
			Shear, lb	Torque, in.-lb	Direct, psi	Torsion, psi	Combined, psi	
1	2	3†	4	5	6	7	8	9
Tee								
IIa	1.5	335	1630	2400	225	180	405	121
IIIa	2.5	323	1190	2900	164	218	382	118
IIIc	2.5	280	1155	2812	159	211	370	132
IVa	3.75	270	712	2616	99	196	295	109
IVc	3.75	331	822	2972	113	224	337	102
Va	5.0	309	730	3500	101	263	364	118
VIa	6.25	322	590	3500	81	263	344	107
Ell								
VIIa	1.5	332	1280	1875	176	171	347	104
VIIIa	3.0	299	880	2550	121	232	353	118
IXa	5.0	282	630	3000	87	273	360	127
Xa	7.0	330	480	3150	66	287	353	107
Rectangular								
XIa	2.5	280	830	2000	115	230	345	123
Nylander*	0	273	6500	0	273	0	273	100
Nylander*	1.48	273	4500	6600	189	143	332	122
Nylander*	3.8	273	2650	10100	111	219	330	121
Nylander*	6.1	273	2180	13200	91	283	374	137
Nylander*	7.9	273	1680	13200	70	283	353	129
Nylander*	∞	273	0	15200	0	330	330	121

*Beam size = 3.74 x 7.87 in., shear and torque not definitely known to be that at first diagonal crack.
†Ultimate tensile strength assumed to be V'/bjd (V' from column 5, Table 1, for test beams, and from shear of beam loaded at $e = 0$ for Nylander's beams).

TABLE 4—TORSIONAL SHEAR STRESSES ASSUMING PLASTIC ACTION

Unit Shear Stress = $\frac{\text{Torque}}{\text{Torsional Rigidity Constant}}$

Section	Torsional Rigidity Constant
	$\frac{\pi D^3}{12}$
	$\frac{b^2}{2}\left(h - \frac{b}{3}\right)$
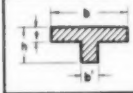	$\frac{t^2}{2}\left(b - \frac{t}{3}\right) + \frac{(b')^2}{2}\left(h - t - \frac{b'}{3}\right) + \frac{(b')^4}{2.5}\frac{t}{(b')^2 + (t)^2}$
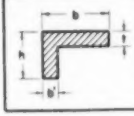	$\frac{t^2}{2}\left(b - \frac{t}{3}\right) + \frac{(b')^2}{2}\left(h - t - \frac{b'}{3}\right) + \frac{(b')^4}{2.5}\frac{t}{(b')^2 + (t)^2}$

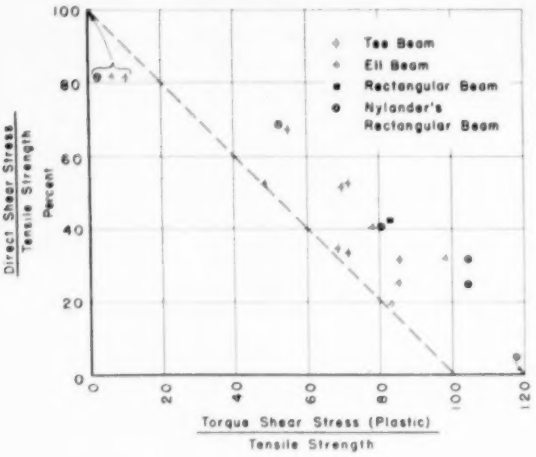

Fig. 7—Ratio of critical stress in combined torsion and direct shear to tensile strength

If the apparent strength in combined direct shear and torsion loading that these test beams show beyond the diagonal cracking condition is to be utilized in design of marginal beams, close study must be given to the effect that this condition of rotation and deflection exerts upon the relative stiffness of the beam and slab.

Theoretically, neither the plastic nor the elastic method is permissible for calculating diagonal stresses after diagonal cracking has occurred. The maximum stress theory of failure for concrete seems to offer no explanation for the 50 percent average increase in strength that the eccentrically loaded test beam showed after cracking occurred. Certainly a considerable redistribution of stress takes place after cracking occurs. The additional strength may be developed by the ability of the compression flange to absorb a larger proportion of the total torque than theoretical calculations indicate. Nylander[5] found that small bending moments exert a favorable effect on the torsional strength of beams longitudinally reinforced.

A study of the results shown in Fig. 6 reveals that for torques causing diagonal cracks in beams of identical cross section and span there is a decrease in deflection and an increase in rotation with larger eccentricities. Likewise, at maximum torques, beams of identical cross section and span show a decrease in deflection as the eccentricity is increased. In contrast, the rotation at maximum torque seems to reach an approximately constant limiting value regardless of the value of eccentricity.

Beam IIa, with a small eccentricity of 1.5 in., shows a smaller rotation at maximum torque than do the other T-beams. This probably does not indicate a change in pattern other than that its ultimate failure was due to deflection rather than to rotation.

This points to the fact that the maximum loading of a reinforced concrete beam in combined direct shear and torsion may be limited by an angular

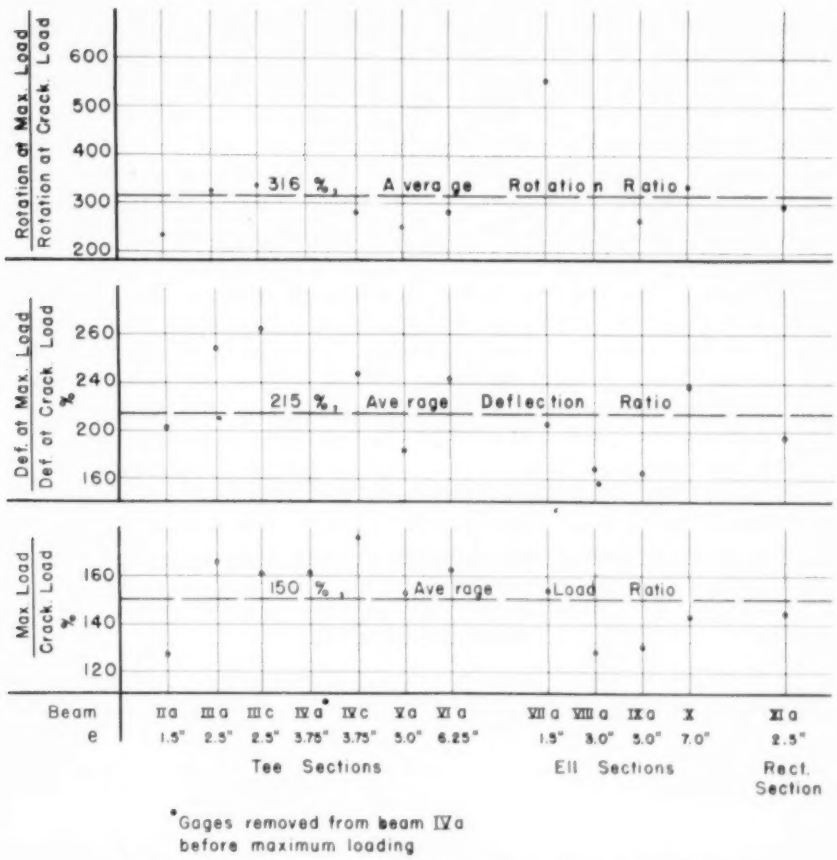

Fig. 8—Ratio of maximum load conditions to cracking load conditions

rotation if the eccentricity of loading is greater than some limiting minimum value. The limiting rotation seems to be dependent upon the cross section rather than the amount of eccentricity.

A great deal more study is needed to explain fully the phenomenon of reinforced concrete after cracking has resulted from this combination of loading.

CONCLUDING REMARKS

There is no conclusive proof that reinforced concrete in combined direct shear and torsion follows a particular criterion of failure. The generally accepted practice in design is to assume the maximum stress criterion, and this has been accepted for a study of various sections of longitudinally reinforced concrete in combined direct shear and torsion.

The ultimate load of the beam loaded in direct shear alone was assumed to be a measure of the ultimate tensile strength of the concrete in each test

group. Cracking loads of the beams in combined direct shear and torsion were accepted as critical loads because of the characteristics of plain concrete in torsion and because of strain characteristics of the test specimens. Nevertheless, combined loads and torques causing diagonal cracks were found to be only some 66 percent of the ultimate loads under combined direct shear and torsion.

Calculated combined stresses at first diagonal cracks when torsion calculation was based on elastic assumptions were found to average 160 percent of ultimate tensile strength. When torsion was based on plastic assumptions, these stresses were found to average 116 percent of ultimate tensile strength. Calculated combined stresses at ultimate loads were similarly 240 and 173 percent of the ultimate tensile strength. Presumably these percentages decrease for small eccentricities since the eccentric load capacity would logically never exceed the concentric load capacity.

The deflection, rotation, and strength characteristics of these test specimens indicate that maximum strength may be limited by a maximum rotation rather than by a maximum stress when torsion is of an important magnitude.

The plastic theory gives more reasonable results in predicting the cracking strength under torsion or combined direct shear and torsion for concrete members than does the more generally used elastic theory.

ACKNOWLEDGMENT

This paper is based upon a thesis by Earl I. Brown, II, submitted in partial fulfillment of the requirements for the degree Doctor of Philosophy in Civil Engineering in the Graduate School of the University of Texas, 1953. The investigations for this thesis were carried out under the guidance of Prof. Phil M. Ferguson.

BIBLIOGRAPHY

1. Ferguson, P. M., and Thompson, J. N., "Diagonal Tension in T-Beams Without Stirrups," ACI JOURNAL, Mar. 1953, *Proc.* V. 49, pp. 665-676.

2. Turner, L., and Davies, V. C., "Plain and Reinforced Concrete in Torsion, with Particular Reference to Reinforced-Concrete Beams," *Selected Engineering Paper* No. 165, Institution of Civil Engineers (England), 1934.

3. Marshall, W. T., and Tembe, N. R., "Experiments on Plain and Reinforced Concrete in Torsion," *The Structural Engineer* (London), Nov. 1941.

4. Marshall, W. T., "Torsional Resistance of Plastic Materials with Special Reference to Concrete," *Concrete and Constructional Engineering* (London), V. 24, No. 4, Apr. 1944.

5. Nylander, H., *Torsion and Torsional Restraint of Concrete Structures* (An English summary is available), Statens Komitte for Byggnadsforskning, No. 3, Stockholm, 1945.

6. Cowan, H. J., and Armstrong, A., "Reinforced Concrete in Combined Bending and Torsion," *Fourth Congress Preliminary Publication* C11, International Assn. for Bridge and Structural Engineering, 1952.

7. Brown, E. I., "Strength of Reinforced Concrete T-Beams Under Combined Direct Shear and Torsion," Unpublished thesis submitted to the University of Texas for the Degree of Doctor of Philosophy, 1953.

8. Prager, W., and Hodge, P. G., *Theory of Perfectly Plastic Solids*, John Wiley & Sons, Inc., New York, N. Y., Section 9, Chapter 3.

Title No. 51-46

Air Entrainment in Cement and Silica Pastes*

By G. M. BRUERE†

SYNOPSIS

The air-entraining capacities of a number of surface-active agents in cement and silica pastes were measured by a standard test procedure. In addition, measurements were made of the foaming properties of surface-active agent solutions with and without electrolyte additions, and of the abilities of surface-active agents to make cement and silica particles hydrophobic by adsorption so that air bubbles adhere to them. These sets of data were used to demonstrate the conditions governing the formation of stable, air-entrained pastes containing surface-active agents, and the mechanisms by which air bubbles are introduced into and retained in pastes.

INTRODUCTION

The literature on air entrainment is concerned largely with its practical aspects, such as measurement and control of air contents, properties and large scale uses of air-entrained and foamed concretes. There is little information describing the mechanism of formation and retention of air bubbles in concrete and cement pastes containing surface-active agents.

Rehbinder and others[1] investigated the physico-chemical principles involved in the manufacture of foamed concrete using soaps of naphthenic and rosin acids, and saponin-glue mixtures as air-entraining agents. They showed that the viscosity of bubble films and mineralization of foam were important factors in stabilizing entrained air bubbles. However, a general mechanism of air entrainment cannot be deduced from these studies because only a limited number of surface-active agents were studied. Scripture and others[2-5] studied the practical factors affecting the amount of air entrained in concrete containing surface-active additions. They showed that the amount of entrained air depended on (1) brand of cement, (2) surface area of cement, (3) cement factor, (4) size grading of sand, (5) sand–total aggregate ratio, (6) slump, (7) size of batch, (8) mixing time, and (9) temperature. Others have tacitly assumed that the ability of surface-active agents to entrain air depends on the foaming power of the agent in solution.

This paper describes measurements of (a) the air-entraining capacities of a number of relatively pure surface-active agents in cement and silica pastes, (b) the foam stabilities and capacities of surface-active agent solutions with

*Received by the Institute June 28, 1954. Title No. 51-46 is a part of copyrighted JOURNAL OF THE AMERICAN CONCRETE INSTITUTE, V. 26, No. 9, May 1955, *Proceedings* V. 51. Separate prints are available at 50 cents each. **Discussion** (copies in **triplicate**) should reach the Institute not later than Sept. 1, 1955. Address 18263 W. McNichols Rd., Detroit 19, Mich.

†Research Officer, Division of Industrial Chemistry, Commonwealth Scientific and Industrial Research Organization, Melbourne, Australia.

and without additions of electrolytes normally present in cement pastes, (c) the foam stabilities and capacities of filtrates from cement and silica pastes containing surface-active agents, and (d) the abilities of surface-active agents to make cement and silica particles hydrophobic so that air bubbles adhere to them. These four sets of data were used to demonstrate the mechanisms by which air bubbles are introduced into and retained in air-entrained pastes.

Although the results of this study apply only to pastes, they provide a basis for investigating the mechanism of air entrainment in concrete. Work is at present being undertaken in this laboratory to determine whether or not the mechanisms of formation and retention of air bubbles in mortars and concretes are similar to those in pastes.

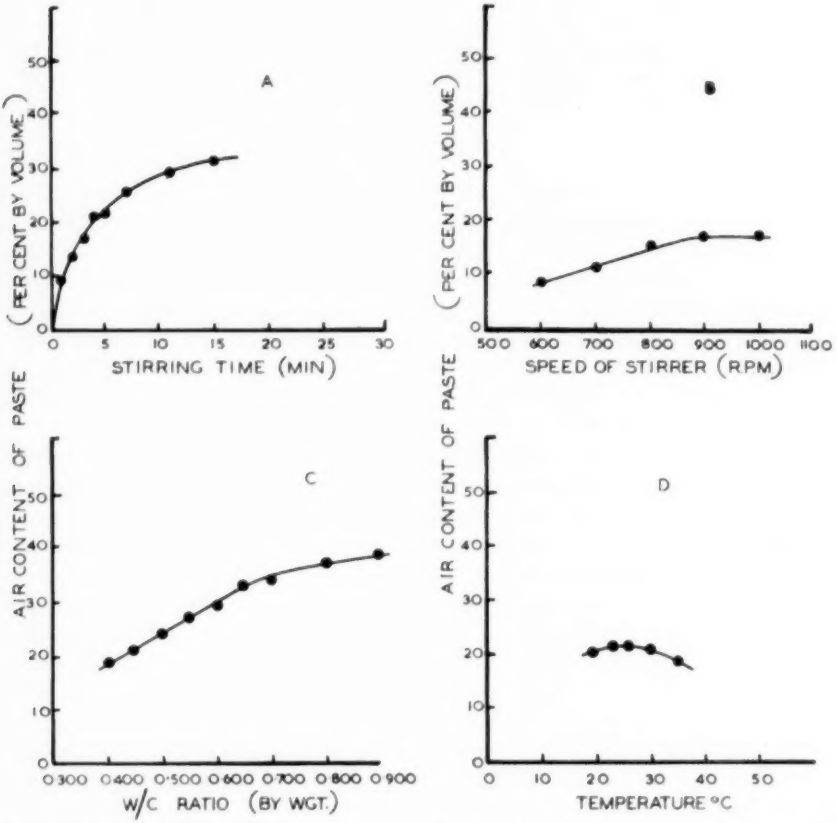

Fig. 1—Effect of various factors on air contents of cement pastes. Air-entraining agent: sodium dodecyl-sulfate, 0.0125 percent by weight of cement. Cement: No. 1

(A) Effect of stirring time on air content. Speed of stirrer 1000 rpm. W/C = 0.450 (by weight). Temperature 25 C
(B) Effect of speed of stirrer on air content. Stirring time 3 min. W/C = 0.450 (by weight). Temperature 25 C
(C) Effect of water-cement ratio on air content. Stirring time 4 min. Speed of stirrer 1000 rpm. Temperature 25 C
(D) Effect of temperature on air content. Stirring time 4 min. Speed of stirrer 1000 rpm. W/C = 0.450 (by weight)

MATERIALS

The surface-active agents studied may be classified conveniently into four groups according to their chemical structures as follows:

(a) Anionic agents: Sodium dodecyl-, tetradecyl-, and hexadecyl-sulfates, and sodium abietate

(b) Cationic agents: Tetradecyl- and hexadecyl-trimethyl-ammonium bromides, and decyl- and dodecyl-amine hydrochlorides

(c) Nonionic agents: "Triton NE"* which is nonionized polyalkylene ether alcohol, and "Lissapol N 300"† which is a long chain ether-linkage compound

(d) Miscellaneous agents: Terpineol, octyl alcohol, saponin, and gelatine

The anionic and cationic agents, terpineol, and octyl alcohol were at least 97 percent pure. The nonionic agents are difficult to obtain free from water. However, the commercial products used had a high percentage of surface-active material and the impurity was mainly water. One sample of each nonionic agent was used for all tests to ensure constant composition. Saponin and gelatine were pure laboratory reagents.

Commercial portland cements which had been stored in airtight containers were used to prepare cement pastes. Silica pastes were prepared from quartz sand which had been washed to remove traces of clay. The sand was ball milled for 12 hr, washed with acid to remove iron, washed with water to remove all traces of acid, and dried at 110 C. The sand used in the flotation tests was coarser than that used to prepare pastes.

The following solutions for the foaming studies were prepared from electrolytes normally present in cement pastes: sodium hydroxide, 10 g per l; calcium hydroxide, 1 g per l; anhydrous sodium sulfate, 10 g per l; anhydrous calcium sulfate, 1 g per l. The electrolytes used were of analytical reagent grade. A solution of all the electrolytes in a cement paste was prepared by vacuum filtering a 2:1 cement-water paste which had been stirred for 5 min at 25 C. A high-alkali cement (No. 1) was used. Some chemical details of which are shown in Table 2.

Distilled water was used in the preparation of solutions and pastes. Glassware which came into contact with surface-active agents was cleaned with hot dichromate cleaning mixture and rinsed with distilled water before use. Tests were done in duplicate at 25 C.

EXPERIMENTAL METHODS

Measurement of air contents of air-entrained pastes

Klein and Walker[6] described a pressure method for measuring air contents of freshly mixed concrete. Because of variations in the uniformity of concrete, ½-cu ft samples are used in this test. Since cement and silica pastes are more homogeneous than concretes, 250-cc samples were found to be adequate for air measurements. A small air meter was constructed to measure air contents of pastes. This apparatus was identical with that described by Klein and Walker,[6] except that the bowl of the air meter had a volume of 250 cc instead of ½ cu ft. The reproducibility of these measurements was good. The scatter rose from 2 percent of the mean at air contents below 10 percent to 5 percent of the mean at air contents of 30 percent.

Method of mixing pastes

For the comparison of air-entraining capacities of surface-active agents in cement and silica pastes, a mixing method was required which would both entrain reproducible amounts of air under standard conditions and entrain large volumes of air for small additions of surface-active agents so that differences between air-entraining capacities of different agents would be emphasized. The mixing method was established by investigating the factors controlling air contents of pastes. Cement pastes containing a fixed concentration of sodium dodecyl-sulfate were mixed with a three-bladed electric stirrer, and the following factors controlling

*"Triton NE" is a product of Rohm and Haas Co., Inc., Philadelphia, Pa.
†"Lissapol N 300" is a product of Imperial Chemical Industries of Australia and New Zealand.

TABLE 1—EFFECT ON AIR CONTENT OF VARYING THE SIZE OF CEMENT PARTICLES*

Particle size of clinker, B.S.S. mesh	Air content of paste, percent by volume
20–52	44.4
52–100	32.0
140–200	24.8
−200	21.0†

*Stirring time 4 min; speed of stirrer 1000 rpm; W/C = 0.450; temperature 25 C; cement clinker No. 1; air-entraining agent sodium dodecyl-sulfate, 0.0125 percent by weight of cement.

†This figure was obtained using ground clinker which contained gypsum as a retarder.

air contents were varied singly: (1) variation in stirring time, (2) variation in speed of stirrer, (3) variation in water-cement ratio, (4) variation in temperature, (5) variation in particle size, and (6) variation in batch of cement.

These results are illustrated in Fig. 1 and Tables 1 and 2 and show that the conditions of mixing should be rigidly controlled. Silica pastes containing tetradecyl-trimethyl-ammonium bromide were tested in the same way and the results showed variations closely similar to those in cement pastes.

Four different brands of cement were used in measuring the effect of different cement batches on air contents of cement pastes. The pertinent variations of these cements are shown in Table 2. There appears to be no direct correlation between air contents of the cement pastes and such factors as surface area, total alkali content, and gypsum content of the cements. However, the reason why pastes made from different cements entrain different amounts of air under standard conditions can be explained by a consideration of the amounts of water required to produce pastes of equivalent consistency. It was observed that, using equal W/C ratios, pastes made form cements No. 2 and 4 were more viscous than those made from cements No. 1 and 3. Cements No. 2 and 4 gave lower air contents than cements No. 1 and 3. However, when air-entrained pastes were produced from all four cements with the W/C ratios adjusted so that all had approximately equal consistencies, it was found that the air contents were approximately equal. To avoid these complications all the data involving cement pastes were obtained with cement No. 1.

The following mixing method was found to be suitable. The mixing water containing a surface-active agent was added to 400 g of cement or silica and the pastes were stirred by hand for 1 min to ensure homogeneity. Cement pastes were prepared with water-cement ratios of 0.450 by weight and silica pastes with water-silica ratios of 0.500 by weight. The pastes were stirred for 4 min with an electric stirrer fitted with a stroboscope, and whose power supply was controlled by a Variac. This enabled the stirring speed to be kept constant during mixing. The cement pastes were mixed at 1000 rpm and the silica pastes at 1200 rpm.

Method of measuring the effect of electrolytes on precipitation, form stability, and foam capacity of surface-active agents in solution

Each electrolyte solution was added separately in 25-ml portions to 100-ml stoppered, measuring cylinders. Then 25 ml of the particular surface-active agent solution being studied were added in turn to each cylinder. The presence of any precipitate was noted after 2 min had elapsed. Finally each cylinder was shaken vigorously by hand for 15 sec. The height of foam 30 sec after shaking, and the time for the foam to collapse were subsequently measured. The foam height is an approximate measure of the ease with which the solution can generate

TABLE 2—EFFECT ON AIR CONTENT OF VARYING THE BATCH OF CEMENT*

Cement batch No.	Surface area of cement, sq cm per g (air permeability)	Total alkali content of cement	SO_3 content of cement	Air content of paste, percent by volume
1	3300	1.09	1.99	14.7
2	3730	0.57	2.56	6.1
3	3480	0.12	1.85	11.0
4	3500	0.25	1.82	5.7

*Stirring time 4 min; speed of stirrer 1000 rpm; W/C = 0.450; temperature 25 C; air-entraining agent sodium dodecyl-sulfate, 0.007 percent by weight of cement.

bubbles and is termed the foam capacity of the solution. The time taken for the foam to collapse is taken as a measure of the foam stability. Surface-active agent solution concentrations were so chosen that when mixed with electrolyte solutions, they had concentrations within the range used in determining air-entraining capacities in pastes. The concentrations of the electrolyte solutions, when mixed with the surface-active agent solutions, were sufficient to ensure the presence of electrolyte in excess of that required for complete reaction with the surface-active agent.

Measurement of foam stability and capacity of filtrates from air-entrained pastes

Pastes containing surface-active agents at various concentrations were vacuum filtered, and the foam stabilities and capacities of the filtrates measured in the usual way. In addition, the foam stabilities and capacities of the mixing water were measured before it was incorporated in the pastes. Comparison of these two sets of data showed the effect of precipitation or adsorption of the surface-active agents on foam stabilities and capacities of the mixing water. Tests made to see if adsorption of surface-active agents on the filter paper affected foam stabilities and capacities of filtrates showed this effect to be very slight.

Measurement of the abilities of surface-active agents to make cement and silica particles hydrophobic so that air bubbles adhere to them

A cylinder flotation test described by Wark[7, p. 72] was used to determine whether bubbles contacted cement and silica particles in the presence of surface-active agents. In this test about 1 g of ground cement clinker (No. 1) or silica was added to a 50-ml stoppered cylinder containing about 30 ml of surface-active agent solution. The solid was allowed to condition for 2 min, then the cylinder was shaken by hand. When the clinker or silica was in a condition to contact air bubbles a large percentage of the mineral floated to the surface attached to bubbles. The cement clinker tests were conducted in the presence of 10 ml of filtrate from a cement paste to simulate the conditions in a cement paste, *e.g.*, pH and presence of electrolytes. Tests showed that different cement clinkers did not influence the results of the flotation tests. The size range of the clinker and silica particles tested was -150 $+200$ B.S.S. mesh. Although this test is only qualitative the results can be graded into three groups.

(1) Excellent bubble-solid contact as evidenced by flotation of 50–100 percent of the solid

(2) Definite bubble-solid contact where less than 50 percent of the solid floated, but many bubbles were in contact with the solid bed

(3) Zero bubble-solid contact where only a few, if any, bubbles were in contact with the bed and none of the solid floated

These tests were conducted in surface-active agent solutions where concentrations ranged from 0–1000 mg per l.

RESULTS

Air-entraining capacities

The air-entraining capacities of effective air-entraining agents in cement pastes are summarized in Fig. 2. Sodium hexadecyl-sulfate, decyl- and dodecyl-amine hydrochlorides, Triton NE, Lissapol N 300, terpineol, octyl alcohol, and gelatine entrained practically no air in cement pastes at all concentrations used. Fig. 3 shows the air-entraining capacities of effective air-entraining agents in silica pastes. Sodium abietate, sodium tetradecyl- and hexadecyl-sulfates, Triton NE, Lissapol N 300, terpineol, octyl alcohol, and gelatine failed to entrain any appreciable quantities of air in silica pastes at all concentrations used. The surface-active agents were studied at concentrations up to about 0.050 percent by weight of the cement or silica except where the agent was not soluble in the higher concentrations.

Fig. 2—Variations of air-entraining capacities of surface-active agents in cement pastes with varying concentrations of agents. Mixing conditions: stirring time 4 min; speed of stirrer 1000 rpm; W/C = 0.450 (by weight); temperature 25 C; cement No. 1

Surface-active agents:

(1) Sodium dodecyl-sulfate
(2) Sodium tetradecyl-sulfate
(3) Sodium abietate
(4) Tetradecyl-trimethyl-ammonium bromide
(5) Hexadecyl-trimethyl-ammonium bromide
(6) Saponin

The slopes of some of the curves in Fig. 2 and 3 tended to zero at high concentrations of surface-active agent indicating that the maximum air content was reached under standard mixing conditions. In mixing an air-entrained paste the rate of increase in air content diminished as the stirring time increased. At the same time it was observed that the vortex in the paste tended to disappear as air was entrained because the air + solid/water ratio increased the viscosity of the paste and decreased the efficiency of mixing. Thus, assuming sufficient air-entraining agent is present, the maximum amount of air that can be entrained under standard mixing conditions is controlled by the efficiency of the stirrer at high paste viscosity.

The air-entrained pastes generally showed little tendency to sediment, and the air was difficult to remove from them even when water was added and the pastes shaken. Such pastes are defined as stable in this paper. Some air-entrained pastes, particularly those with high water contents, readily segregated into three zones, a sediment of solid particles, a layer of

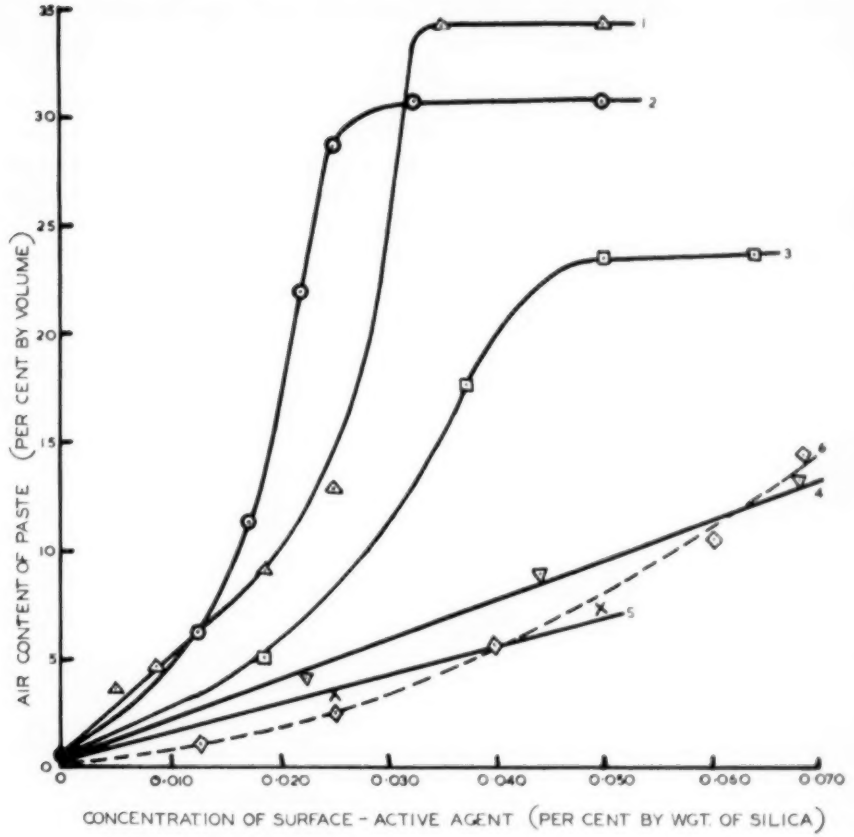

Fig. 3—Variations of air-entraining capacities of surface-active agents in silica pastes with varying concentrations of agents. Mixing conditions: stirring time 4 min; speed of stirrer 1200 rpm; W/S = 0.500 (by weight); temperature 25 C

Surface-active agents:

(1) Decyl-amine hydrochloride
(2) Dodecyl-amine hydrochloride
(3) Tetradecyl-trimethyl-ammonium bromide
(4) Hexadecyl-trimethyl-ammonium bromide
(5) Saponin
(6) Sodium dodecyl-sulfate

water, and a layer of foam mixed with fine solid particles. These pastes are defined as unstable.

The sizes of entrained bubbles were very small, the size range estimated from photographs of set cement pastes containing sodium dodecyl-sulfate being about 0.05–0.001 cm in diameter with the great preponderance of the bubbles in the 0.025 to 0.002-cm range.

Effect of electrolytes on precipitation, foam stability, and foam capacity in surface-active agent solutions

These data are contained in Tables, 3, 4, and 5. Precipitation of a surface-active agent by an electrolyte should reduce both the foam stability and

capacity, the reduction depending on the completeness of precipitation. Solutions of sodium tetradecyl- and hexadecyl-sulfates in the presence of calcium ions, and dodecyl-amine hydrochloride in the presence of sulfate ions follow this relationship. However, solutions of sodium dodecyl-sulfate and sodium abietate, although precipitated by calcium ions, retain their capacity for forming stable foams. This anomalous behavior has been explained by Bartsch,[8] who showed that hydrophobic particles could stabilize a foam. When solutions of sodium dodecyl-sulfate and sodium abietate containing calcium ions were filtered, both the foam stabilities and capacities

TABLE 3—EFFECT OF ELECTROLYTES ON PRECIPITATION OF SURFACE-ACTIVE AGENTS AT 25 C

Surface-active agent	Concentration of surface-active agent when mixed with addition solution, mg per l	Precipitation of surface-active agent in presence of electrolytes					
		Water	Sodium hydroxide	Calcium hydroxide	Sodium sulfate	Calcium sulfate	Cement filtrate
Sodium dodecyl-sulfate	250	–	–	+	–	+	+
Sodium tetradecyl-sulfate	50	–	–	+	–	+	+
Sodium hexadecyl-sulfate	50	–	+	+	+	+	+
Sodium abietate	500	–	–	+	–	+	+
Decyl-amine hydrochloride	250	–	+	+	–	–	+
Dodecyl-amine hydrochloride	150	–	+	+	+	+	+
Tetradecyl-trimethyl ammonium bromide	250	–	–	–	–	–	–
Hexadecyl-trimethyl ammonium bromide	250	–	–	–	–	–	–
Triton NE	250	–	–	–	–	–	–
Lissapol N 300	250	–	–	–	–	–	–
Saponin	500	–	+	+	–	–	+
Gelatine	1000	–	–	–	–	–	–
Octyl alcohol	100	–	–	–	–	–	–
Terpineol	250	–	–	–	–	–	–

+ denotes that the surface-active agent is precipitated by a particular electrolyte.
– denotes that the surface-active agent is not precipitated by a particular electrolyte.

TABLE 4—EFFECT OF ELECTROLYTES ON FOAM STABILITY OF SURFACE-ACTIVE AGENT SOLUTIONS AT 25 C

Surface-active agent	Concentration of surface-active agent mixed with addition solution, mg per l	Foam stability of surface-active agent solution (time for foam to collapse)					
		Water	Sodium hydroxide	Calcium hydroxide	Sodium sulfate	Calcium sulfate	Cement filtrate
Sodium dodecyl-sulfate	250	>15 hr	12 hr	>15 hr	12 hr	>15 hr	3 hr
Sodium tetradecyl-sulfate	50	6 hr	1½ hr	5 sec	6 hr	5 sec	5 sec
Sodium hexadecyl-sulfate	50	5 hr	0	0	0	0	0
Sodium abietate	500	1½ hr	3 hr	>15 hr	2 hr	>15 hr	>15 hr
Decyl-amine hydrochloride	250	30 sec	38 min	1½ hr	13 sec	30 sec	2 hr
Docecyl-amine hydrochloride	150	35 sec	>15 hr	>15 hr	5 sec	5 sec	>15 hr
Tetradecyl-trimethyl ammonium bromide	250	30 min	20 min	>15 hr	20 min	25 min	>15 hr
Hexadecyl-trimethyl ammonium bromide	250	>15 hr	10 min	>15 hr	>15 hr	>15 hr	>15 hr
Triton NE	250	>15 hr	>15 hr	>15 hr	>15 hr	>15 hr	>15 hr
Lissapol N 300	250	>15 hr	>15 hr	>15 hr	>15 hr	>15 hr	>15 hr
Saponin	500	>15 hr	>15 hr	>15 hr	>15 hr	>15 hr	>15 hr
Gelatine	1000	>15 hr	>15 hr	>15 hr	>15 hr	>15 hr	>15 hr
Octyl alcohol	100	12 sec	5 sec	5 sec	5 sec	5 sec	5 sec
Terpineol	250	8 sec	8 sec	10 sec	8 sec	8 sec	10 sec

TABLE 5—EFFECT OF ELECTROLYTES ON FOAM CAPACITY OF SURFACE-ACTIVE AGENT SOLUTIONS AT 25 C

Surface-active agent	Concentration of surface-active agent mixed with addition solution, mg per l	Foam capacity of surface-active agent solution (height of foam in cm)					
		Water	Sodium hydroxide	Calcium hydroxide	Sodium sulfate	Calcium sulfate	Cement filtrate
Sodium dodecyl-sulfate	250	15	16	15	16	16	16
Sodium tetradecyl-sulfate	50	1.5	2	0	2	0	0
Sodium hexadecyl-sulfate	50	1.5	0	0	0	0	0
Sodium abietate	500	12	12	3	12	3	3
Decyl-amine hydrochloride	250	1	3	5	0	0	3
Dodecyl-amine hydrochloride	150	1	3	3	0	0	3
Tetradecyl-trimethyl ammonium bromide	250	10	12	16	12	12	16
Hexadecyl-trimethyl ammonium bromide	250	16	16	16	16	16	16
Triton NE	250	6	6	6	6	6	6
Lissapol N 300	250	5	5	5	5	5	5
Saponin	500	12	12	12	12	12	12
Gelatine	1000	5	5	6	6	6	6
Octyl alcohol	100	0	0	0	0	0	0
Terpineol	250	0	0	0	0	0	0

of their filtrates were reduced to low values. This showed that the precipitated calcium compounds stabilized the foams.

A comparison of the air-entraining capacities of surface-active agents in cement and silica pastes with the precipitation and foaming data in Tables 3, 4, and 5 established three facts:

(1) Agents may be precipitated, but provided the foam stabilities and capacities of their solutions are not reduced to zero, they can entrain air in pastes. Sodium dodecyl-sulfate and sodium abietate behave in this way in cement pastes.

(2) Agents which are completely precipitated, so that the foam stabilities and capacities of their solutions are reduced to zero, entrain no air in pastes. Sodium hexadecyl-sulfate in cement pastes is an example of this type of behavior.

(3) Agents may be unaffected by electrolytes, the foam stabilities and capacities of their solutions may be high, and yet they entrain little or no air in pastes. The nonionic agents in cement and silica pastes are examples of this type of behavior.

Foam stabilities and capacities of filtrates from cement and silica pastes containing surface-active agents

Table 6 shows that in many cases the foam stabilities and capacities of paste filtrates are lower than those in the mixing water before addition to the pastes. This indicates that the concentrations of the surface-active agents in the mixing water were reduced; such reductions were due to precipitation of the agent or to adsorption of the agent on the solid particles.

A comparison of the air-entraining capacities of surface-active agents in cement and silica pastes with the foam stabilities and capacities of filtrates from these pastes showed that:

(1) Agents may be adsorbed or precipitated in pastes so that the foam stabilities and capacities of the mixing water in pastes are reduced to low values, yet entrain large volumes of air. Decyl- and dodecyl-amine hydrochlorides in silica pastes, and sodium dodecyl-sulfate and sodium abietate in cement pastes behave in this way.

(2) Agents may be neither precipitated nor adsorbed very strongly in pastes, so that the foam stabilities and capacities of the mixing water remain relatively high,

TABLE 6—EFFECT OF PRECIPITATION AND ADSORPTION OF SURFACE-ACTIVE AGENTS IN PASTES ON THE FOAM STABILITIES AND CAPACITIES IN THE MIXING WATER AT 25 C

Surface-active agent	Initial concentration in mixing water, mg per l	Mixing water before adding to pastes		Filtrate from cement paste $W/C = 0.450$		Filtrate from silica paste $W/S = 0.500$	
		FS*	FC,†cm	FS*	FC,†cm	FS*	FC,†cm
Sodium dodecyl-sulfate	50	3½ min	3	45 sec	1.5	—	—
	100	2½ hr	7	1 min	2	2½ hr	6.5
	500	>15 hr	17	3 min	4	>15 hr	17
	1000	>15 hr	>19	4 min	4.5	>15 hr	>19
Sodium tetradecyl-sulfate	50	6 hr	1.5	0	0	5 hr	1
	100	>15 hr	1.5	0	0	>15 hr	1.5
Sodium hexadecyl-sulfate	50	5 hr	1.5	0	0	4 hr	1.5
Sodium abietate	100	2 min	0.5	10 sec	0	1½ min	0.5
	500	1½ hr	12	13 sec	0	1½ hr	11
	1000	> 3 hr	11	12 sec	0	> 3 hr	10.5
Decyl-amine hydrochloride	100	12 sec	0	6 min	0.5	0	0
	500	30 sec	1.5	> 1 hr	1	3 sec	0
Dodecyl-amine hydrochloride	100	30 sec	1	0	0	1 sec	0
	250	> 5 hr	4.5	0	0	5 sec	0
	500	>15 hr	8	1 sec	0	10 sec	0
Tetradecyl-trimethyl ammonium bromide	50	40 sec	4	4 min	1.5	0	0
	100	2½ min	8	1 hr	2.5	—	—
	375	> 5 hr	>17	—	—	1 min	2.5
	500	> 8 hr	>17	> 5 hr	11	1½ min	4
	750	> 8 hr	>17	—	—	1½ min	4
Hexadecyl-trimethyl ammonium bromide	50	>15 hr	9	1 sec	0	0	0
	100	>15 hr	13	3 min	1	2 sec	0
	500	>15 hr	>16	> 8 hr	3	1 hr	1.5
	1000	>15 hr	>16	> 8 hr	4.5	> 5 hr	3
Triton NE	50	>15 hr	3	5 sec	0	5 sec	0
	100	>15 hr	4	2½ min	1	30 sec	1
	500	>15 hr	8.5	> 4 hr	4	>12 hr	6
	1000	>15 hr	10	> 4 hr	7	>15 hr	9
Lissapol N 300	50	>15 hr	2	20 sec	0.5	10 sec	0
	100	>15 hr	3.5	20 min	0.5	30 min	3
	500	>15 hr	6	3 hr	3.5	> 5 hr	2
Saponin	100	>15 hr	4	30 sec	1	5 sec	0
	500	>15 hr	12	30 min	2	>15 hr	6
	1000	>15 hr	15	> 4 hr	4	>15 hr	6
Gelatine	500	>15 hr	5	30 sec	1.5	>15 hr	4.5
	1000	>15 hr.	5	3 min	4.5	>15 hr	5
Octyl alcohol	100	12 sec	0	10 sec	0	10 sec	0
	250	12 sec	0	10 sec	0	10 sec	0
Terpineol	250	8 sec	0	8 sec	0	8 sec	0
	1000	8 sec	0	8 sec	0	8 sec	0

*FS = Foam stability.
†FC = Foam capacity.

yet entrain little or no air in pastes. Examples of this behavior are the nonionic agents, and sodium tetradecyl- and hexadecyl-sulfates in silica pastes.

Abilities of surface-active agents to make cement and silica particles hydrophobic so that air bubbles may adhere to them

Tables 7 and 8 summarize the flotation data for cement clinker and silica respectively in solutions of surface-active agents of varying concentrations. It will be seen that in some cases the solid particles float at low concentrations of surface-active agent, but at high concentrations flotation ceases. Wark[9] suggested that this effect is due to bubble armoring.

TABLE 7—FLOTATION DATA FOR CEMENT CLINKER IN SURFACE-ACTIVE AGENT SOLUTIONS OF VARIOUS CONCENTRATIONS WHICH CONTAIN CEMENT FILTRATE*

Surface-active agent	Concentration						
	0 mg per l	5 mg per l	15 mg per l	50 mg per l	100 mg per l	500 mg per l	1000 mg per l
Sodium dodecyl-sulfate	0	+	++	++	++	++	++
Sodium tetradecyl-sulfate	0	+	+	+	+	–	–
Sodium hexadecyl-sulfate	0	+	+	+	–	–	–
Sodium abietate	0	+	++	++	++	++	++
Decyl-amine hydrochloride	0	0	0	0	0	0	0
Dodecyl-amine hydrochloride	0	0	0	0	0	0	0
Tetradecyl-trimethyl-ammonium bromide	0	+	+	+	+	0	0
Hexadecyl-trimethyl-ammonium bromide	0	+	+	+	+	0	0
Triton NE	0	0	0	0	0	0	0
Lissapol N 300	0	0	0	0	0	0	0
Saponin	0	0	0	0	0	0	0
Gelatine	0	0	0	0	0	0	0
Octyl alcohol	0	0	0	0	0	–	–
Terpineol	0	0	0	0	0	0	0

*Temperature 25C; size of clinker −150 +200 B.S.S. mesh.
0 denotes zero flotation.
+ denotes definite contact between cement and bubbles but poor flotation.
++ denotes excellent flotation.
– denotes agent not soluble.

A comparison of the air-entraining capacities of surface-active agents in cement and silica pastes with the flotation data in Tables 7 and 8 showed that in most cases agents which entrain air in pastes are also adsorbed on the solid particles of the pastes making them hydrophobic so that air bubbles adhere to them. Sodium dodecyl-sulfate in silica pastes and saponin in cement and silica pastes appear to be exceptions to the above relationship. These cases will be discussed later.

DISCUSSION

Air entrainment in cement and silica pastes appears to depend on two major factors. Firstly, after any precipitation or adsorption, the foam stability and foam capacity of the surface-active agent remaining in the mixing water of the paste should be finite but not necessarily great. Secondly, the surface-active agent should be adsorbed on the solid particles of the

TABLE 8—FLOTATION DATA FOR SILICA IN SURFACE-ACTIVE AGENT SOLUTIONS OF VARIOUS CONCENTRATIONS*

Surface-active agent	Concentration						
	0 mg per l	5 mg per l	25 mg per l	50 mg per l	100 mg per l	500 mg per l	1000 mg per l
Sodium dodecyl-sulfate	0	0	0	0	0	0	0
Sodium tetradecyl-sulfate	0	0	0	0	0	–	–
Sodium hexadecyl-sulfate	0	0	0	0	–	–	–
Sodium abietate	0	0	0	0	0	0	0
Decyl-amine hydrochloride	0	+	++	++	++	0	0
Dodecyl-amine hydrochloride	0	+	++	++	++	0	–
Tetradecyl-trimethyl-ammonium bromide	0	+	++	++	++	0	0
Hexadecyl-trimethyl-ammonium bromide	0	+	++	++	++	0	0
Triton NE	0	0	0	0	0	0	0
Lissapol N 300	0	0	0	0	0	0	0
Saponin	0	0	0	0	0	0	0
Gelatine	0	0	0	0	0	0	0
Octyl alcohol	0	0	0	0	0	–	–
Terpineol	0	0	0	0	0	0	0

*Temperature 25C; size of silica −150 +200 B.S.S. mesh.
0 denotes zero flotation.
+ denotes definite contact between silica and bubbles but poor flotation.
++ denotes excellent flotation.
– denotes agent not soluble.

paste making them hydrophobic so that air bubbles may adhere to them.

Additional proof that the adherence of air bubbles to solid particles is a necessary factor of air entrainment was provided by a study of the influence on air entrainment of an activator and a depressant of flotation. Neither sodium dodecyl-sulfate nor sodium abietate floated silica, but in the presence of calcium hydroxide as an activator, both agents floated silica excellently. Fig. 4 shows that sodium dodecyl-sulfate and sodium abietate did not entrain much air when used in low concentrations in silica pastes; however, in the presence of calcium hydroxide both agents entrained large volumes of air and these pastes were very stable. The behavior of dodecyl-amine hydrochloride, which floats silica and forms very stable air-entrained silica pastes, can be modified by additions of gelatine which depress the flotation of silica.

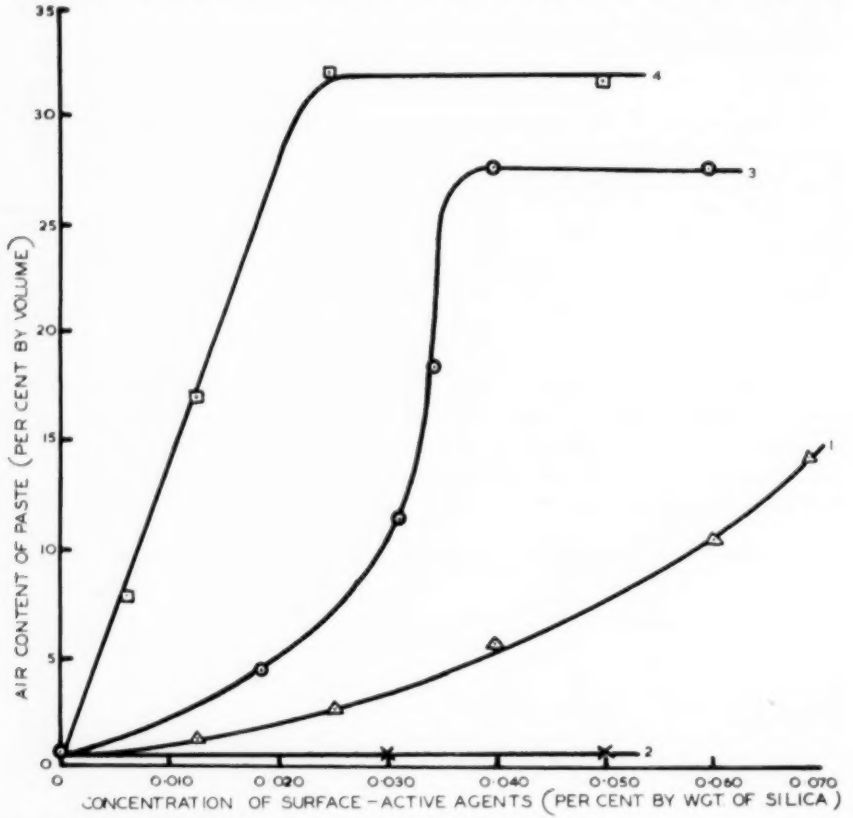

Fig. 4—Effect of calcium hydroxide on the air-entraining capacities of sodium dodecyl-sulfate and sodium abietate in silica pastes. Mixing conditions: stirring time 4 min; speed of stirrer 1200 rpm; W/S = 0.500 (by weight); temperature 25 C

Surface-active agents:

(1) Sodium dodecyl-sulfate
(2) Sodium abietate
(3) Sodium dodecyl-sulfate + $Ca(OH)_2$
(4) Sodium abietate + $Ca(OH)_2$

TABLE 9—COMPARATIVE AIR-ENTRAINING CAPACITIES OF SINGLE AND MIXED SURFACE-ACTIVE AGENTS IN SILICA PASTES AT 25 C*

Conditioning agent	Concentration, percent by weight of silica	Foaming agent	Concentration, percent by weight of silica	Air content of paste, percent
Hexadecyl-trimethyl-ammonium bromide	0.025	—	—	4.2
Dodecyl-amine hydrochloride	0.0175	—	—	6.2
—	—	Octyl alcohol	0.0125	0.5
—	—	Terpineol	0.045	0.5
Hexadecyl-trimethyl-ammonium bromide	0.025	Octyl alcohol	0.0125	29.9
Hexadecyl-trimethyl-ammonium bromide	0.025	Terpineol	0.045	27.8
Dodecyl-amine hydrochloride	0.0175	Octyl alcohol	0.0125	21.8
Dodecyl-amine hydrochloride	0.0175	Terpineol	0.045	30.9

*Stirring time 4 min; speed of stirrer 1200 rpm; W/S ratio 0.500 (by weight).

It was found that air-entrained silica pastes containing dodecyl-amine hydrochloride with gelatine additions were very unstable and the entrained air escaped readily.

Studies of air-entraining capacities of mixed surface-active agents in cement and silica pastes emphasized further that the solid particles must be in a hydrophobic condition before stable air-entrained pastes can be produced. Air-entrained silica pastes were prepared using the combined action of two types of surface-active agents; one was a foaming agent which did not float silica and the other was a cationic conditioning agent which floated silica. The cationic agents were added to the pastes at low concentrations so that when used singly they did not entrain much air. Table 9 shows that silica pastes containing combinations of conditioning agents hexadecyl-trimethyl-ammonium bromide or dodecyl-amine hydrochloride and foaming agents octyl alcohol or terpineol, had air contents which were much greater than the sums of air contents of silica pastes containing the single agents. Table 10 shows that the same effect occurs in cement pastes with conditioning agents tetradecyl- and hexadecyl- trimethyl-ammonium bromides and foaming agent octyl alcohol. These results show that agents like octyl alcohol and terpineol which have low foam stabilities and capacities in solution are able to form stable air-entrained pastes provided the solid particles are in a hydrophobic condition.

The behavior of sodium dodecyl-sulfate in silica pastes indicated that the major factor controlling the retention of air bubbles in pastes is not a high solid + air/water ratio but the adherence of air bubbles to hydrophobic particles. Sodium dodecyl-sulfate which does not float silica, and whose solutions generate large volumes of stable foam, entrain large volumes of

TABLE 10—COMPARATIVE AIR-ENTRAINING CAPACITIES OF SINGLE AND MIXED SURFACE-ACTIVE AGENTS IN CEMENT PASTES AT 25 C*

Conditioning agent	Concentration, percent by wt. of cement	Foaming agent	Concentration, percent by wt. of cement	Air content of paste, percent
Tetradecyl-trimethyl ammonium bromide	0.0125	—	—	10.7
Hexadecyl-trimethyl-ammonium bromide	0.0125	—	—	4.2
—	—	Octyl alcohol	0.0025	0.5
Tetradecyl-trimethyl-ammonium bromide	0.0125	Octyl alcohol	0.0025	18.0
Hexadecyl-trimethyl-ammonium bromide	0.0125	Octyl alcohol	0.0025	9.2

*Stirring time 4 min; speed of stirrer 1000 rpm; W/C ratio 0.450 (by weight); cement No. 1.

air in silica pastes when present in concentrations greater than 0.075 percent by weight of silica. However, despite the high solid + air/water ratio such pastes are very unstable. In contrast with this behavior, sodim dodecylsulfate is able to form very stable air-entrained silica pastes of high air content when used in the presence of ferric iron or calcium hydroxide both of which activate the flotation of silica.

Saponin entrained large volumes of air in cement and silica pastes when present in concentrations greater than about 0.05 percent by weight of the solid. These pastes were stable despite the fact that saponin does not float either cement or silica. A possible explanation of this anomalous behavior of saponin comes from a consideration of the size of saponin bubbles. Rehbinder[1] showed that in foamed concrete saponin formed bubbles whose diameters were up to five times smaller than those formed by naphthenic soap. Hence saponin bubbles, because of their extremely small size, should rise very slowly from pastes. Consequently air-entrained pastes made from saponin should be stable despite the absence of bubble-solid contact.

On the basis of the results and discussion presented above the following mechanisms are postulated for the formation and retention of air bubbles in cement and silica pastes.

1. When a surface-active agent is added to a paste its concentration may be reduced to a low value by precipitation or by adsorption on the solid particles. Air entrainment can obviously only take place if the concentration of the agent remaining in the mixing water is sufficient to generate air bubbles when the paste is stirred. When the solid particles are made hydrophobic by adsorption of the agent, the generated air bubbles will adhere to them. This process stabilizes bubbles of low stability and fixes bubbles in position uniformly in the paste preventing their coalescence, and allows the air content of the paste to build up as mixing progresses. When mixing ceases, bubbles are retained in the paste by virtue of their attachment to solid particles which weight them and prevent their escape. Similarly the attached bubbles tend to float the large solid particles and prevent their sedimentation. In addition the attachment of bubbles to solid particles tends to bind the particles together and increase the viscosity of the paste by the process of adhesional flocculation (Bartsch[8]), thus increasing the stability of the paste.

2. The behavior of saponin in pastes suggests that stable air-entrained pastes can be formed also by agents which possess a high foam capacity in the paste and are able to form very small bubbles which do not coalesce and whose rate of escape from the paste is slow.

CONCLUSIONS

1. The major conditions governing the formation of stable, air-entrained cement and silica pastes containing surface-active agents are:

(a) The residual concentration of surface-active agent in the mix water of a paste, after any precipitation or adsorption, must be sufficient to generate fine air bubbles.

(b) The surface-active agent must be adsorbed on the solid particles of the paste, making them hydrophobic, so that air bubbles adhere to them.

2. The conditions governing the formation of stable, air-entrained cement and silica pastes containing saponin appear to be a good foaming capacity in the mix water, and the ability of saponin to form ultrafine bubbles which do not coalesce.

3. The results of this paper apply only to pastes and at present should not be extrapolated to explain air entrainment in concrete.

REFERENCES

1. Rehbinder, P. A., Petrova, N. N., Smirnova, A. M., and Polozhintseva, E. N., *Izvestiya Akademii Sci. USSR*, O.T.N., V. 4, 1937, p. 593.

2. Scripture, E. W., Jr., Hornibrook, F. B., and Bryant, D. E., "Influence of Size Grading of Sand on Air Entrainment," ACI JOURNAL, Nov. 1948, *Proc.* V. 45, pp. 217-228.

3. Scripture, E. W., Jr., and Litwinowicz, F. J., "Some Factors Affecting Air Entrainment," ACI JOURNAL, Feb. 1949, *Proc.* V. 45, pp. 433-444.

4. Scripture, E. W., Jr., and Litwinowicz, F. J., "Effects of Mixing Time, Size of Batch and Brand of Cement on Air Entrainment," ACI JOURNAL, May 1949, *Proc.* V. 45, pp. 653-664.

5. Scripture, E. W., Jr., Benedict, S. W., and Litwinowicz, F. J., "Effect of Temperature and Surface Area of the Cement on Air Entrainment," ACI JOURNAL, Nov. 1951, *Proc.* V. 48, pp. 205-212.

6. Klein, W. H., and Walker, Stanton, "A Method for Direct Measurement of Entrained Air in Concrete," ACI JOURNAL, June 1946, *Proc.* V. 42, pp. 657-668.

7. Wark, I. W., *Principles of Flotation*, Australian Institute of Mining and Metallurgy, Melbourne, 1938.

8. Bartsch, O., *Kolloidchem. Beihefte*, V. 20, 1924, p. 1.

9. Wark, I. W., *Journal of Physical Chemistry*, V. 40, 1936, p. 661.

Title No. 51-47

Eccentric Bending in Two Directions of Rectangular Concrete Columns*

By LU-SHIEN HU†

SYNOPSIS

Four charts are presented for checking the stresses in a rectangular reinforced concrete section subjected to bending in two directions with or without normal compressive force. These charts can be used for sections with symmetrical as well as nonsymmetrical steel arrangement. The only limitation of the use of these charts is the rectangularity of the section.

The assumption that the slope of the neutral axis is the same as that for a homogeneous section is used in preparing the charts. The maximum error due to this assumption is shown to be on the safe side and of negligible magnitude even for the worst cases. Four numerical examples are given to illustrate the use of the charts.

INTRODUCTION

Principles of structural design may be classified into two large groups, namely, elastic and plastic design. Most parts of structures are designed according to elastic theory while plastic theory is now largely confined to bearing and steel details. In designing reinforced concrete columns, both elastic and plastic theories have been used. The ACI Building Code gives column formulas which are based upon plastic theory; the American Assn. of State Highway Officials Specifications specifies the use of elastic theory. This paper is confined to elastic theory of eccentrically loaded reinforced concrete sections.

Because of the invalidity of the principle of superposition, the problem of reinforced concrete sections subjected to bending in two directions is usually solved by trial methods. A certain section is first assumed, either from experience or from approximate computations, and then verified if it is adequate. To find the stresses of the assumed section, the position of the neutral axis is first determined by trial. The present paper deals with the verification of the stresses, not the direct design of the section.

This problem is not new. Methods of attack may be grouped into two types: (1) general methods and (2) charts or graphs. General methods, analytic or graphic, are usually successive approximations which take considerable time and labor to find the result. Parker and Scanlon[1] gave an

*Received by the Institute Sept. 2, 1954. Title No. 51-47 is a part of copyrighted JOURNAL OF THE AMERICAN CONCRETE INSTITUTE, V. 26, No. 9, May 1955, *Proceedings* V. 51. Separate prints are available at 50 cents each. **Discussion** (copies in **triplicate**) should reach the Institute not later than Sept. 1, 1955. Address 18263 W. McNichols Road, Detroit 19, Mich.

†Designer, Hardesty and Hanover, New York, N. Y.

analytic, and Andersen[2] a graphic method, both using the assumption that the slope of the neutral axis of the reinforced concrete section was the same as that of a homogeneous section. Parker and Scanlon used the assumption only as a first approximation and corrected successively. Andersen showed that the deviation of the direction of the neutral axis of a cracked plain concrete section from that of a homogeneous section is in general very small. For rectangular sections, Ingerslev[3] considered first the greater bending moment with normal compression, if any; found the neutral axis and stresses by any method; and then superposed the stresses due to the smaller bending moment alone. The error due to the superposition was finally corrected by successive approximation. Without successive correction, the results computed from this method are not exact, but are good approximations.

For rectangular sections, charts have been worked out to save time and labor. They are generally based upon certain assumptions or limitations, the most used being: (1) steel concentrated at four corners, (2) coverage of steel is a certain fixed percentage of the sides of the section, (3) ratios of moments of inertia of steel to concrete are the same in both directions, and (4) square section with symmetric steel.

These assumptions limit the use or the accuracy of the charts. Roussopoulos[4] presented a group of charts for rectangular sections subjected to bending in two directions with normal force, using assumptions (2) and (3). He has not considered large eccentricities or pure bending. Andersen[5] presented a group of charts, using assumptions (1) and (4).

This paper gives four charts which do not use any of the four assumptions listed above. These charts include large eccentricities and pure bending and can be used also for the case of nonsymmetrical steel arrangement.

ASSUMPTIONS AND LIMITATIONS

The charts presented in this paper are based upon the following assumptions: (1) plane deformation and Hooke's law, (2) concrete takes no tension, and (3) slope of the neutral axis is the same as that for a homogeneous section. The first two assumptions are commonly used for elastic analysis of reinforced concrete structures; the third is discussed in detail on p. 927.

The charts are subjected to the following limitations: (1) rectangular sections, and (2) normal compressive force, which may equal zero.

EQUILIBRIUM EQUATIONS

As derived in Appendix 1, the equilibrium equations of a rectangular section b x d with symmetrical reinforcement (*i.e.*, $\mu = 0$), subjected to normal compressive force N with eccentricities $e_x b$ and $e_y d$ in the direction of b and d, respectively, are

$$\frac{N}{bdf_c} = \frac{chk}{6} - np\left(\frac{1}{2h} + \frac{1}{2k} - 1\right) \quad (1)$$

$$\frac{N}{bdf_c} e_x = \frac{chk}{6}\left(\frac{1}{2} - c_h\right) + nq_x \frac{1}{12h} \quad (2)$$

Fig. 1—Forces on column section

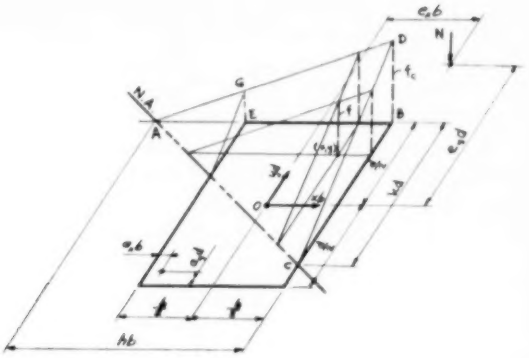

$$\frac{N}{bdf_c} e_y = \frac{chk}{6}\left(\frac{1}{2} - c_d\right) + nq_y \frac{1}{12k} \quad \ldots\ldots (3)$$

and the steel stress is

$$f_s = nf_c\left(1 - \frac{1 - a_x}{h} - \frac{1 - a_y}{k}\right) \quad \ldots\ldots (4)$$

in which h and k define the position of neutral axis; c, c_b, and c_d are known functions of h and k; f_c is the maximum concrete stress; p is the percentage of steel area; q_x and q_y are the percentages of steel moment of inertia in the appropriate direction on b and d; and $a_x b$ and $a_y d$ are the concrete protection to center of bars in x- and y-directions, respectively (see Fig. 1).

If the slope of the neutral axis is assumed the same as that of the homogeneous sections, $m = k/h = e_x/e_y$ (see Appendix 2), equilibrium Eq. (2) and (3) can be replaced by equation $\Sigma M_{N.A.} = 0$, which can be expressed as

$$\frac{N}{bdf_c} e_y (1 + m^2) = \frac{chk}{6}\left[m\left(\frac{1}{2} - c_b\right) + \left(\frac{1}{2} - c_d\right)\right] + \frac{Qnp}{12k} \quad \ldots\ldots (5)$$

where $Q = (m^2 nq_x + nq_y)/(np)$.

For pure bending, $N = 0$, Eq. (1) and (5) become

$$\frac{chk}{6} - np\left(\frac{1}{2h} + \frac{1}{2k} - 1\right) = 0 \quad \ldots\ldots (6)$$

$$\frac{M_y}{bd^2 f_c}(1 + m^2) = \frac{chk}{6}\left[m\left(\frac{1}{2} - c_b\right) + \left(\frac{1}{2} - c_d\right)\right] + \frac{Qnp}{12k} \quad \ldots\ldots (7)$$

Eq. (4) remains the same.

Fig. 2 shows a section with nonsymmetrical steel arrangement. The actual section is b x d; the imaginary section is b' x d'. If the neutral axis is as shown, the additional area (b' x d' − b x d) introduces no stresses, thus no error. Nonsymmetrical steel arrangement is usually used when there is excessive tensile stress, *i.e.*, for large eccentricities. In case of large eccentricity, the neutral axis is moved toward the compression side and only a small portion, if any, of the additional area (b' x d' − b x d) is in compression. Since this small area is near the neutral axis, error due to this additional stress is negli-

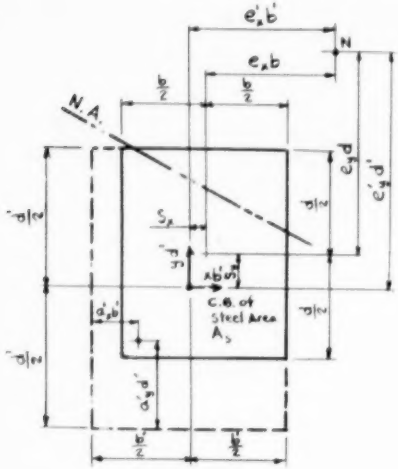

Fig. 2—Section with nonsymmetrical steel arrangement

gible. In such cases, Eq. (1) to (7) can also be used for the case of nonsymmetrical steel arrangement if b is replaced by b', d by d', e by e', a by a', and nq by $nq' = nq\ (1 + \mu)$.

One numerical example (Example 4) is given later on nonsymmetrical arrangement, which shows good approximations.

PLOTTING OF CHARTS

Eq. (1), (4), (5), (6), and (7) are the fundamental equations from which the charts are plotted. The accuracy of these equations hinges on the assumption made for the slope of the neutral axis, which is discussed later.

In Eq. (1), (5), (6), and (7), there are four known quantities: e_y, $m = e_x/e_y$, np, and Q and two unknown quantities k ($h = k/m$) and $N/(bdf_c)$. Maximum steel stress can easily be computed from Eq. (4) after k and f_c are obtained.

Proportionality between N/bdf_c or M_y/bd^2f_c and Q

The quantity N/bdf_c or M_y/bd^2f_c and the factor Q appear in Eq. (5) and (7) only and are all linear. As far as these factors are concerned, N/bdf_c or M_y/bd^2f_c is linearly proportional to Q, if m is considered as the slope of the neutral axis.

Variation of np

Effect of variation on np on e_y has been studied for the case of pure bending. $M_d/(bd^2f_c)$ was plotted against np for $m = 0$, 0.5, 1.0 and $Q = 1$ and 3. Values of $np = 0.03$, 0.10, and 0.30 have been selected for which charts are plotted. For intermediate values of np, linear interpolation may be used with negligible error. This is assumed also for bending with normal compression.

Kern and modified kern

The kern may be defined as that area of the section through which the

compressive force N must pass if the force N is to produce, at all points in the given section, the same kind of normal stress, *i.e.*, compressive stress throughout. For any compressive force applied within the kern, the principle of superposition can be used with exact results. If a small error in maximum stresses is allowed, superposition can still be used for force applied within a certain area of the section which is called the modified kern.

Let α be the ratio of tensile stress f_t to the compressive stress f_c of a reinforced concrete section with concrete capable of taking tension. The modified kern distances e_x and e_y in the direction of x and y, respectively, are

$$e_{ox} = \frac{1}{6}\,\frac{1 + nq_x}{1 + np}\,\frac{1 + \alpha}{1 - \alpha} = \frac{1 + \alpha}{1 - \alpha}\,e_{ox}$$

$$e_{oy} = \frac{1}{6}\,\frac{1 + nq_y}{1 + np}\,\frac{1 + \alpha}{1 - \alpha} = \frac{1 + \alpha}{1 - \alpha}\,e_{oy}$$

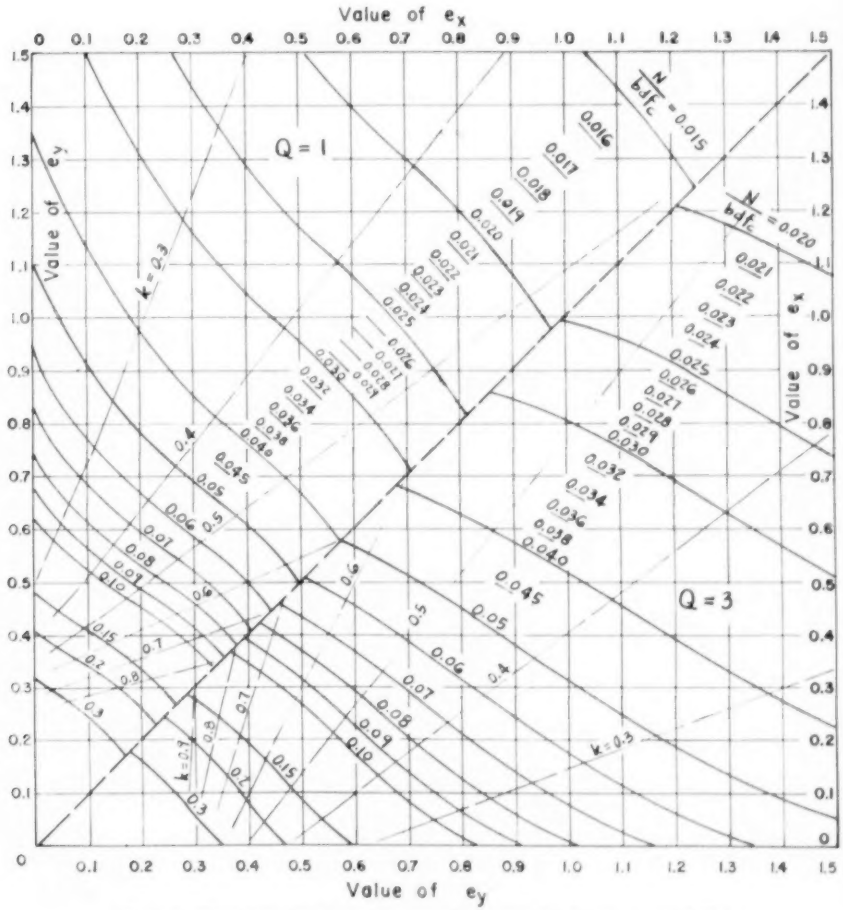

Fig. 3—Chart for bending with normal compressive force, $np = 0.03$

The kern distances are then

$$e_{ox} = \frac{1}{6}\,\frac{1 + nq_x}{1 + np}$$

$$e_{oy} = \frac{1}{6}\,\frac{1 + nq_y}{1 + np}$$

The German specification[6] uses $\alpha = 0.35$ which gives a modified kern about twice the kern area.

Ranges of charts

There are four charts: Fig. 3, 4, and 5 for bending with normal compressive force, and Fig. 6 for pure bending. Fig. 3 is plotted for $np = 0.03$, Fig. 4 for $np = 0.10$, and Fig. 5 for $np = 0.30$. Linear interpolation may be used for intermediate np values. Each chart is further divided by its diagonal

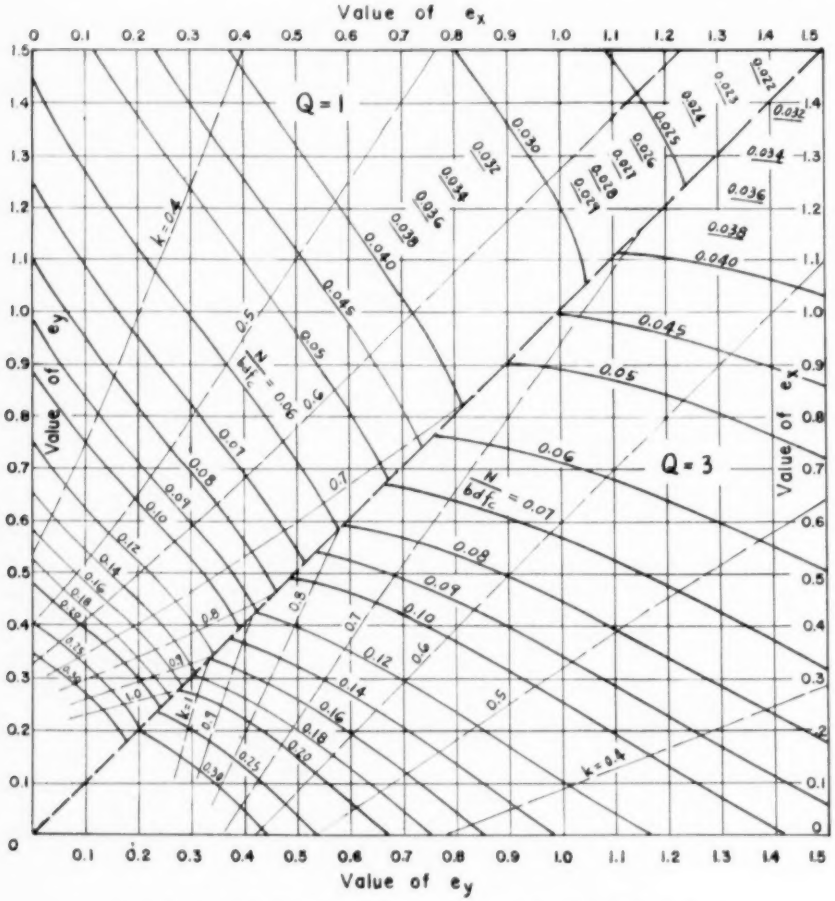

Fig. 4—Chart for bending with normal compressive force, $np = 0.10$

into two parts, one for $Q = 1$ and another for $Q = 3$. For any other Q values, linear interpolation or extrapolation may be used. The range of eccentricities e_x and e_y, $e_y \leqq e_x$, plotted is 0 to 1.5; for large eccentricities, the effect of normal force is small and Fig. 6 may be used.

ASSUMPTION OF SLOPE OF NEUTRAL AXIS

As mentioned previously, the usefulness of the charts depends on the accuracy of the assumption made concerning the slope of the neutral axis.

Plain concrete section

For a plain concrete section, $np = nq = 0$ and Eq. (1), (2), and (3) become

$$\frac{N}{bdf_c} = \frac{chk}{6}$$

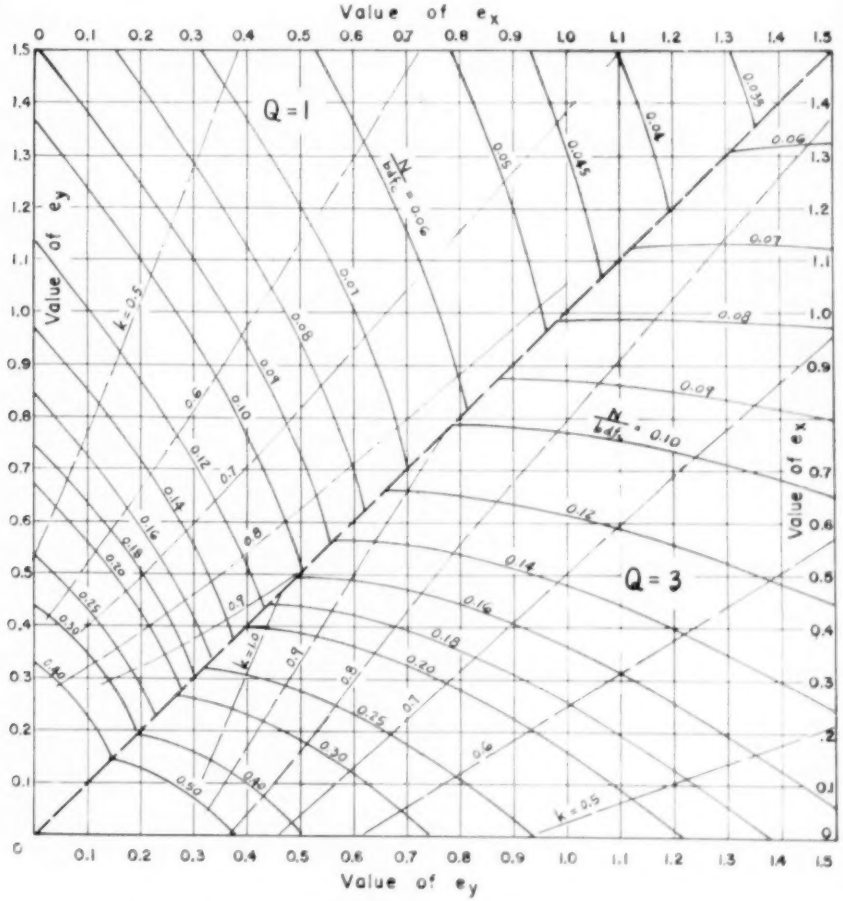

Fig. 5—Chart for bending with normal compressive force, $np = 0.30$

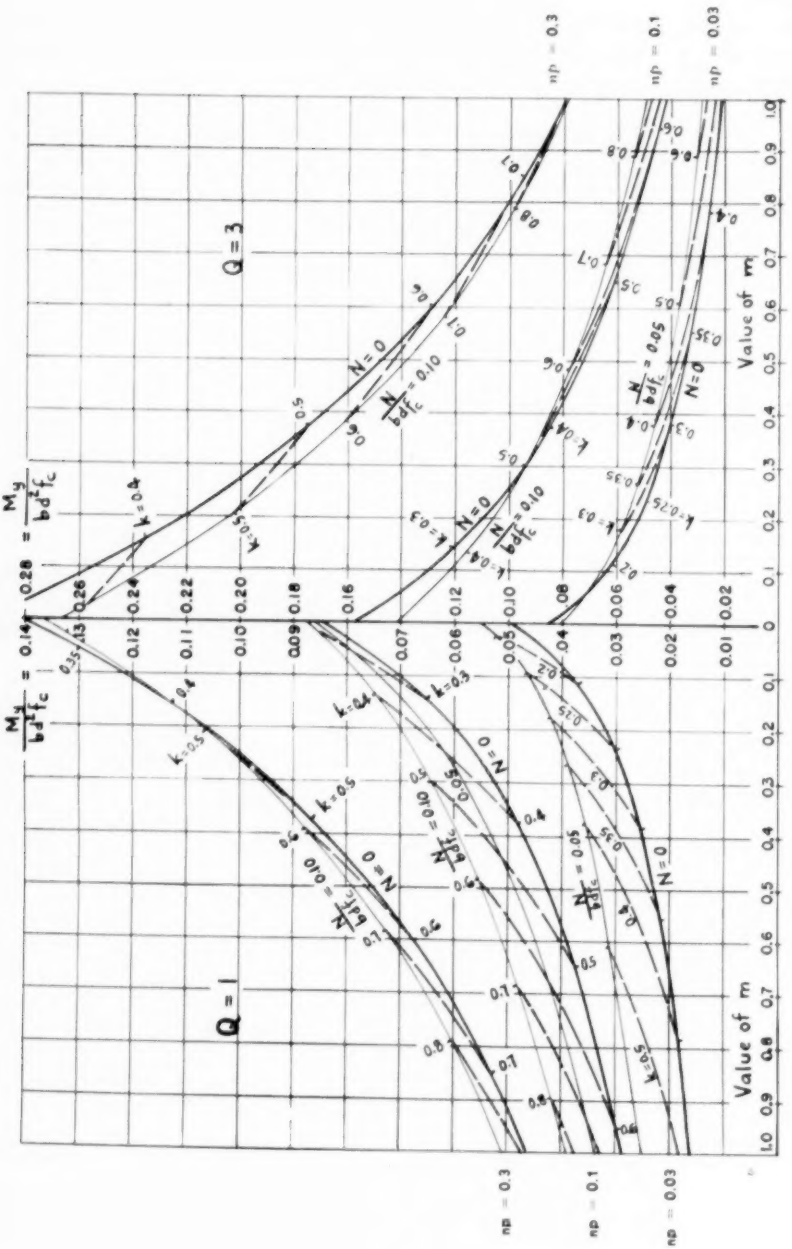

Fig. 6—Chart for pure bending

$$e_x = \tfrac{1}{2} - c_b$$
$$e_y = \tfrac{1}{2} - c_d$$

From the last two equations, the value of $e_x h/e_y k$ can be obtained as

$$\frac{e_x h}{e_y k} = \frac{\tfrac{1}{2} - c_b}{\tfrac{1}{2} - c_d} \frac{h}{k}$$

The value h/k is the slope of the neutral axis of the plain concrete section, and e_y/e_x the slope of the homogeneous section. Therefore, the greater the value $e_x h/e_y k$ differs from unity, the greater is the difference of the slope of the neutral axes. This value has a maximum at $h = 1$. For $h = 1$ and $k \leqq 1$

$$e_x h/e_y k = (2 - h)\, h/[(2 - k)\, k] = 1/[(2 - k)\, k]$$

which has a maximum at $k = 0$. A few values are tabulated below:

k	0	0.1	0.2	0.3	0.4	0.5	0.6	0.7
$e_x h/e_y k$	∞	5.25	2.78	1.96	1.56	1.33	1.19	1.10

Although the slope of the neutral axis may be rather different, the error in stress is usually small as shown in the following section.

Error on stress

Plain concrete section—Using the assumed slope of the neutral axis, the equilibrium equations of the plain concrete sections are

$$N/bdf_c = ehk/6 = ek^2/6m$$
$$e_y(1 + m^2) = m(\tfrac{1}{2} - c_b) + (\tfrac{1}{2} - c_d)$$

Position of the neutral axis, k, can be solved from the second equation and f_c then computed from the first. The approximate computation gives exact results for $m = 0$ and for $m = 1$. The maximum error is, therefore, probably near $m = 0.5$. The following figures should indicate the magnitude of errors.

			h	k	$f_c/(N/bd)$
$e_x/e_y = 0.5$	$e_y = 0.4$	Exact	1.215	0.398	12.5
		Approximate	1.0	0.5	12.0
	$e_y = 0.3$	Exact	1.53	0.798	5.1
		Approximate	1.56	0.78	5.1

The errors for plain concrete sections are rather small; the errors for reinforced concrete sections should be smaller. Considering other uncertainties in concrete structures, this amount of error is acceptable.

Reinforced concrete section—Two results are shown in the following for $e_x/e_y = 0.5$, where the error is nearly maximum. The following results are for sections with $np = 0.1$, $nq_x = 0.15$, $nq_y = 0.20$, $a_x = 0.10$, $a_y = 0.05$.

		h	k	$f_c/(N/bd)$	$f_s/(N/bd)$
$e_y = 1.0$	Exact	1.124	0.550	14.8	22.6
	Approximate	1.11	0.555	14.9	22.7
$e_y = 2.0$	Exact	1.026	0.489	15.2	27.7
	Approximate	0.98	0.49	15.4	28.2

USE OF CHARTS

Steps of computation

The following steps of computation are outlined for using the charts.

1. Assume a section, with arrangement of steel.

2. Compute the following sectional constants: A_c, A_s, I_x^s, I_y^s, I_x^c, I_y^c, $np = nA_s/A_c$, $nq = nI_s/I_c$. For nonsymmetrical steel arrangement, compute also I^s_{xy}, μ_x, μ_y, and use $nq(1 + \mu)$ instead of nq. In the computation for cases of nonsymmetrical steel, use $b' = b + 2s_x$ and $d' = d + 2s_y$ instead of b and d, respectively.

3. Compute the following load constants: $e_x = M_x/Nb$, $e_y = M_y/Nd$, and $m = e_x/e_y$. For nonsymmetrical steel arrangement, use $e_x' = (M_x/N + s_x)/b'$ and $e_y' = (M_y/N + s_y)/d'$ instead of e_x and e_y, respectively. In case of pure bending use $m = M_x d/(M_y b)$.

4. Compute $Q = (nq_y + m^2 nq_x)/np$.

5. Find N/bdf_c and k from Fig. 3, 4, and 5, or M_y/bd^2f_c and k from Fig. 6. In case of large eccentricities, which fall outside of Fig. 3, 4, and 5, Fig. 6 will be used as follows: First considering $N = 0$, with known values of m, np, and Q, find M_y/bd^2f_c; then with $N/bdf_c = M_y/(bd^2f_c)/e_y$, find the corrected M_y/bd^2f_c. Repeat until there is no correction on M_y/bd^2f_c.

6. Compute $h = k/m$.

7. Find f_c and f_s, $f_s = nf_c\left(1 - \frac{1 - a_x}{h} - \frac{1 - a_y}{k}\right)$.

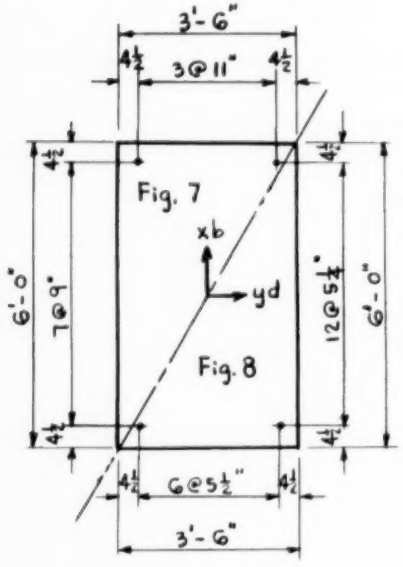

Fig. 7 (upper left diagonal section)—Column section of Example 1, 20—#11 bars. Fig. 8 (lower right diagonal section)—Column section of Example 2, 36—#11 bars

Numerical examples

Four numerical examples show the use of the charts. The first example shows the use of charts for small or moderate eccentricities, the second for large eccentricities or pure bending, the third for the approximation of sections somewhat different from rectangular, and the fourth for nonsymmetrical steel arrangement. Exact results are given in the parentheses following the approximate results from the charts.

Example 1—A section, as shown in Fig. 7, with 20—#11 bars, subjected to $N = 135$ kips, $M_x = 810$ ft-kips, and $M_y = 635$ ft-kips. The computations are self-explanatory.

$A_s = 20 \times 1.56 = 31.2$ sq in. $A_c = 6 \times 3.5 = 21.0$ sq ft $np = 0.103$
$I_x^s = 116.8$ sq in.-sq ft $I_x^c = 6^3 \times 3.5/12 = 63.0$ ft^4 $nq_x = 0.129$
$I_y^s = 48.6$ sq in.-sq ft $I_y^c = 6 \times 3.5^3/12 = 21.44$ ft^4 $nq_y = 0.157$
$e_x = (810/135 = 6.00)/6.0 = 1.000$
$e_y = (635/135 = 4.71)/3.5 = 1.345$ $m = 1.000/1.345 = 0.743$
$Q = (0.157 + 0.743^2 \times 0.129 = 0.228)/0.103 = 2.21$

From Fig. 4 and 5:

	$Q \rightarrow$	1	2.21	3
$np = 0.10$	N/bdf_c	0.0283	(0.0368)	0.0423
	k	0.585	(0.603)	0.615
$np = 0.30$	N/bdf_c	0.0445	(0.0651)	0.0785
	k	0.710	(0.735)	0.752

By interpolation,

$np = 0.103$ $N/bdf_c = 0.0368 + (0.028 \times 0.003/0.2 = 0.0004) = 0.0372$
$k = 0.603 + (0.132 \times 0.003/0.2 = 0.002) = 0.605$
$h = 0.605/0.743 = 0.814$
$f_c = 135/(21.0 \times 144 \times 0.0372) = 1.20$ ksi (exact 1.19 ksi)
$f_s = (1 - 0.9375/0.814 + 0.893/0.605)(10 \times 1.20)$
$= -1.628 \times 10 \times 1.20 = -19.5$ ksi (exact -19.3 ksi)

Example 2—A section, as shown in Fig. 8, with 36—#11 bars, subjected to $N = 45$ kips, $M_x = 545$ ft-kips, and $M_y = 897$ ft-kips. Neglect the normal force N.

$np = 0.1855$ $nq_x = 0.242$ $nq_y = 0.269$
$m = 545 \times 3.5/(897 \times 6.0) = 0.354$ $Q = 1.616$

From Fig. 6:

	$Q \rightarrow$	1	1.616	3
$np = 0.10$	M_y/bd^2f_c	0.0495	(0.0612)	0.0875
	k	0.40	(0.40)	0.40
$np = 0.30$	M_y/bd^2f_c	0.0890	(0.1195)	0.180
	k	0.50	(0.50)	0.50

By interpolation,

$np = 0.1855$ $M_y/(bd^2f_c) = 0.0612 + (0.0583 \times 0.0855/0.2) = 0.0861$

$k = 0.40 + (0.10 \times 0.0855/0.2) = 0.444$

$h = 0.444/0.354 = 1.255$

$f_c = 897/(6.0 \times 3.5^2 \times 144 \times 0.0861) = 0.984$ ksi (exact 0.947 ksi)

$f_s = 10 \times 0.984\,(1 - 0.9375/1.255 - 0.893/0.444 = 1.758)$

$= -17.3$ ksi (exact -16.7 ksi)

Example 3—A section, as shown in Fig. 9, with 24—#11 bars, subjected to $N = 111$ kips, $M_x = 295$ ft-kips, and $M_y = 874$ ft-kips.

This section is not rectangular. For approximation, use actual section for the computation of np and nq, but use full dimensions for b and d. Accuracy depends on the deviation from rectangularity of the section.

$np = 0.1746$ $nq_x = 0.238$ $nq_y = 0.247$

$e_x = 0.625$ $e_y = 2.250$ $m = 0.278$ $Q = 1.518$

From Fig. 6:

	$Q \rightarrow$	1	1.518	3
$np = 0.10$	M_y/bd^2f_c	0.057	(0.067)	0.097
	k	0.395	(0.386)	0.360
$np = 0.30$	M_y/bd^2f_c	0.097	(0.120)	0.186
	k	0.500	(0.505)	0.520

$np = 0.1746$ $M_y(bd^2f_c) = 0.067 + (0.053 \times 0.0746/0.2) = 0.087$

$k = 0.386 + (0.119 \times 0.0764/0.2) = 0.430$

$h = 0.430/0.278 = 1.547$

$f_c = 874/(4.25 \times 3.5^2 \times 144 \times 0.087) = 1.34$ ksi (exact 1.30 ksi)

$f_s = 10 \times 1.35\,(1 - 0.838/1.547 - 0.893/0.430)$

$= -21.7$ ksi (exact -21.3 ksi)

Note here that in obtaining M_y/bd^2f_c from Fig. 6, $N = 0$ was assumed at first and corrected successively.

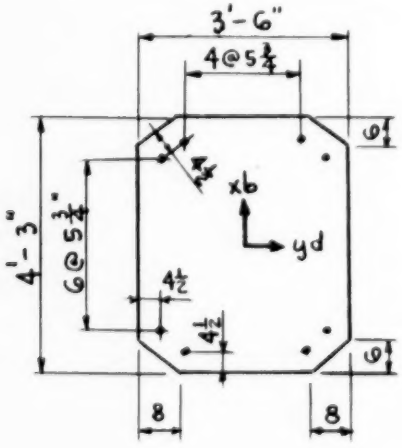

Fig. 9—Column section of Example 3, 24—#11 bars

Example 4—Same section as shown in Fig. 7 for Example 1 except that nine bars near compression corner are removed which leaves the section with only 11—#11 bars on the two sides near the tension corner. Loads on the section are the same as in Example 1.

$s_x = 3 \times 31.5/11 = 8.59$ in. $\quad s_y = 7 \times 16.5/11 = 10.50$ in.
$b = 72 + 2 \times 8.59 = 89.18$ in. $\quad d' = 42 + 2 \times 10.50 = 63.00$ in.
$e_x b = 72$ in. $\quad e_x' b' = 80.59$ in. $\quad e_x' = 0.904$
$e_y d = 56.4 \quad e_y' b' = 66.9 \quad e_y' = 1.063 \quad m = 0.904/1.063 = 0.85$

About the center of gravity of steel,
$I_x^s = 8680$ in.^{4} $\quad I_y^s = 2020$ in.^{4} $\quad A_s = 11 \times 1.56 = 17.16$ sq in.
$I^s{}_{xy} = -(17.16 \times 8.59 \times 10.50) - (1.56 \times 31.5 \times 16.5) = -2360$ in.^{4}
$\mu_x = -0.452 \quad \mu_y = -0.700$
$A_c = 89.18 \times 63.00 = 5620$ sq in. $\quad I_x^c = 3{,}723{,}400 \quad I_y^c = 1{,}858{,}000$ in.^{4}
$np = 0.0305, \quad nq_x' = 0.0127, \quad nq_y' = 0.0032, \quad Q = 0.408$

From Fig. 3, $np = 0.03$:

$Q \rightarrow$	0.408	1.0	3.0
$N/b'd'f_c$	(0.0187)	0.0201	0.0268
k	(0.48)	0.485	0.515

For $np = 0.0305 = 0.03$ (say), $\quad k = 0.48/0.85 = 0.565$
$f_c = 135/(0.0187 \times 5620) = 1.29$ ksi (exact 1.30 ksi)
$a_x' = (8.59 \times 2 + 4.5)/89.18 = 0.243 \quad a_y' = (10.50 \times 2 + 4.5)/63.0 = 0.405$
$f_s = 10 \times 1.29(1 - 0.757/0.565 - 0.595/0.48) = -20.3$ ksi (exact -20.1 ksi)
(Exact: $k = 0.670, \quad k = 0.422$)

CONCLUSION

The preceding numerical examples were picked at random and were intended to illustrate the use of the charts rather than for comparison of the results with the exact method.

Magnitude of error for the assumption of slope of neutral axis has been shown on p. 929. Error on the maximum concrete stress f_c is smaller than that on the maximum steel stress f_s; both are on the safe side. In general, the maximum error is about 1 percent in maximum concrete stress and 3 percent in maximum steel stress.

Another error is introduced by using linear interpolation for intermediate values of np between 0.03 and 0.10, and between 0.10 and 0.30. Maximum error due to this interpolation is about 2 percent in maximum stresses, also on the safe side. The total maximum error, therefore, is about 3 percent in maximum concrete stress f_c and 5 percent in maximum steel stress f_s. In ordinary cases, errors are smaller than the maximum given above.

The four charts presented in this paper for bending in two directions, with or without normal compression, of the rectangular reinforced concrete sections eliminate the ordinary trial solution. Although certain approximate assumptions are used in preparing the charts, the small error is believed acceptable for concrete structures.

BIBLIOGRAPHY

1. Parker, L. G., and Scanlon, J. J., "A Simple Analysis for Eccentrically Loaded Concrete Sections," *Civil Engineering*, V. 10, No. 10, Oct. 1940, pp. 656-657.

2. Andersen, Paul, "A Graphical Method of Analyzing Eccentrically Loaded Concrete Sections," *Civil Engineering*, V. 10, No. 1, Jan. 1940, pp. 37-39.

3. Ingerslev, E., "Rectangular Members Subjected to Moments in Two Directions," *Concrete and Constructional Engineering* (London), V. 47, No. 11, Nov. 1952, pp. 353-354.

4. Roussopoulos, A., "Die allgemeine Loesung des Problems des excentrisch beanspruchten Eisenbetonquerschnitts," *Beton und Eisen*, Mar. 1939, pp. 79-87.

5. Andersen, Paul, "Design Diagrams for Square Concrete Columns Eccentrically Loaded in Two Directions," ACI JOURNAL, Nov. 1941, *Proc.* V. 38, pp. 149-164.

6. *Deutsche Industrie Normen* (DIN) 1045, §27.

7. Pucher, Adolf, "Ueber die schiefe Biegung in Eisenbetonstaeben," *Der Bauingeneiur* (Berlin), V. 21, May 1940, pp. 131-136.

8. Loeser, B., *Bemessungsverfahren*, Wilhelm Ernst und Sohn, Berlin, 1950.

APPENDIX 1—DERIVATION OF FORMULAS

Geometric relations and forces

Consider a section as shown in Fig. 1, with known steel. In addition to the notations as shown in the figure, the following notations are used:

$n = E_s/E_c$ = modulus of elasticity of steel to that of concrete

$p = A_s/A_c$ = total area of steel to that of concrete

$q = I_s/I_c$ = moments of inertia of steel to that of concrete

ΔA_s = area of one reinforcement

I^s_{xy} = product moment of inertia of reinforcement, equal to zero for symmetrical reinforcement

$\mu_x = \dfrac{b}{md}\dfrac{I^s_{xy}}{I_x^s}$ = equal to zero for symmetrical reinforcement

$\mu_y = \dfrac{md}{b}\dfrac{I^s_{xy}}{I_y^s}$ = equal to zero for symmetrical reinforcement

$x(y)$ = subscript, indicating the quantity in $x(y)$ − direction

= linear dimension in $x(y)$ − direction, divided by $b(d)$

$f(x,y)$ = stress at point (x,y), compression as positive

Δf_x = change of average stress from $x = 0$ to $x = \frac{1}{2} - a_x$

$C = chkbdf_c/6$ = total compressive force in concrete

c = coefficient for total compressive force in concrete

$c_0b(c_1d)$ = distance of resultant of force C from edge $BC(AB)$

$T = nA_sf(0, 0)$ = total tensile force in steel

$m = e_x/e_y$

$H = (h - 1)/h$ } $H(K) = 0$

$K = (k - 1)/k$ } when $h(k) \leq 1$

As shown in Fig. 1, coordinates x and y are nondimensional; any linear dimension in the x- or y-direction is divided by b or d to give x or y, respectively. Since the deformation is a plane and Hooke's law holds, stress at any point (x, y) is

$$f(x,y) = f_c\left[1 - (0.5 - x)/h - (0.5 - y)/k\right] \quad \text{(a)}$$

By substituting for the corresponding x and y values,

$$f(-s_x, -s_y) = f_c\left[1 - (0.5 + s_x)/h - (0.5 + s_y)/k\right]$$

$$f(-0.5, 0.5) = f_c(1 - 1/h)$$

$$\Delta f_x = f_c(0.5 - a_x)/h \qquad \Delta f_y = f_c(0.5 - a_y)/k$$

The stress prisms $ABCD$ and $AEFG$ are

$C_1 = hkbdf_c/6$ and $C_2 = H^3hkbdf_c/6$

respectively. The total compressive force in concrete is then

$C = C_1 - C_2 = chkbdf_c/6$

in which $c = 1 - H^3$. The resultant of the force C_1 is $AB/4$ from edge BC, and $BC/4$ from AB. Similar relations exist for the force C_2. The location of the resultant of the force C is found by taking moments about edges BC and AB separately as

$c_b b = (hb/4)\,[(1 - 4H^3 + 3H^4)/(1 - H^3)]$
$c_d d = (kd/4)\,[(1 - H^4)/(1 - H^3)]$

Following the same process, the coefficients c, c_b, and c_d are found and summarized in the following for various cases.

$$
\left.\begin{array}{ll}
h \leqq 1 & c = 1 \\
k \leqq 1 & c_b = h/4 \\
 & c_d = k/4 \\
 & \\
h \geqq 1 & c = 1 - H^3 \\
k \leqq 1 & c_b = (h/4)\,(1 - 4H^2 + 3H^4)/(1 - H^3) \\
 & c_d = (k/4)\,(1 - H^4)/(1 - H^3) \\
 & \\
h \leqq 1 & c = 1 - K^3 \\
k \geqq 1 & c_d = (k/4)\,(1 - 4K^3 + 3K^4)/(1 - K^3) \\
 & c_b = (h/4)\,(1 - K^4)/(1 - K^3) \\
 & \\
h \geqq 1 & c = 1 - H^3 - K^3 \\
k \geqq 1 & c_b = (h/4)\,(1 - 4H^3 + 3H^4 - K^4)/(1 - H^3 - K^3) \\
\dfrac{1}{h} + \dfrac{1}{k} \geqq 1 & c_d = (k/4)\,(1 - H^4 - 4K^3 + 3K^4)/(1 - H^3 - K^3)
\end{array}\right\} \quad \text{(b)}
$$

Considering the nonsymmetric arrangement of steel, the total steel stresses can be considered as due to three causes: the total tensile force T at the centroid of steel, and two moments $M_x{}^s$ and $M_y{}^s$ about x- and y- axes, respectively.

$$T = nA_s f\,(-s_x, -s_y) = np\,[(0.5 + s_x)/h + (0.5 + s_y)/k - 1]\,bdf_c$$

$$M_x{}^s = \Sigma\,\Delta A_s f_s\,(x, y)\,xb = \Sigma\,\Delta A_s n f_c \left(1 - \frac{0.5 - x}{h} - \frac{0.5 - y}{k}\right) xb$$

$$= nf_c b\left[\frac{1}{hb^2} I_x{}^s + \frac{1}{kbd} I^s{}_{xy}\right]$$

$$= nq_x \frac{b^2 df_c}{12h}\left(1 + \frac{h}{md}\frac{I^s{}_{xy}}{I_x{}^s} = 1 + \mu_x\right)$$

$$M_y{}^s = nq_y \frac{bd^2 f_c}{12k}\left(1 + \frac{md}{b}\frac{I^s{}_{xy}}{I_y{}^s} = 1 + \mu_y\right)$$

Equilibrium equations

Three equilibrium equations, $F = 0$, $M_x = 0$, and $M_y = 0$, between all the forces on the column, give the following fundamental equations:

$$N = C - T = \frac{c}{6} hkbdf_c - np\left(\frac{1 + s_x}{2h} + \frac{1 + s_y}{2k} - 1\right) bdf_c$$

$$Ne_x b = \frac{c}{6} hkbdf_c\,(\tfrac{1}{2} - c_b)\,b + nq_x \frac{1}{12h} b^2 df_c\,(1 + \mu_x)$$

$$Ne_y d = \frac{c}{6} hkbdf_c\,(\tfrac{1}{2} - c_d)\,d + nq_y \frac{1}{12k} bd^2 f_c\,(1 + \mu_y)$$

These equations can be written in terms of nondimensional quantities as follows:

$$\frac{N}{bdf_c} = \frac{chk}{6} - np\left(\frac{1 - s_x}{2h} + \frac{1 + s_y}{2k} - 1\right) \quad (1)$$

$$\frac{N}{bdf_c} e_x = \frac{ckh}{6}(\tfrac{1}{2} - c_b) + nq_x \frac{1}{12h}(1 + \mu_x) \quad (2)$$

$$\frac{N}{bdf_c} e_y = \frac{chk}{6}(\tfrac{1}{2} - c_d) + nq_y \frac{1}{12k}(1 + \mu_y) \quad (3)$$

The maximum steel stress can be obtained by substituting the corresponding coordinates of the extreme steel,

$x = -(0.5 - a_x)$ and $y = -(0.5 - a_y)$, in Eq. (a)

$$f_s = nf_c\left(1 - \frac{1 - a_x}{h} - \frac{1 - a_y}{k}\right) \quad (4)$$

For special case of bending in one direction only, $e_x = 0$, the foregoing equations are reduced to

$$\frac{N}{bdf_c} = \frac{k}{2} - np\left(\frac{1 + s_x}{2k} - 1\right) \quad (1a)$$

$$\frac{N}{bdf_c}e_y = \frac{k}{2}\left(\tfrac{1}{2} - \frac{k}{3}\right) + nq_y\frac{1}{12k}(1 + \mu_y) \quad (3a)$$

$$f_s = nf_c\left(1 - \frac{1 - a_y}{k}\right) \quad (4a)$$

APPENDIX 2—SLOPE OF NEUTRAL AXIS FOR HOMOGENEOUS SECTIONS

For homogeneous sections, sections of the same material capable of taking both tension and compression, the stress at any point may be expressed as (see Fig. 1)

$$f = \frac{N}{bd} + \frac{M_x\,xb}{I_x} + \frac{M_y\,yd}{I_y} = \frac{N}{bd}(1 + 12e_x\,x + 12e_y\,y)$$

For the position of neutral axis, $f = 0$.

When $x = 0.5$, $y = -(1 + 6e_x)/(12e_y) = 0.5 - k$

$k = (1 + 6e_x + 6e_y)/(12e_y)$

When $y = 0.5$, $x = -(1 + 6e_y)/(12e_x) = 0.5 - h$

$h = (1 + 6e_x + 6e_y)/(12e_x)$

The slope of the neutral axis is then $m = k/h = e_x/e_y$.

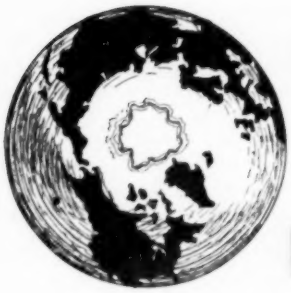

Letters from Readers*

BY WAY OF SYNOPSIS

BRYANT MATHER offers a suggestion for a uniform set of permeability units.

A tentative standard for designing continuity splices is suggested by J. EDWARD MARTIN.

A design procedure for individual, centrally-loaded, square footings is presented by HARRY ZAREMBA and ROBERT FORSTER.

Tables giving coefficients for two-way slab design are presented by ANTONIO M. GOMEZ.

Permeability Units (LR 51-20)

The permeability of a porous material is given by the volume of flow of a fluid during unit time through a volume of the material having unit cross-sectional area and unit thickness when unit pressure difference exists between the ends. In addition to defining the properties of the fluid, there are thus five quantities involved each of which must be expressed in some units of measurement. A variety of units have been used as follows:

Amount of flow	Time	Area	Thickness	Pressure difference
cc (or ml)	sec	cm^2	mm	cm head
l	min	ft^2	cm	ft head
gram	hr	dm^2*	in.	atm
mm^3	day		ft	psi
μl**	year			dynes per cm^2
cu ft				
bbl				
gal.				

*Sq decimeters.
**Microliters.

It may be noted that when the expression of permeability includes a factor for the viscosity of the fluid, for example:

$$K = \frac{\text{poises} \times \text{cm}^3 \times \text{cm}}{\text{sec} \times \text{cm}^2 \times \text{atm}}$$

K has the dimensions L^2.[18] The coefficient K_2 as used by Powers and Brownyard[16, p. 886] is in sq cm. If viscosity is not included, the dimensions are those of rate L/T. In certain fields, values for coefficient of permeability are expressed as rate (cm per sec).[19] The constant K_1 as used by Powers and Brownyard[16, p. 865] defined as "depending on the properties of the porous medium and the kinematic viscosity of the fluid" has the units cm per sec. In other cases where specimen dimensions and other test conditions are constant, permeability has been expressed in amount of flow (volume or weight) per unit time.[11-14]

The choice of units has varied with the nature of the investigations made and with the customs of the technology involved. The American Petroleum Institute Code No. 27[1] gives a table for converting between six different sets of units as follows:

*A part of copyrighted JOURNAL OF THE AMERICAN CONCRETE INSTITUTE, V. 26, No. 9, May 1955. *Proceedings* V. 51. Separate prints of the entire Letters from Readers section are available at 50 cents each. Address 18263 W. McNichols Rd., Detroit 19, Mich.

Amount of flow	Time	Area	Thickness	Pressure difference
1. cc	sec	cm^2	cm	atm
2. cc	sec	cm^2	cm	dynes per cm^2
3. cu ft	sec	ft^2	ft	psi
4. cc H_2O (20 C)	sec	cm^2	cm	cm H_2O
5. bbl H_2O (20 C)	day	ft^2	ft	psi
6. gal. H_2O (20 C)	min	ft^2	ft	ft H_2O

Norton[2] gives a table of nine combinations that have been employed by various workers in the field of gas permeation as follows:

Amount of flow	Time	Area	Thickness	Pressure difference
1. cc	sec	cm^2	mm	cm
2. cc	hr	cm^2	mm	atm
3. g	sec	cm^2	mm	atm
4. mm^3	day	cm^2	mm	atm
5. cc	sec	cm^2	mm	atm
6. cc	sec	cm^2	mm	cm
7. μl*	hr	cm^2	mm	atm
8. cc	sec	cm^2	cm	atm
9. cc	hr	dm^2	mm	atm

*Microliters.

Determinations of the permeability of concrete have been reported in several different sets of units, and a number of reports have given relative data for the specimens tested without indicating some of the quantities needed for a complete expression of permeability. Those noted include:

Amount of flow	Time	Area	Thickness	Pressure difference	Reference
cu ft	sec	ft^2	ft	ft head	3, 4, 10
cc	hr or day	ft^2	in.	psi	5
gal.	hr	ft^2	—	psi	6, 7, 8
cc	hr	ft^2	—	ft head	9
gram	day	—	—	—	11
gram	hr	ft^2	—	—	12
cc	hr	—	—	psi	13
l	hr	—	—	—	14

Powers and Brownyard[16, p. 865] introduce their discussion of permeability of portland cement paste by giving an expression for permeability in terms of cc, sec, cm^2, cm, and cm head, in the order of the above tabulations.

Powers, Copeland, Hayes, and Mann[17] in a further discussion of permeability of cement paste give an expression in terms of cc, sec, cm^2, cm, and dynes per cm^2.

Fancher, Lewis, and Barnes[15] have defined the unit of permeability in cgs units as the *darcy*, stating that a porous medium has a permeability of 1 darcy if, in a section 1 sq cm in area perpendicular to the flow, 1 cc of fluid of unit viscosity travels 1 cm per sec under a pressure drop of 1 atmosphere. This unit has been generally adopted in the petroleum industry and in certain other fields. API Code 27[1] restates the definition as follows: "A medium has a permeability of 1 darcy when the rate of flow through it in milliliters per second per square centimeter of cross section area, of a fluid of one centipoise viscosity, under a pressure of one atmosphere per centimeter and conditions of viscous flow, is unity." "Conditions of viscous flow" means that the rate of flow is sufficiently low to be directly proportional to the pressure or hydraulic gradient. One millidarcy = 0.001 darcy.

It will be noted that the units of the darcy are those given as Item 1 in the table taken from API Code 27 and as Item 8 in the list taken from Norton's paper. The units given by Powers and associates[16, 17] differ only in the units for pressure drop.

It is suggested that, for simplicity, uniformity, and ease of presentation, serious consideration be given to the use of the darcy (or millidarcy) as the unit of permeability in as many sorts of measurements as possible.

REFERENCES

1. "Standard Procedure for Determining Permeability of Porous Media," *Code* No. 27, American Petroleum Institute, 2nd Edition, Apr. 1942.

2. Norton, Francis J., "Helium Diffusion Through Glass," *Journal*, American Ceramic Society, V. 36, Mar. 1953, p. 90.

3. Cook, Herbert K., "Permeability Tests of Lean Mass Concrete," *Proceedings*, American Society for Testing Materials, V. 51, 1951, p. 1156.

4. Ruettgers, Arthur, Vidal, E. N., and Wing, S. P., "An Investigation of the Permeability of Mass Concrete with Particular Reference to Boulder Dam," ACI JOURNAL, Mar.-Apr. 1935, *Proc.* V. 31, pp. 382-416.

5. McMillan, F. R., and Lyse, Inge, "Some Permeability Studies of Concrete," ACI JOURNAL, Dec. 1929, *Proc.* V. 26, pp. 101-142.

6. Norton, Paul T., Jr., and Pletta, Dan H., "The Permeability of Gravel Concrete,"

ACI JOURNAL, May 1931, *Proc.* V. 27, pp. 1093-1132.

7. Washa, George W., "The Efficiency of Surface Treatments on the Permeability of Concrete," ACI JOURNAL, Sept.-Oct. 1933, *Proc.* V. 30, pp. 1-8.

8. Washa, George W., "Comparison of the Physical and Mechanical Properties of Hand Rodded and Vibrated Concrete Made with Different Cements," ACI JOURNAL, June 1940, *Proc.* V. 36, pp. 617-648.

9. Dunagan, W. M., "Methods for Measuring the Passage of Water Through Concrete," *Proceedings*, American Society for Testing Materials, V. 39, 1939, p. 866.

10. Wiley, George, and Coulson, D. C., "A Simple Test for Water Permeability of Concrete," ACI JOURNAL, Sept.-Oct. 1937, *Proc.* V. 34, pp. 65-76.

11. Pearson, J. C., and Adams, R. F., "Low Head Permeability Tests of Mortar Pots," ACI JOURNAL, Feb. 1939, *Proc.* V. 35, pp. 285-288.

12. Barre, H. J., "Some Observations of the Water Vapor Permeability of Concrete," *Proceedings*, American Society for Testing Materials, V. 39, 1939, p. 860.

13. Davis, Raymond E., Kelly, J. W., Troxell, G. E., and Davis, Harmer E., "Properties of Mortars and Concretes Containing Portland-Puzzolan Cements," ACI JOURNAL, Sept.-Oct. 1935, *Proc.* V. 32, pp. 80-114.

14. Mary, M., discussion of the Ruettgers-Vidal-Wing paper "An Investigation of the Permeability of Mass Concrete with Particular Reference to Boulder Dam," ACI JOURNAL, Sept.-Oct. 1935, *Proc.* V. 32, pp. 125-129.

15. Fancher, G. H., Lewis, J. A., and Barnes, K. B., "Some Physical Characteristics of Oil Sands," *Bulletin* No. 12, Pennsylvania State College Mining and Industrial Experiment Station, 1953, pp. 65-163.

16. Powers, T. C., and Brownyard, T. L., "Studies of the Physical Properties of Hardened Portland Cement Paste," ACI JOURNAL, *Proc.* V. 43, Oct. 1946, pp. 101-132; Nov. 1946, pp. 249-336; Dec. 1946, pp. 469-504; Jan. 1947, pp. 549-604; Feb. 1947, pp. 669-712; Mar. 1947, pp. 845-880; Apr. 1947, pp. 933-992.

17. Powers, T. C., Copeland, L. E., Hayes, J. C., and Mann, H. M., "The Permeability of Portland Cement Paste," ACI JOURNAL, Nov. 1954, *Proc.* V. 51, pp. 285-300.

18. Dallavalle, J. M., *Micromeritics*, 2nd Edition, 1948, Putnam Publishing Co., New York, N. Y., p. 265.

19. Hvorslev, M. J., "Time Lag and Soil Permeability in Ground-Water Observations," *Bulletin* No. 36, Waterways Experiment Station, 1951.

BRYANT MATHER,
Jackson, Miss.

Continuity Splices (LR 51-21)

The ACI Building Code contends that continuity splices in reinforcing bars should be avoided in regions where concrete is in tension. It goes on to say that where such splices are necessary, special precautions shall be taken.

From these remarks of the ACI Building Code each engineer proceeds on his own interpretations of what "special considerations" he shall take. There are numerous points of view that may be taken by different designers on criteria that need to be satisfied if one is to make an effective splice, but there is no recommended practice to be found in engineering codes or texts.

To reach a point of consistent practice we have prepared a tentative specification for making such continuity splices in hope that the proper committees of the American Concrete Institute and other code and industry committees will consider them to the end that the industry shall have an effective yardstick to control these splices.

Modest research into trade practices points up some glaring, dangerous misconceptions of conditions to be maintained to preserve continuity. A number of reinforcing steel placing crews were interviewed, as were a number of highly experienced field inspectors, regarding the conditions that they normally

maintained when making continuity splices. We were not able to establish anything approaching a uniform practice. Quite the contrary, many field practices are extremely dangerous; to wit, lapping beam bars in a vertical plane.

On the other hand, in discussing the problem with a number of structural designers, we find a reasonably consistent opinion on conditions to be maintained. Therefore, it is apparent that the intention of the designers is not reaching the placing crews and we think the subject is worthy of considerable attention by structural engineers.

Our studies of the subject indicate that there are two principal factors that need specific consideration by designers. These should be accounted for by appropriate notation on engineering drawings.

First, the general notes of structural drawings need to clearly establish that the lap shall be made with the two bars at the same effective depth (Fig. 1).

Secondly, stresses in the concrete due to wedging action of deformations on the bars needs consideration and we suggest stirrups of ¼ bar diameter to resist these forces.

The following tentative specification is submitted in the hope that it will prompt considerable discussion, and such comment will be of value to the appropriate ACI committee.

Tentative design criteria for tension splices in reinforcing concrete

Until such time as additional test data become available to more accurately define the conditions which must be met in making continuity splices in regions of tension, the following procedure is recommended as conservative practice.

I—Lapped splices

(a) The length of lap shall be computed from the relation

$$L = (f_s D)/4u$$

where f_s is the actual steel stress (to be taken at not less than 10,000 psi), D is the diameter of the bar in in., and u is the allowable bond stress and shall have the following values, not to exceed 245 psi for top bars or 350 psi for all others:

Top bars*	without stirrups	$u = 0.038 f_c'$
Top bars	with stirrups	$u = 0.07 f_c'$
All others	without stirrups	$u = 0.055 f_c'$
All others	with stirrups	$u = 0.10 f_c'$

*As defined in ACI Building Code.

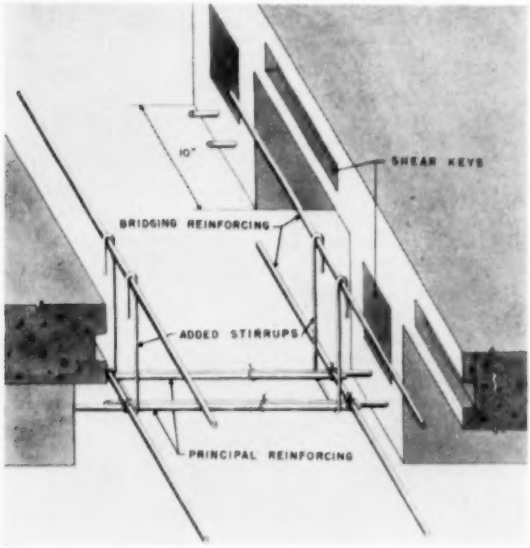

Fig. 1—Splice provisions at section of maximum moment

(b) In all such splices the bars shall be in contact and wired together side by side at the same effective depth. The clear distance between adjacent pairs of spliced bars shall not be less than one bar diameter or 1 in. whichever is greater. Such bars may be offset by bending where the slope is not more than 1 in 12.

(c) Where such splices occur in joist-type construction, bridging shall be required at each end of the splice.

(d) When stirrups are used, one shall be placed at each end of the lap splice and the diameter of such stirrup shall be $\frac{1}{4}$ the bar diameter and not less than $\frac{1}{4}$ in.

II—Welded splices

(a) Lapped splices shall be made with a $\frac{3}{16}$-in. minimum fillet weld which may be designed using one-half allowable weld stress.

(b) Butt welds may be employed using full weld stress and with proper end preparation prior to welding.

(c) For all grades of reinforcing steel the welding electrode shall be AWS-E7016.

(d) Where such splices occur in joist-type construction, bridging shall be required at the splices.

Discussion

The formula $L = (f_s D)/4u$ needs no further explanation as it may be found in any standard textbook on reinforced concrete design. Allowable bond stress, however, must be carefully chosen and its magnitude must come from tests with a proper factor of safety (F.S.) applied. For this discussion a factor of safety of 2 has been used. If $mf_c' = u$ then using an ultimate value of u from tests,

$$m = \frac{u}{f_c' \text{ (F.S.)}}$$

Substituting in the first equation yields

$$u = \frac{f_s D}{4 L} \text{ or } m = \frac{f_s D}{4 L f_c' \text{ (F.S.)}}$$

From reference 1, pp. 16 and 32, the solution is $m = 60D/(4 \times 30D \times 4700 \times 2) = 0.053$ and from reference 2, p. 887, the solution for the allowable is $m = 225/4000 = 0.056$. As the latter reference employed the new A305 bars, it was concluded that allowable bond stress for reinforcing conforming to ASTM A305 should be $u = 0.055 f_c'$ when no special ties or stirrups are used. If ties are used to take care of splitting tensile stresses which arise from wedging action of deformations, the value of u may go to present code values. This is made clear by reference 2, p. 886, under conclusion item 4(a).

It was considered wise to use blocking at tension lap splices in joists and to side lap and wire tie such bars to minimize splitting tendencies arising from bar eccentricities. Also to avoid sections of unreinforced concrete lapped bars must be in the direction of stress and at the same effective depth. This conclusion is verified by reference 3, Sec. 2610 (e).

The only factor which needs special consideration under welded splices is in the choice of a proper welding electrode. As reinforcing steel of intermediate grade has approximately twice as much carbon content as structural steel, care must be exercised in welding such a bar or its structural strength will be lowered. Therefore the low hydrogen electrode AWS-E7016 must be used.

It is believed that within these working stresses and conditions the recommendations outlined will safeguard the splices against the types of failures outlined in references 1 and 2. The method advocated for computing length of lap is rational as it relates factors known to influence the strength of such a splice, and its performance is based on test values reduced by a factor of safety consistent with reinforced concrete design. By using this procedure a safe design is obtained, but flexibility is not sacrificed.

References

1. Kluge, Ralph W., and Tuma, Edward C., "Lapped Bar Splices in Concrete Beams," ACI JOURNAL, Sept. 1945, *Proc.* V. 42, pp. 13-33.

2. Ferguson, Phil M., Turpin, Robert D., and Thompson, J. Neils, "Minimum Bar Spacing as a Function of Bond and Shear Strength," ACI JOURNAL, June 1954, *Proc.* V. 50, pp. 869-887.

3. *Uniform Building Code*, 1952 Edition, V. 2, Pacific Coast Building Officials Conference, Los Angeles, Calif.

J. EDWARD MARTIN, Chief of Engineering, Albert C. Martin and Associates, Architects and Engineers, Los Angeles, Calif.

Simplified Design Procedure for Individual, Centrally-Loaded, Square Footings (LR 51-22)

Although individual, centrally-loaded, reinforced concrete, square footings present little design difficulty, they can at times create tedious work if encountered in large numbers with wide ranges in superimposed load. On frequent occasions, a designer finds sources of tabulated footing designs limited in scope or not in accord with the flexural and bond criteria of Sec. 1204(e) and Sec. 1205(e) of the ACI Building Code. For these reasons, the writers have been prompted to develop a general design procedure which reduces the conventional trial and error design processes to a minimum, and affords great rapidity in checking footing proportions.

The procedure is applicable to all concrete compressive strengths equal to or greater than 2500 psi which according to the ACI Building Code have a constant maximum allowable unit shear stress (75 lb per sq in.). In the rare event that a lower concrete strength is used, extension in application can be made readily by preparing a graph similar to Fig. 1 for the appropriate unit shear stress.

Notation

W = load on footing exclusive of footing weight and overburden, kips
P = unit soil pressure under footing due to W, ksf
u = unit bond stress, ksi
f_s = unit steel stress, ksi
B = side dimension of footing, in.
b = side dimension of either a square column, square pier, or, if round columns or metallic bases rest directly on footing, side dimension as determined from consideration of Sec. 1208(a) or Sec. 1204(b-3) of the ACI Building Code, in.
d = effective depth of footing, in.
D_t = theoretical diameter of reinforcing bar when u and f_s are equal to maximum allowable values simultaneously, in.
D = selected nominal diameter of reinforcing bar, in.
N = number of reinforcing bars in each direction

Method

The method is as follows:

(1) Determine required footing area in usual manner from W, overburden, assumed weight of footing, and allowable soil bearing pressure.

(2) Compute P, and ratio B/b.

(3) From Fig. 1, determine

$$d/b = \phi\,(P, B/b) = \frac{-(P+vj)+\left[P(P+2vj)(B/b)^2+(vj)^2\right]^{1/2}}{2(P+2vj)} \quad \text{(a)}$$

and compute $d = b\,\phi\,(P, B/b)$. This is the minimum effective depth required for allowable unit shear stress (v = 75 lb per sq in., j = 7/8). Note: In using Eq. (a), P and v must be in the same units.

At this point, if concrete columns rest directly on the footing, the designer can at his discretion increase d for proper development of dowels or retain computed value and increase number of dowels where column design permits.

(4) Calculate theoretical bar diameter by equating the general mathematical expressions for effective depth of footing required for both allowable bond and flexural stresses. It is not predicated upon the length of bar given by $L = (f_s D)/4u$ necessary to develop the induced bar stress since, in general, this requirement is more than satisfied by the footing proportions determined from the allowable soil pressure.

Effective depth of footing required by allowable bond stress is

$$d = \frac{W(B-b)}{2\pi juBD_tN} \times 0.85 \quad \text{(1)}$$

Effective depth required by allowable steel stress is

$$d = \frac{W(B-b)^2}{2\pi jf_sBD_t^2N} \times 0.85 \quad \text{(2)}$$

Equating (1) and (2) gives

$$D_t = \frac{u}{f_s}(B-b) \quad \text{(b)}$$

using allowable unit stresses

(5) Select a nominal bar diameter D nearest D_t, then, (a) if $D < D_t$, compute u from Eq. (b) using f_s = 20 ksi and $D_t = D$ or (b) if $D > D_t$, compute f_s from Eq. (b) using u = allowable bond stress and $D_t = D$.

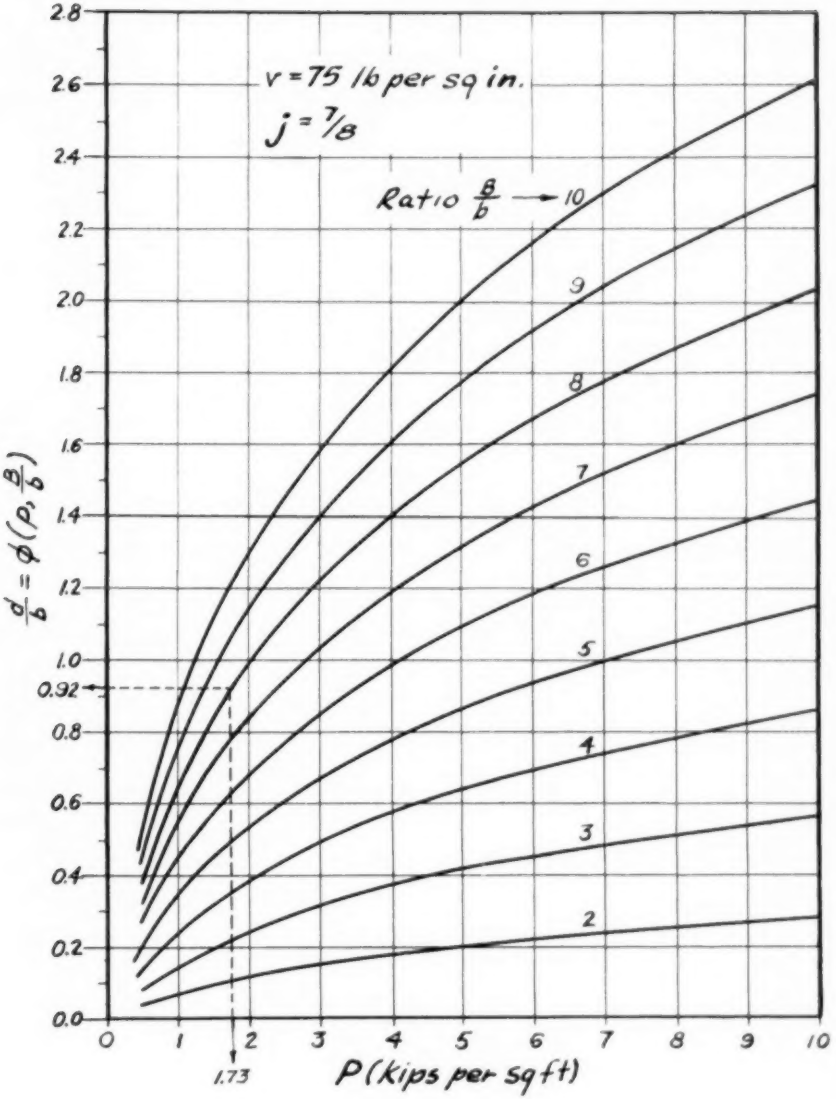

Fig. 1—Relationship between the d-b ratio and P for various B-b ratios

(6) Determine number of bars by substituting the expression for theoretical bar diameter in either Eq. (1) or (2).

$$N = \frac{Wf_s}{6.47Bda^2} \quad \ldots\ldots\ldots\ldots\ldots\ldots\ldots\ldots\ldots\ldots (c)$$

using a and f_s from 5a or 5b depending on how D was selected. It will be noted that the unit concrete compressive stress is not considered in the procedure since this stress is never a critical factor of footing design.

Sample design

Data: Assume allowable soil bearing pressure $P = 2$ ksf, $W = 200$ kips, $f_c' = 2500$ psi, $a = 0.20$ ksi allowable, $b = 16$ in., $f_s = 20$ ksi. Assumed footing weight = 11 percent of $W = 22$ kips.

(1) Area $= 222/2 = 111$ sq ft
$B = 10.53$ ft or, say 10 ft 9 in. $= 129$ in.
(2) $P = 200/10.75^2 = 1.73$ ksf
$B/b = 129/16 = 8.06$
(3) From Fig. 1, $\phi\,(P, B/b) = 0.92$
$d = 16 \times 0.92 = 14.7$ in., say 15 in.

(4) $D_t = \dfrac{0.2}{20}(129 - 16) = 1.13$ in.

(5) Select #8 bars, $D = 1.0$ in. $(D < D_t)$

and, $a = \dfrac{1.0 \times 20}{129 - 16} = 0.177$ ksi

$(f_s = 20$ ksi)

(6) $N = \dfrac{200 \times 20}{6.47 \times 129 \times 15 \times 0.177^2} =$

10.2, say 11—#8 bars

Thus, design is complete and footing size is 10 ft 9 in. square, total depth $= 15 + 4 = 19$ in., and reinforcement is 11—#8 bars each way.

HARRY ZAREMBA and ROBERT FORSTER, Senior Engineers, H. K. Ferguson Co., Engineers and Builders, Cleveland, Ohio

Coefficients for Two-Way Slab Design (LR 51-23)

Below are tables giving coefficients for two-way slab design according to Method 1 of "Building Code Requirements for Reinforced Concrete (ACI 318-51)," Chapter 7, Section 709c.

The reason for compiling the tables was to have available for design purposes coefficients for bending moments, for different types of support, as a function of the ratio of the spans $\epsilon = L_1/L$.

Sample calculations are given below for each support condition.

Case 1 (Table 1)—Four discontinuous edges

$M = c_1 B w L^2$, $M_1 = c B_1 w L_1^2$

If $B = B_1 = 1/8$, then, $C = 1/8 c_1$, $C_1 = 1/8 c$

i.e., $r = \epsilon = \dfrac{L_1}{L} = 0.90$

From ACI 318-51 p. 616, $c = 0.40$, $c_1 = 0.27$ therefore

$C = 1/8\ 0.27 = 0.034$, $C_1 = 1/8\ 0.40 = 0.05$

Values of C and C_1 for values of ϵ from 0.5 to 2 are tabulated.

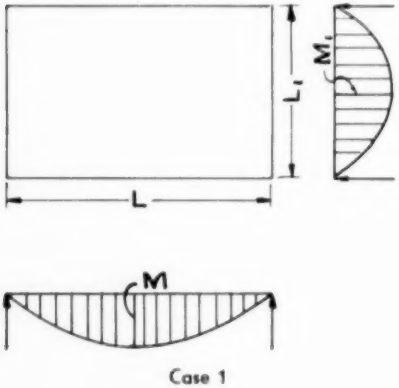

Case 1

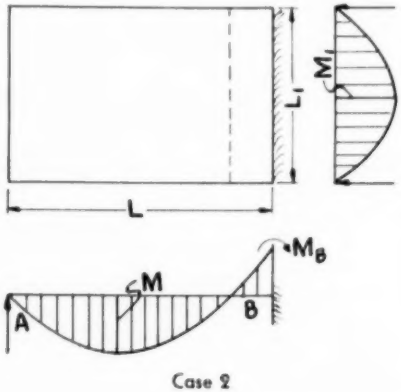

Case 2

Case 2 (Table 2)—One edge continuous

$M = {}^1\!/_{12} c_1 w L^2$, $M_1 = {}^1\!/_8 c w L_1^2$,
$M_B = {}^1\!/_8 c_1 w L^2$

$$r = \frac{L_1}{0.87L} = 1.15\frac{L_1}{L} = 1.15\epsilon$$

i.e., $\epsilon = 0.90$, $r = 1.15 \times 0.90 = 1.035$
For $r = 1.035$, from ACI 318-51, p. 616

$$c = 0.33 - 0.05 \times \frac{3.5}{10} = 0.33 - 0.0175 = 0.3125$$

$$c = 0.33 + 0.06 \times \frac{3.5}{10} = 0.33 + 0.021 = 0.351$$

Then, $C = {}^1\!/_{12}\,0.351 = 0.0292$
$C'' = {}^1\!/_8\,0.351 = -0.0438$
$C_1 = {}^1\!/_8\,0.3125 = 0.0391$

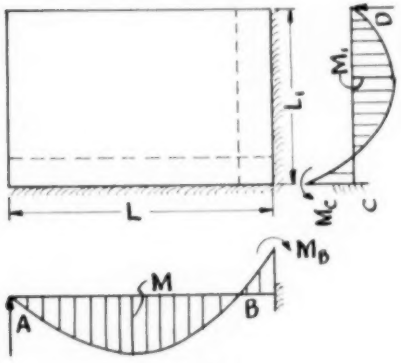

Case 3

Case 3 (Table 3)—Two adjacent edges continuous

$M = {}^1\!/_{12} c_1 w L^2$, $M_1 = {}^1\!/_{12} c w L_1^2$,
$M_B = -{}^1\!/_{10} c_1 w L^2$, $M_c = -{}^1\!/_{10} c w L_1^2$

$$r = \frac{0.87L_1}{0.87L} = \frac{L_1}{L} = \epsilon$$

i.e., $r = \epsilon = 0.90$

From ACI 318-51, p. 616 $c = 0.40$, $c_1 = 0.27$
then, $C = {}^1\!/_{12}\,0.27 = 0.0225$
$C'' = -{}^1\!/_{10}\,0.27 = -0.027$ (for M_B)
$C_1 = {}^1\!/_{12}\,0.40 = 0.0333$
$C_1' = -{}^1\!/_{10}\,0.40 = -0.040$ (for M_c)

Case 4 (Table 4)—Two opposite edges continuous

$M = {}^1\!/_{16} c_1 w L^2$, $M_1 = {}^1\!/_8 c w L_1^2$,
$M_A = M_B = -{}^1\!/_{10} c_1 w L^2$

$$r = \frac{L_1}{0.76L} = 1.318\frac{L_1}{L} = 1.318\,\epsilon$$

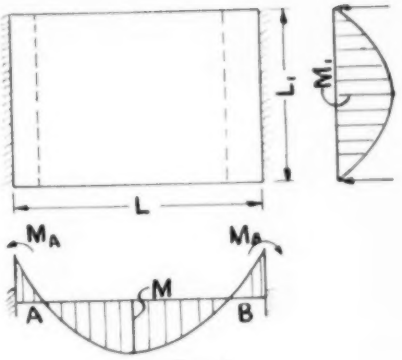

Case 4

i.e., $\epsilon = 0.90$, $r = 1.318 \times 0.90 = 1.185$
From ACI 318-51, p. 616

$$c = 0.28 - 0.05\frac{8.5}{10} = 0.28 - 0.0425 = 0.2375$$

$$c_1 = 0.39 + 0.06\frac{8.5}{10} = 0.39 + 0.051 = 0.441$$

Then, $C = {}^1\!/_{16}\,0.441 = 0.0276$,
$C'' = -{}^1\!/_{10}\,0.441 = 0.0441$
$C_1 = {}^1\!/_8\,0.2375 = 0.0295$,

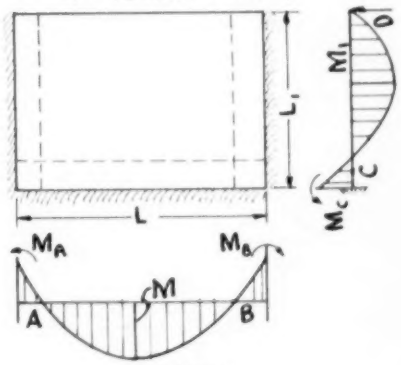

Case 5

Case 5 (Table 5)—Three continuous edges

$M = {}^1\!/_{16} c_1 w L^2$, $M_1 = {}^1\!/_{12} c w L_1^2$,
$M_A = M_B = -1/11 c_1 w L^2$, $M_c = -{}^1\!/_{10} c w L_1^2$
$r = 0.87L_1/0.76L = 1.145L_1/L = 1.145\epsilon$
i.e., $\epsilon = 0.90$, $r = 1.145 \times 0.90 = 1.03$
From ACI 318-51, p. 616
$c = 0.33 - 0.05 \times {}^3\!/_{10} = 0.33 - 0.015 = 0.315$
$c_1 = 0.33 + 0.06 \times {}^3\!/_{10} = 0.33 + 0.018 = 0.348$
Then, $C = {}^1\!/_{16} c_1 = {}^1\!/_{16}\,0.348 = 0.0219$
$C_1 = {}^1\!/_{12} c = {}^1\!/_{12}\,0.315 = 0.0262$
$C'' = -1/11 c_1 = -1/11\,0.348 = -0.0316$
$C_1' = -{}^1\!/_{10} c = -{}^1\!/_{10}\,0.315 = -0.0315$

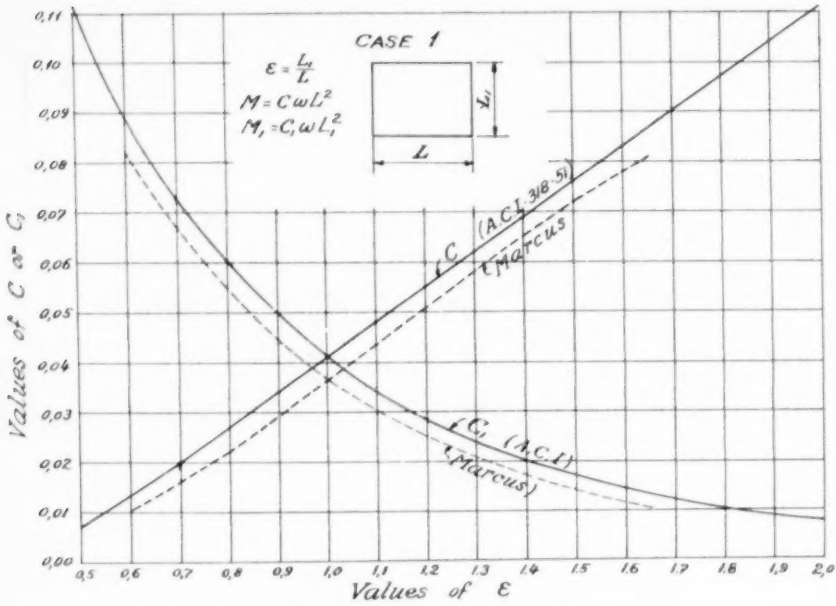

Fig. 1—C and C_1 as a function of ϵ

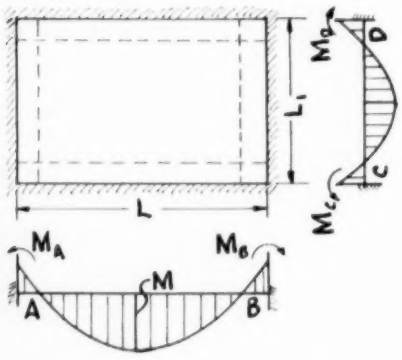

Case 6

Case 6 (Table 6)—Four edges continuous

$M = \frac{1}{16}c_1\omega L_1^2, \qquad M_1 = \frac{1}{16}c\omega L_1^2$

$M_A = M_B = -1/11c_1\omega L^2$

$M_C = M_D = -1/11c\omega L_1^2$

$$r = \frac{0.76L_1}{0.76L} = \frac{L_1}{L} = \epsilon$$

i.e., $r = \epsilon = 0.90$

From ACI 310-51, p. 616,

$c = 0.40, \qquad c_1 = 0.27$

Then $C = \frac{1}{16}\,0.27 = 0.0169$

$C_1 = \frac{1}{16}\,0.40 = 0.025$

$C' = -1/11\,0.27 = -0.0246$

$C_1' = -1/11\,0.40 = -0.0364.$

TABLE 1—FOUR DISCONTINUOUS EDGES

ϵ	C	C_1
0.50	0.0075	0.111
0.55	0.0106	0.099
0.60	0.0137	0.0875
0.65	0.0169	0.080
0.70	0.020	0.0725
0.75	0.0237	0.0662
0.80	0.0269	0.060
0.85	0.0306	0.0545
0.90	0.0340	0.050
0.95	0.0375	0.0452
1.00	0.0412	0.0412
1.05	0.0445	0.0378
1.10	0.0481	0.035
1.15	0.0517	0.0315
1.20	0.0552	0.0288
1.25	0.0587	0.026
1.30	0.0620	0.0238
1.35	0.0657	0.0219
1.40	0.0692	0.020
1.45	0.0726	0.0188
1.50	0.0762	0.017
1.55	0.0798	0.0156
1.60	0.0832	0.0144
1.65	0.0868	0.0131
1.70	0.0904	0.0119
1.75	0.0939	0.0108
1.80	0.0975	0.010
1.85	0.101	0.0094
1.90	0.104	0.00875
1.95	0.108	0.0081
2.00	0.111	0.0075

TABLE 2—ONE EDGE CONTINUOUS

ϵ	C	C_1	C'
0 50	0 00766	0 0934	−0 0115
0 55	0 010	0 0822	−0 0150
0 60	0 0123	0 0725	−0 0185
0 65	0 0150	0 0660	−0 0225
0 70	0 0178	0 0596	−0 0267
0 75	0 0206	0 0537	−0 0309
0 80	0 0234	0 0482	−0 0351
0 85	0 0263	0 0435	−0 0384
0 90	0 0292	0 0391	−0 0438
0 95	0 0318	0 0355	−0 0476
1 00	0 0348	0 0318	−0 0522
1 05	0 0385	0 0284	−0 0577
1 10	0 0405	0 0256	−0 0607
1 15	0 0434	0 0228	−0 0651
1 20	0 0464	0 0208	−0 0696
1 25	0 0486	0 0190	−0 0729
1 30	0 0506	0 0177	−0 0759
1 35	0 0529	0 0161	−0 0784
1 40	0 0554	0 0146	−0 0829
1 45	0 0585	0 0132	−0 0875
1 50	0 0615	0 0119	−0 0920
1 55	0 0646	0 0106	−0 0967
1 60	0 0671	0 0096	−0 1006
1 65	0 0695	0 00875	−0 104
1 70	0 0720	0 0081	−0 108
1 75	0 0741	0 0075	−0 111
1 80	0 0743	0 0073	−0 1114
1 85	0 0746	0 0071	−0 1118
1 90	0 0748	0 0069	−0 1122
1 95	0 0751	0 0067	−0 1126
2 00	0 0753	0 0065	−0 113
ϵ'*	C_1	C	C_1'

*$\epsilon' = L/L_1$, with side L continuous.

TABLE 3—TWO ADJACENT EDGES CONTINUOUS

ϵ	C	C_1	C'	C_1'
0 50	0 005	0 0741	−0 006	−0 089
0 55	0 0071	0 0658	−0 0085	−0 079
0 60	0 0092	0 0584	−0 0110	−0 070
0 65	0 0113	0 0534	−0 0136	−0 064
0 70	0 0133	0 0484	−0 016	−0 058
0 75	0 0158	0 0442	−0 019	−0 053
0 80	0 0179	0 0400	−0 0215	−0 048
0 85	0 0204	0 0363	−0 0245	−0 0436
0 90	0 0227	0 0333	−0 0272	−0 040
0 95	0 025	0 0302	−0 030	−0 0362
1 00	0 0275	0 0275	−0 033	−0 033
1 05	0 0296	0 0252	−0 0356	−0 0302
1 10	0 0321	0 0234	−0 0385	−0 028
1 15	0 0345	0 0210	−0 0414	−0 0252
1 20	0 0370	0 0192	−0 0442	−0 023
1 25	0 0392	0 0173	−0 0470	−0 0208
1 30	0 0413	0 0158	−0 0495	−0 019
1 35	0 0438	0 0146	−0 0526	−0 0175
1 40	0 0462	0 0133	−0 0554	−0 016
1 45	0 0484	0 0125	−0 0572	−0 015
1 50	0 0508	0 0113	−0 0610	−0 0136
1 55	0 0532	0 0104	−0 0638	−0 0125
1 60	0 0555	0 0096	−0 0666	−0 0115
1 65	0 0579	0 0088	−0 0695	−0 0105
1 70	0 0603	0 0079	−0 0724	−0 0095
1 75	0 0625	0 00716	−0 075	−0 0086
1 80	0 0650	0 00666	−0 078	−0 0080
1 85	0 0671	0 00625	−0 0805	−0 0075
1 90	0 0695	0 00583	−0 0834	−0 0070
1 95	0 0718	0 00541	−0 0862	−0 0065
2 00	0 0741	0 005	−0 089	−0 0060

TABLE 4—TWO OPPOSITE EDGES CONTINUOUS

ϵ	C	C_1	C'
0 50	0 0084	0 0781	−0 0135
0 55	0 0104	0 0693	−0 0166
0 60	0 0128	0 0606	−0 0205
0 65	0 0153	0 0538	−0 0245
0 70	0 0178	0 0477	−0 0284
0 75	0 0202	0 0422	−0 0324
0 80	0 0226	0 0376	−0 0362
0 85	0 0252	0 0335	−0 0403
0 90	0 0276	0 0295	−0 0442
0 95	0 0300	0 0262	−0 0480
1 00	0 0324	0 0229	−0 0519
1 05	0 0350	0 0205	−0 0560
1 10	0 0368	0 0187	−0 0589
1 15	0 0385	0 0169	−0 0616
1 20	0 0405	0 0155	−0 0649
1 25	0 0428	0 0138	−0 0686
1 30	0 0456	0 0121	−0 0730
1 35	0 0482	0 0105	−0 0773
1 40	0 0506	0 0095	−0 0809
1 45	0 0528	0 0086	−0 0844
1 50	0 0548	0 0077	−0 0876
1 55	0 0556	0 00738	−0 0892
1 60	0 0557	0 00720	−0 0895
1 65	0 0559	0 00702	−0 0897
1 70	0 0561	0 00684	−0 0900
1 75	0 0563	0 00666	−0 0903
1 80	0 0565	0 00648	−0 0906
1 85	0 0567	0 00630	−0 0909
1 90	0 0569	0 00612	−0 0911
1 95	0 0571	0 00594	−0 0914
2 00	0 0573	0 00575	−0 0916
ϵ'*	C_1	C	C_1'

*$\epsilon' = L/L_1$, with sides L continuous.

TABLE 5—THREE CONTINUOUS EDGES

ϵ	C	C_1	C'	C_1'
0 50	0 00575	0 0625	−0 00836	−0 0751
0 55	0 0075	0 0548	−0 0109	−0 0657
0 60	0 00925	0 0483	−0 0135	−0 058
0 65	0 01125	0 044	−0 0164	−0 053
0 70	0 0133	0 0397	−0 0194	−0 048
0 75	0 01545	0 0358	−0 0225	−0 043
0 80	0 0176	0 0322	−0 0256	−0 039
0 85	0 0197	0 0290	−0 0286	−0 035
0 90	0 0219	0 0261	−0 0319	−0 0312
0 95	0 0239	0 0237	−0 0348	−0 0284
1 00	0 0261	0 0212	−0 0380	−0 0255
1 05	0 0283	0 0189	−0 0412	−0 0230
1 10	0 0304	0 0171	−0 0442	−0 0205
1 15	0 0325	0 0152	−0 0472	−0 0184
1 20	0 0348	0 0139	−0 0506	−0 0167
1 25	0 0365	0 0127	−0 0531	−0 0152
1 30	0 0381	0 0118	−0 0554	−0 0142
1 35	0 0397	0 0108	−0 0577	−0 0129
1 40	0 0416	0 0098	−0 0605	−0 0117
1 45	0 0439	0 0088	−0 0639	−0 0106
1 50	0 0461	0 0079	−0 0670	−0 0095
1 55	0 0486	0 0071	−0 0706	−0 0085
1 60	0 0504	0 0064	−0 0734	−0 0077
1 65	0 0522	0 0059	−0 0760	−0 0071
1 70	0 0540	0 0054	−0 0785	−0 0065
1 75	0 0556	0 0050	−0 0808	−0 0060
1 80	0 0558	0 0049	−0 0811	−0 0058
1 85	0 0560	0 00474	−0 0814	−0 00565
1 90	0 0562	0 0046	−0 0816	−0 0055
1 95	0 0564	0 0045	−0 0819	−0 00535
2 00	0 0566	0 00435	−0 0822	−0 00522
ϵ'*	C_1	C	C_1'	C''

*$\epsilon' = L/L_1$, with side L_1 discontinuous.

TABLE 6—FOUR EDGES CONTINUOUS

ϵ	C	C_1	C'	C_1'
0 50	0 0038	0 0556	−0 0055	−0 0809
0 55	0 00531	0 0494	−0 0077	−0 0720
0 60	0 00688	0 0440	−0 010	−0 0638
0 65	0 00844	0 0400	−0 0123	−0 0582
0 70	0 010	0 0363	−0 0146	−0 0528
0 75	0 0119	0 0332	−0 0173	−0 0483
0 80	0 01345	0 0296	−0 0196	−0 0431
0 85	0 0153	0 0272	−0 0223	−0 0396
0 90	0 017	0 025	−0 0248	−0 0364
0 95	0 01875	0 0226	−0 0274	−0 0329
1 00	0 0206	0 0206	−0 030	−0 030
1 05	0 0222	0 0189	−0 0323	−0 0275
1 10	0 0241	0 0175	−0 0351	−0 0255
1 15	0 0259	0 0158	−0 0377	−0 0231
1 20	0 0276	0 0144	−0 0402	−0 0210
1 25	0 0296	0 0130	−0 0431	−0 0189
1 30	0 0310	0 0119	−0 0451	−0 0173
1 35	0 0329	0 0110	−0 0479	−0 016
1 40	0 0346	0 010	−0 0504	−0 0146
1 45	0 0363	0 0094	−0 0521	−0 0137
1 50	0 0381	0 0085	−0 0554	−0 0124
1 55	0 040	0 0078	−0 0582	−0 0114
1 60	0 0416	0 0072	−0 0605	−0 0105
1 65	0 0434	0 0066	−0 0632	−0 0097
1 70	0 0452	0 0060	−0 0659	−0 0088
1 75	0 0469	0 0054	−0 0682	−0 0079
1 80	0 0487	0 0050	−0 0710	−0 0073
1 85	0 0504	0 0047	−0 0734	−0 0068
1 90	0 0521	0 0044	−0 0758	−0 0064
1 95	0 0539	0 0041	−0 0785	−0 0060
2 00	0 0556	0 0038	−0 0809	−0 0055

I have drawn graphs* showing the calculated values of C and C_1 for the different types of support with respect to ϵ. The dotted lines are the corresponding values of Dr. Marcus.† Fig. 1 corresponds to Table 1.

In my opinion, the ACI coefficients, although higher than Marcus', permit simpler calculation since total load is used. Marcus' method requires the separation of dead load from live load.

ANTONIO M. GOMEZ, Professor of Reinforced Concrete Structures, National University of Colombia, Bogotá, Colombia

*Fig. 1 is the graph of Case 1. Those desiring graphs of the remaining five cases may obtain them from ACI headquarters at cost of reproduction.

†Löser, *Bemessungsverfahren*, 13th Edition, Wilhelm Ernst u. Sohn, Berlin, 1951.

Current Reviews*

of Significant Contributions in Foreign and Domestic Publications

Bridges

Description of some prestressed concrete bridges built in Germany (in French)

ARTHUR BRANDES, *Precontrainte* (Brussels), V. 4, No. 1, Jan.-June 1954, pp. 31-39

AUTHOR'S SUMMARY

Four bridges using the Blaton-Magnel system of prestressing are described. Bridge across the Ems at Sustrum is a statically indeterminate structure with three spans of 18.5, 37, and 18.5 m. Each of the main beams is 1.4 m deep. The bridge is prestressed both longitudinally and transversally. The two central piers are prestressed vertically.

Bridge across the Ems at Greven has seven spans with a total length of 210 m. The central span is simply supported on the ends of two cantilevers. Bridge across the Ruhr at Untermaubach has three spans of 16.6, 33.2, and 16.6 m. Bridge across a highway at Walldorf has a 35.17-m span and total depth of 1.07 m; the cross section is box shaped.

Reconstruction of the Battant Bridge at Besancon (in French)

J. CLOUET, *Precontrainte* (Brussels), V. 3, No. 2, July-Dec. 1953, pp. 67-73

AUTHOR'S SUMMARY

Battant Bridge, replacing an old masonry bridge, spans 62.5 m with an effective width of 16 m. It consists of ten two-hinged prestressed arch girders bound together by transverse prestressing. Each longitudinal and transverse cable consisted of twelve 5 mm diameter high tensile steel wires tensioned initially to a stress exceeding 120 kg per sq mm. Stirrups of high tensile steel (four 5-mm diameter wires) tensioned by two jacks were employed. Decentering of the arch girders was carried out by distending flat jacks embedded in shims of stirruped concrete and arranged beneath the springers of the arches.

Two prestressed concrete bridges across the new canal surrounding Ghent (in French)

D. VANDEPITTE, *Precontrainte* (Brussels), V. 4, No. 1, Jan.-June, 1954 pp. 3-13

AUTHOR'S SUMMARY

Describes in detail bridge "W7" and adds some data on bridge "W9," which is of the same type but has somewhat longer spans.

Bridge W7 has three spans, respectively 85, 170, and 85 ft long. The cross section of the abutments is similar to that of a quay wall of the Christiani and Nielsen type. The superstructure is monolithic and comprises 11 continuous prestressed concrete beams, the total depth of which is 8 ft 10 in. above the intermediate supports and 4 ft 11 in. at the center of the center span. The cables are outside the concrete cross section of the main beams and have been embedded in mortar after tensioning. In elevation they are polygonal. There are three changes of direction: above the piers and at the center of the beam. The cables are anchored by means of sandwich plates.

The author discusses the cracks that appeared in the superstructure before pre-

*A part of copyrighted JOURNAL OF THE AMERICAN CONCRETE INSTITUTE, V. 26, No. 9, May 1955, *Proceedings* V. 51. Address 18263 W. McNichols Rd., Detroit 19, Mich. Where the English title only is given in a review, the book or article reviewed is in English. If it is followed by a foreign title the work reviewed is in that language. In those cases where the foreign title cannot conveniently be set in type or is not available, the language of the original article is indicated in parenthesis following the English title. Copies of articles or books reviewed are **not** available through ACI. Available addresses of publishers are listed in the June "Current Reviews" each year. In most cases ACI can furnish addresses of publications added later.

stressing, the concreting and prestressing operations, the lowering of the falsework, the working stresses in the main beams, the vertical and longitudinal deformations of the superstructure during and after prestressing, and the quantities of materials required. He explains why he preferred I-beams above box girders and exterior above interior cables, and why he made the webs 10 in. thick, thicker than necessary for resisting shearing forces.

Note on the transverse moments in a prestressed concrete bridge slab

R. E. Rowe, *Magazine of Concrete Research* (London), V. 6, No. 18, Dec. 1954, pp. 149-150

Author's Summary

Deals with the application of the theories of Massonnet and Guyon to a flat slab bridge model. Particular mention is made of the distribution and the absolute values of the transverse moments in relation to the theoretical values. Only one slab has been tested but further tests on slabs of different span/breadth ratios are now in progress.

High-strength cables for tie rods (in Hungarian)

E. Bolcskei, *Melegyitestudomanyi Szemle*, V. 2, No. 10, 1952, pp. 52-53

Hungarian Technical Abstracts V. 5, No. 4, 1954

Use of high-strength cables for tie rods in reinforced concrete arch bridges is described. Compared with tie rods produced from mild steel plates, 50 to 70 percent less steel is required. The cable may be made of parallel wires or of a single or more strands. The elongation increases considerably due to the greater stress occurring in the steel and the lower Young's modulus. The ensuing disadvantages can be eliminated to a great extent by prestressing the bridge to eliminate the effects of live loads as well as by setting the structure under pressure by hydraulic presses applied in the crown. Even then, additional moments arise in the arches which require a slight additional reinforcement.

Construction

New forms of shell structures

Indian Concrete Journal (Bombay), V. 28, No. 7, July 1954, pp. 246-250

Describes briefly some of the forms of shell roofs; corrugated shells, straight corrugated roofs, roofs with doubly curved surfaces, prismatic structures, and lamella type roofs.

Construction of moving forms (in Hungarian)

I. Mester, *Magyar Epitoipar*, V. 2, No. 7, 1953, pp. 201-210

Hungarian Technical Abstracts V. 6, No. 3, 1954

Design of moving forms, and organization and phases of work are described.

Design, development and construction of foundations for turbo-compressors for compressor plant LL-370 (in Spanish)

E. Paulet, *Revista del Colegio de Ingenieros de Venezuela* (Caracas), No. 222, Sept. 1954, pp. 7-10

Reviewed by Joseph J. Waddell

This plant consists of ten turbo-compressors of 5000 hp. The turbines use gas at a temperature of 760 C, and are connected to centrifugal gas compressors turning at 5000 rpm. These compressors raise the pressure of the pumped gas to 141 kg per sq cm.

Specifications for the turbines required that the supporting structure could deflect no more than 0.0508 cm. This and other considerations led to the selection of reinforced concrete for the bases.

The bases rest on a grillage of reinforced concrete beams which in turn are supported on concrete piles 48 m long. Bases were precast some distance from the site, transported to the site on barges, and there placed on the supporting structure with cranes.

This article gives a brief outline of the design, and describes the construction and placement of the bases.

Metal forms (Coffrage metalliques)

M. J. Ricouard, Editions Eyrolles, Paris, 1954, 232 pp., 1950 Fr

Author's Summary

The use of metal forms has developed considerably in all countries, but especially in France and its colonies in the last ten years. This book shows principal works in which there has been a particular interest in the utilization of forms and the substantial economies which can be effected. While a wood form can be used only a few times, the metal form can be re-used 500 to 1000 times. Its installation is more rapid and the surface obtained is more regular—all factors which increase the value of this technique.

Described are the general characteristics of metal forms, the importance of organizing the plant, and establishing work standards.

This first study is terminated by an analysis of the procedure for using metal forms presented in a clear and concise fashion in which the engineer will find all the necessary elements for the utilization of this procedure.

The last part, and the most important, reviews the different particular cases which can be presented. The many illustrations show the construction of forms and the results obtained.

Woodhead new tunnel: Construction of a 3-mile main double-line railway tunnel

PETER A. SCOTT and JOHN I. CAMPBELL, *Proceedings*, Institution of Civil Engineers (London), Part I, V. 3, No. 5, Sept. 1954, pp. 506-563 (including discussion)

Reviewed by ARON L. MIRSKY

Describes difficulties encountered during construction of 3.04-mile long double-track tunnel which replaces two old, badly deteriorated single-track masonry-lined tunnels. Mass concrete lining, 21 in. thick, was used for the full length of the tunnel; the floor was not concreted. The contract was of the cost-plus-fixed-fee type, with provisions for bonus or penalty based on the actual cost and date of completion.

Abstracts of this paper have appeared in *The Engineer* (London), V. 197, No. 5121, Mar. 19, 1954, pp. 418-420, and in *Engineering* (London), V. 178, No. 4614, July 2, 1954, pp. 20-22.

Concrete quality control at Woodhead new tunnel

FREDERICK A. SHARMAN, *Proceedings*, Institution of Civil Engineers (London), Part I, V. 3, No. 5, Sept. 1954, pp. 564-578

Reviewed by ARON L. MIRSKY

Mix proportioning and batching, transporting, and placing some 145,000 cu yd of concrete tunnel lining (77,600 cu yd within payment line, 67,000 cu yd overbreak filling) are discussed. (See also preceding review.)

New electronic factory at Charleroi (in French)

JACQUES ROBIN, *Precontrainte* (Brussels), V. 4, No. 1, Jan.-June 1954, pp. 24-30

AUTHOR'S SUMMARY

Factory building covers an area of 25,000 sq m with prestressed concrete beams bearing on columns 15 m from center to center in two directions. The main beams have a reversed V-shape and were concreted at the foot of their columns and then hoisted into position; their total height is 1.2 m, the top and bottom flange width is 150 cm and the thickness of the web is 13 cm. The secondary beams, placed every 3.75 m, rest on the principal ones; they are continuous beams, the continuity being assured by means of threaded alloy steel bars prestressed by turning the nuts. They have a total depth of 70 cm, a top and bottom flange 40 cm wide and are each made of five prefabricated blocks, the two prestressing cables being placed on either side of the web. The secondary beams carry small reinforced concrete purlins placed at 2.5 m center to center, and these carry pumice concrete slabs. For part of the covered area a floor designed for a superimposed load of 200 kg per sq m is suspended from the roof beams.

Deep well at Eskilstuna (Grundvattensbrunn i Eskilstuna)

B. RITHANDER and S. E. SVENSSON, *Betong* (Stockholm), V. 38, No. 4, 1953, pp. 261-268

Reviewed by EIVIND HOGNESTAD

Discusses the structural design and construction methods of a well about 75 ft deep with an internal diameter of 10 ft. Slip-forms were used.

Water towers in reinforced concrete (in Danish)

PREBEN C. WISTISEN, *Beton Teknik* (Copenhagen), V. 19, No. 3, Oct. 1953, pp. 155-164

AUTHOR'S SUMMARY

Describes four elevated reinforced concrete water tanks of various capacities: 1500 and 54 cu m, and two of 130 cu m.

Civil engineering construction under water

JOHN R. MALCOLM and JOHN A. LEWIS, *Proceedings*, Institution of Civil Engineers (London), Part III, V. 3, No. 3, Dec. 1954, pp. 738-788 (including discussion)

Reviewed by ARON L. MIRSKY

Valuable monograph-type paper covering all aspects of underwater construction (construction in the dry, *i.e.*, inside cofferdams or caissons, is excluded). First part of paper covers design and materials, second part methods and plant. Material is quite up-to-date; even underwater television is briefly discussed.

Concrete shell roof construction in India

E. P. NICOLAIDES and R. N. BANERJEE, *Indian Concrete Journal* (Bombay), V. 28, No. 7, July 1954, pp. 239-245

Reviews briefly fundamentals and advantages of shell construction. Some of India's concrete shell roofs are described. These are grouped under barrel vaults, north-light shells, conoidal shells, and prestressed shells.

Dams

Buttress dams: Pracana Dam

J. G. Pinto Machado, *Memorias da Ordem dos Engenheiros* (Lisbon), V. 1, No. 4, 1954
Reviewed by J. Laginha Serafim

Presents different types of buttress dams and compares them with gravity dams from the point of view of economy and safety. Design of Pracana Dam is examined and construction phases of the buttresses are indicated.

Owen Falls, Uganda, hydroelectric development

Charles R. Westlake, Reginald W. Mountain, and Thomas A. L. Paton, *Proceedings*, Institution of Civil Engineers (London), Part I, V. 3, No. 6, Nov. 1954, pp. 630-669 (including discussion); *Proceedings*, Institution of Electrical Engineers (London), Part I, V. 101, No. 132, Nov. 1954, pp. 347-368 (including discussion)

Owen Falls: Constructional problems

Dennis P. Bertlin and Henry Olivier, *Proceedings*, Institution of Civil Engineers (London), Part I, V. 3, No. 6, Nov. 1954, pp. 670-719 (including discussion); abstracted in *Proceedings*, Institution of Electrical Engineers (London), Part I, V. 101, No. 132, Nov. 1954, pp. 369-372

Development and utilization of hydroelectric power in Uganda

J. M. Stock and J. C. Littlow, *Proceedings*, Institution of Electrical Engineers (London), Part I, V. 101, No. 132, Nov. 1954, pp. 373-390
Reviewed by Aron L. Mirsky

First paper discusses the project as a whole, with especial reference to the economics of the scheme (see also *Engineering* Apr. 16 and 23, 1954; "Current Reviews," ACI Journal, *Proc.* 51, Sept. 1954, p. 102).

Second paper discusses, besides the more usual topics of control of water during construction, excavation and production of concrete (both cast-in-place and precast), such relatively unusual items as health pests and diseases.

Third paper covers the electrical problems encountered in generating and transmitting the power.

All three papers together constitute a valuable account of the development of a large source of hydroelectric power "from the ground up."

Grout curtain for a Rocky Mountain dam foundation

E. Parrag, *The Engineering Journal* (Montreal), V. 38, No. 1, Jan. 1955, pp. 13-17
Reviewed by Aron L. Mirsky

Extensive and costly grouting was required for dam on Bull River in British Columbia. Although dam was relatively small (87 ft maximum height, 445 ft length at crest, requiring 22,500 cu yd of concrete), grout curtain at upstream face and consolidation grouting at toe comprised almost 5 percent of the cement and almost 7 percent of the cost of the new facility.

Development of modern cableways for construction purposes in Germany and in America (Die Entwicklung der neuzeitlichen Kabelkrane fuer Bauzwecke in Deutschland und in Amerika)

W. Franke, *Der Bauingenieur* (Berlin), V. 29: No. 1, Jan. 1954, pp. 20-30; No. 3, Mar. 1954, pp. 93-99

Cableways or concreting platforms? Problems of conveying mass concrete for dams (Kabelkrane oder Betonierbuehnen? Probleme der Massenbetoneinbringung bei Talsperren)

Friedrich Meschan, *Der Bauingenieur* (Berlin), V. 29, No. 3, Mar. 1954, pp. 77-85
Reviewed by Aron L. Mirsky

First article describes German and American cableways used in dam construction, particularly in concreting. Second article, after discussing various methods of placing concrete for dams, describes the cableways which were adopted on the basis of cost analyses for the construction of the Mooser and Drossen dams. Much of the plant used for these two dams had previously been used in the construction of the Kaprun and Limberg dams.

Concreting at Konar Dam

F. Stoecklin-Schlegel and A. K. Sinha, *Indian Concrete Journal* (Bombay), V. 28, No. 10, Oct. 1954, pp. 399-408, 411

Dam is partly a gravity type concrete structure linked with earth embankments on either side. It involved 420,000 cu yd of concrete in dam, retaining walls, and stilling basin. Items covered include aggregate, batching, and mixing plants; transportation and placing; and curing. Major attention is given to construction control, including such items as consistency, gradation, moisture content, bulking, and batching errors. Strength and age-strength relationships are also covered thoroughly.

Cleveland Dam, British Columbia

The Engineer (London), V. 198, No. 5162, Dec. 31, 1954, pp. 921-922
Reviewed by Aron L. Mirsky

Brief description of gravity type dam on Capilano River. Project is designed to furnish 200 million gal. per day to the Greater Vancouver area.

Design

Particular type of continuous girder on yielding elastic supports (Un particolare tipo di trave continua su appoggi elasticamente cedevole)

Vincenzo Francioso. *Il Cemento* (Milan), V. 50, No. 2-10, Feb.-Oct. 1953, pp. 69-73

Reviewed by G. Mianulli

The author has investigated the special case of a collapsible bridge supported on floats. Influence lines have been developed by an approximate method, assuming that the girders have infinitely great stiffness. An example illustrates the design procedure.

Relaxation method applied to the solution of frames (in Portuguese)

J. Araujo Sobreira. *Tecnica* (Lisbon), V. 29, No. 241, 242, 243, and 244, Apr., May, June, July 1954

Reviewed by J. Laginha Serafim

Applies Sowthwell relaxation method to the computation of moments and deflections of hinged frames, statically indeterminate, to show the use of the same method for the solution of continuous beams and rigid frames. Same examples are given showing the advantages of this method when compared with the moment-distribution method (Hardy Cross) as it gives the deformation of the structure and allows a progressive checking of the computations.

Analysis of statically indeterminate structures

John I. Parcel and Robert B. Moorman. John Wiley & Sons, Inc., New York, N. Y., 1955, 566 pp., $9.50

A book suitable for a series of courses in structural analysis, including graduate study. It is also a worthy addition to the practicing engineer's reference library since it concentrates material ordinarily scattered through several books.

The technique of combining theory and application should be particularly appreciated. Each method is developed carefully and as simply as possible, and followed by complete numerical examples in a systematic design office procedure. Tabulations of necessary constants for unusual problems that are particularly helpful for practical applications of theory include ratios of deflection due to moment and shears for a wider range of beams, constants for multiple arches on elastic piers, and complete equations for various beam loadings. The subject matter includes a complete treatment of the general theory and classical methods of determining deflections, followed by a general treatment of modern methods, including an ingenious modified moment distribution method combining sidesway correction in the direct distribution. Continuous beams, rigid frames, and arches are treated in the principal sections of the book, which then concludes with chapters on secondary stresses and suspension bridges. Classical and modern methods are derived and applied to examples of secondary stress analysis. The elastic theory and deflection theory of suspension bridge analysis is included.

The authors promise a second, companion volume to develop methods for more complex problems such as plates and shells, deflection theory in arches, space frames, and dynamic problems of bridges and buildings.

Deformation of thin shells (in Hungarian)

E. Bolcskei. *Magyar Epitoipar*, V. 2, No. 3, 1953, pp. 93-100

Hungarian Technical Abstracts V. 6, No. 2, 1954

Author establishes general principles in relation to the deformation of thin shells applicable to any type of surface and load. Stress distribution in thin shells and its solution by stress functions is dealt with. Unit strains and unit distortions are defined in terms of position vectors and displacement functions. Deformations and displacement of the shell surface are defined by the differential equations thus deduced. Displacement functions are established for inner stresses, changes of temperature, and the settling of supports. The method is used to calculate the deformations of various statically determinate shell types. The method is also applicable to statically indeterminate shells.

Demonstration apparatus for structural problems. Visual aid for moment distribution calculations

R. J. Wilkins. *Engineering* (London), V. 178, No. 4632, Nov. 5, 1954, p. 595

Reviewed by Amos L. Mirsky

Description of simple apparatus—rods, corner joints, and loading pulleys—from which models of structures may be formed, to illustrate sign conventions, effect of continuity, and sidesway. While this visual aid would find its largest application in teaching, reviewer believes it might also find a niche in design offices, as a help in visualizing the results of calculations.

Materials

Proceedings of the Third International Symposium of the Chemistry of Cement—London, 1952

Cement and Concrete Association, London, England, 1954, 950 pp., 89

This meeting was a continuation of the exchange of ideas between research cement chemists. The first meeting was held in London in 1918; the second in Stockholm, in 1938. Papers presented on cement constituents included "The Tri-Calcium Silicate Phase," by J. W. Jeffrey; "The Di-Calcium Silicate Phase," by R. W. Nurse; "Tri-Calcium Aluminate," by Fred Ordway; "The Ferrite Phase," by G. Malquori and V. Cirilli; "The Alkali Phases in Portland Cement Clinker," by Terry F. Newkirk; "Interstitial Phases in Portland Cement Clinker," by Herbert Insley; and "Studies on the Constitution of Portland Cement Clinker," by R. H. Bogue.

Studies on the effects of hydration were offered in several papers: "The Structures of Cement Hydration Compounds," by J. D. Bernal; "The Reactions and Thermochemistry of Cement Hydration at Ordinary Temperature," by Harold H. Steinour; and "The Reactions of Cement Hydration at Elevated Temperatures," by George L. Kalousek. The controversial question of the effect of cement on concrete durability was considered in the papers "The Physical Structure of Cement Products and Its Effect on Durability," by F. E. Jones; and "Chemical Aspects of the Durability of Cement Products," by T. Thorvaldson.

A number of papers and discussions on special cements developed for modern use included "The Constitution of Aluminous Cement," by T. W. Parker; "Slag Cements," by F. Keil; "Expansive Cements," by H. Lafuma; "Oil Well Cements," by W. C. Hansen; "Masonry Cement," by Charles E. Wuerpel; and "Development of Cements for Special Uses in the United States," by Myron A. Swayze. Two papers dealing with manufacturing problems were "The Influence of the Fineness of Cement Raw Mixes on Their Burnability," by T. Heilmann and "Thermodynamics of the Cement Kiln," by H. Gygi and F. Guye.

One paper was presented on concrete technology emphasizing modern structural developments in the field, not for the purpose of adding to the knowledge of the chemistry of cement, but to survey new developments in the use of concrete and to promote discussion of their effects on cement technology. The paper "Some Recent Developments in the Design and Construction of Concrete Structures," by A. R. Collins, discussed structural advances, such as shell roofs and prestressed concrete; advances in construction technique, such as precasting and textured surface finishes; and concluded with the thought that the increasing use of exposed concrete for a wider range of structures has focused attention on the problems of improving the appearance of exposed surfaces and in particular on crazing, efflorescence, and other forms of surface blemishes, indicating that perhaps the cement technologist can contribute to an improvement of the performance of concrete in these respects.

Technical and economic aspects of the manufacture and use of lightweight concrete and of the use of coal waste in construction (Quelques aspects techniques et economiques de la fabrication et l'emploi des betons legers et de l'utilisation des dechets de l'exploitation houillere dans la construction)

A. Jarrige, *Revue des Materiaux de Construction* (Paris), No. 471, Dec. 1954, pp. 343-352; No. 472, Jan. 1955, pp. 1-8

Reviewed by Phillie L. Melville

After a good review of the advantages and uses of lightweight concrete, sundry methods of manufacture are considered. Waste from power stations using coal is a useful aggregate of the sintered or expanded shale type. Fly ash can also be used, if of a suitable kind, as a pozzolanic agent. The use of fly ash seems to be on the increase due to many potential advantages.

Evaluation of air-entraining admixtures for concrete

Frank H. Jackson and Albert G. Timms, *Public Roads*, V. 27, No. 12, Feb. 1954, pp. 259-267

Authors' Summary

This investigation was undertaken to determine the acceptability of a number of commercial admixtures for use in the production of air-entrained portland cement concrete for highway pavements and bridges. The complete program involved evaluation of 27 materials, each of which was tested in concrete to determine its ability to entrain

air, as well as its effect on flexural and compressive strength and on durability. As the result of the evaluation study, 26 of the 27 materials which were received for test have been classified as acceptable for use as air-entraining admixtures.

Except for a few relatively minor deviations, the 27 admixtures met the 88-percent strength requirement at the three ages of test. They also complied with the requirement for durability, although in this respect the various materials differed considerably in performance. These differences could not be related directly to total air content, but it is possible that they were influenced by differences in the distribution or spacing of the air voids.

ASTM standards on cement (with related information)

American Society for Testing Materials, Philadelphia, Pa., May 1954, 254 pp., $2.75

Presents the various American Society for Testing Materials standard and tentative specifications, methods of chemical analysis, and methods of physical testing pertaining to cement. An appendix includes information on analytical balances and weights, a manual of cement testing, list of selected references on portland cement, and information on the methoxyl method for determining Vinsol resin in portland cement.

Direct titration of Al_2O_3 in clinker and cement (Dosage direct de la teneur en Al_2O_3 du clinker et du ciment)

K. Gloor and R. Rentsch, *Revue des Materiaux de Construction* (Paris), No. 470, Nov. 1954, pp. 304-307
Reviewed by Phillip L. Melville

Describes a simple gravimatric method to titrate aluminium in clinker and cements. Examples are worked out.

Pavements

Air-entrained concrete test road

Research Report No. 5, Ohio Department of Highways, June 1954, 35 pp.
Highway Research Abstracts Sept. 1954

In 1940 the Ohio Department of Highways constructed a test road of 51 test sections. Principal test features were use of portland cements and combinations of portland and natural cements with and without air-entraining additions. Other features were sections with "Pozzolith" added to the concrete, portland cement with calcium stearate, and sections with surface hardened with a mixture of iron, sand, and cement, known as "metallic shake." Principal air-entraining agents were Vinsol resin, beef tallow, and petroleum distillate.

Effect of type of finishing was also studied. On half the project concrete was struck off and finished with regular type of finishing machine. On the other half concrete was struck, compacted, and finished with a vibratory-screed finishing machine.

The report discusses subgrades and traffic, materials, construction equipment, proportioning and mixing, yield and air content, workability, bleeding, compressive and transverse strengths, freeze-and-thaw tests, and condition surveys—all supplemented with tables, graphs, and photographs. Condition surveys have been made annually since the project was built.

Report on the construction of reinforced concrete pavement

G. Albert Hill, *American Highways*, V. 32, No. 4, Oct. 1953, pp. 7, 22-25

Reports on test section of reinforced concrete pavement using only contraction joints at about 40-ft intervals. Intermediate groove type dummy joints were eliminated and expansion joints were restricted to critical locations such as at bridges and intersecting roads. Various types of contraction joints (full plate, half plate, and dummy joint groove) and load transfer assemblies were incorporated in the test section. Data on joint movement and crack occurrence, and performance of joint assemblies and joint filler materials is presented.

Precast concrete

Cutting costs of handling precast slabs

H. S. Freeman, *Concrete*, V. 62, No. 5, May 1954, pp. 10-11

Transportation of precast concrete channel roof slabs (2 ft x 6 ft x $3\frac{3}{4}$ in.) from plant to construction site by railroad flatcar and handling the slabs, bundled in groups of ten, by fork lift truck reduced erection costs about 6 cents per sq ft.

Precast concrete shell-roofed building

The Engineer (London), V. 198, No. 5160, Dec. 17, 1954, pp. 854-855
Engineering (London), V. 179, No. 4642, Jan. 14, 1955, p. 56
Reviewed by Aron L. Mirsky

Workshop block of new technical college at Kingston-upon-Hull is a 312 x 192 ft

single story building planned on a 24-ft module. The main frames are eight-bay continuous portal frames precast in two basic units (the column and north-light strut, and the curved rib); when the gutter units are connected to the main frames, the result is a series of portal frames in the lateral direction as well. Shell roof units span 24 ft, are 16 ft wide, and 2.5 in. thick. Casting and prestressing is done on the site.

Prestressed concrete

Prestressed concrete

GUSTAVE MAGNEL, 3rd Edition, McGraw-Hill Book Co., Inc., New York, N. Y., 1954, 340 pp., $8

Magnel's well-known earlier edition has been somewhat expanded. The revisions include many new test results, ultimate strength prediction methods, and a larger treatment of continuous structures. Every effort has been made to enable a practicing designer to utilize the technique. Most refreshing is the author's admission that "the problem of the ultimate strengths of a statically indeterminate structure (in prestressed concrete) is not yet solved." Suggested working stresses, assumptions, and simplified formulas are given, following reports on tests and applications in successful service. The book should be most valuable to practicing designers, students, and teachers, as well as an indication of questions requiring further investigation. (See also review of French edition, "Current Reviews," ACI JOURNAL, Nov. 1954, *Proc.* V. 51, p. 309.)

Criteria for prestressed concrete bridges

Bureau of Public Roads, 1954, 25 pp., 15 cents (Available from Superintendent of Documents, Government Printing Office, Washington 25, D. C.)

The nearest approach to an official building code for prestressed concrete construction in the United States, these criteria are suitable for all prestressed construction except that they specify safety factors for bridge loads, cover for bridge exposures, and diaphragms for distributing concentrated bridge loads. Manufacturers of prestressed products will note with interest that the criteria allow temporary tensile stresses in the concrete at the time of fabrication. All designers will appreciate the criteria on ultimate strength, principal tensile stress, and end anchorage bearing stress as well as simple approximate formulas for the computation of the ultimate strength. Tables of probable friction losses are included. Manufacturers of the high-tensile steel for prestressing will appreciate the extremely general requirements on this material which specifically allow bonded as well as unbonded steel. A definite preference is indicated for the bonded steel with suggestions for grouting. The protection required for unbonded steel includes galvanizing and coating with waterproof material. One minor criticism from the standpoint of uniformity is that the notation employed, although entirely rational and simple, does not conform with that adopted by ACI-ASCE Committee 323. The work of the committee is recognized, however, in the preface which states that the criteria will be reviewed upon the publication of a report by the committee. This booklet is highly recommended to anyone engaged in research, design, manufacture, or construction of prestressed concrete.

Set of cement silos in prestressed concrete (in French)

G. SAMBITO, *Precontrainte* (Brussels), V. 4, No. 1, Jan.-June 1954, pp. 40-45

AUTHOR'S SUMMARY

Gives first the principles of design for circular silos, laying particularly stress on the joint between the cylindrical shell and the foundation slab. Then comes the description of a set of eight silos built at Naples; their internal diameter is 11.4 m for a height of 22.4 m with a shell thickness of 15 cm; the total capacity is 3400 tons; the foundations are on piles. Details are given about the prestressing. The wires were wrapped helicoidaly round the cylinder (Stahlton patent); their diameter is 4 mm and the stress 8800 kg per sq cm.

Prestressed concrete reservoir construction

G. M. JONES, *Commonwealth Engineer* (Melbourne), V. 42, No. 3, Oct. 1, 1954, pp. 91-95

Describes two prestressed concrete reservoirs in Australia. A 2,000,000-gal. capacity reservoir has a diameter of 128 ft and a wall height of 28 ft 3 in. Wall tapers from 10 in. at the base to 7 in. at the top. Base slab was reinforced concrete 4 in. thick. Wall was prestressed vertically and horizontally, and formed in the usual manner. The 750,000-gal. tank walls were constructed by shotcreting instead of standard concreting methods.

Prestressed concrete foundation

D. E. Oelschlager, *Civil Engineering*, V. 25, No. 1, Jan. 1955, pp. 42-45

An 8000-ton forging press posed a foundation problem because of limited foundation width and an allowable soil bearing load of 3200 psf. A slab type foundation of minimum dimensions and weight was used. To provide flexural strength, the two beams, one on each side of the press pit, were prestressed before constructing the rest of the superstructure. A 24-in. slab extended the full width of the foundation. This prestressed section, called the sill girder, was prestressed for 70 ft of its 86-ft length. Girder was tapered toward ends on a 1 to 4 slope to reduce foundation weight. Sidewalls of foundation were tied to sill girder, making the whole act as a composite beam section.

Prestressed concrete pipes for water supply in Belgium (in French)

J. Capel, *Precontrainte* (Brussels), V. 3, No. 2, July-Dec. 1953, pp. 74-83

Author's Summary

Description of prestressed concrete water pipeline between two Belgian dams. The core concrete was placed by centrifugal process, the external coating by vacuum processing.

Properties of concrete

Compaction and flow of concrete

M. P. Poucher, *Magazine of Concrete Research* (London), V. 6, No. 18, Dec. 1954, pp. 139-148

Author's Summary

Tests are briefly described for a comparison between the workability and mobility of concrete mixes suitable for compaction by vibration. Variations in the mix proportioning for high-quality concretes are discussed, stress being placed on the concrete containing a high proportion of the maximum sized aggregate.

Comparison of electrical properties of various cements and concretes

E. Hammond and T. D. Robson, *The Engineer* (London), V. 199, No. 5165, Jan. 21, 1955, pp. 78-80; No. 5166, Jan. 28, 1955, pp. 114-115

Reviewed by Aron L. Mirsky

Tests of resistivity, capacitance, and dielectric strength were conducted on concretes made with (1) ordinary, (2) high-early-strength, and (3) high-alumina cements. All other factors, including aggregate and mix, were held constant, to permit comparison of results for the three cements. Paper includes details of methods of measuring resistance; advantages of external versus immersed electrodes are discussed. Results indicated specimens made with high-alumina cement had higher resistances than those made with portland cement under all conditions and at all ages.

Surface finishes of concrete

J. G. Wilson, *British Constructional Engineer* (London), V. 5, No. 2, Sept. 1954, pp. 56-57, 59

Various types of architectural finishes are covered briefly: (1) board-marked finishes including smooth and rough surfaces; raised, recessed, and overlapping joints; (2) finishes from special formwork linings; (3) exposed aggregate finishes including brushing, tooling, and grinding; and (4) applied finishes including painting, rendering, and precast slabs.

Specific heat of cement pastes and reaction heat of concrete during setting and hardening (Spezifische Warme von Zementpasten und Reaktionswarme des Betons wahrend des Abbindens und Erhartens)

J. Siegmann, *Zement-Kalk-Gips* (Wiesbaden), V. 7, No. 10, Oct. 1954, pp. 390-395

Author's Summary

As an experiment the specific heat of various kinds of cement paste was calorimetrically measured independent of the water-cement ratio. As reference data the unreliable considerations with regard to hydration water were replaced by the mass ratio p and the specific heat c_m of that cement paste which in the hardened state contains neither unset cement nor free water. These data permit the reliable computation of the specific heat in cement pastes for any kind of water-cement ratio on the basis of a specific mixing rule. The relationships between the temperature curve formed in the adiabatic calorimeter, the quantity of cement which has set per unit of cement used initially, and the reaction heat are explained theoretically. An example demonstrates how these data are ascertained on the basis of the temperature curve.

Self-desiccation in portland cement pastes

L. E. Copeland and R. H. Bragg, *ASTM Bulletin*, No. 204, Feb. 1955, pp. 34-39

The rates of hydration of cement pastes cured in sealed containers are compared with cement pastes continuously moist cured. For water-cement ratios greater than about

5½ gal., the rate in sealed paste was practically the same as moist-cured paste at ages up to 1 year. The authors conclude that the experiments reported show that to obtain the maximum possible rate of hydration at a constant temperature, concrete must be kept saturated, or nearly so, for water-cement ratios less than about 5½ gal. per sack. For higher water-cement ratios, the rate of curing in sealed specimens is the same as that in specimens kept fully saturated. This indicates that if a curing membrane were perfectly impervious, a membrane cure would be just as effective as a water cure for all but the richer grades of concrete.

Computation of shrinkage and thermal stresses in massive structures

OLGIERD C. ZIENKIEWICZ. *Proceedings*, Institution of Civil Engineers (London), Part I, V. 4, No. 1, Jan. 1955, pp. 88-100

Reviewed by ARON L. MIRSKY

Author applies relaxational methods to solution of complex problems of shrinkage and thermal stress. Simplifying assumptions made are that the material is homogeneous and isotropic and has constant elastic properties, that the known temperature and shrinkage values are applied *after* the material has set and developed the above properties, and that the problems are two-dimensional (plane stress or plane strain). While these assumptions are far from valid for a material like concrete, results do offer some assistance in estimating stresses due to shrinkage and temperature change in large and important structures. Application of method to discontinuous shrinkage, such as occurs when fresh concrete is bonded to old concrete (*e.g.*, in increasing the height of a dam) or to rock, is outlined.

Evaluation of concrete block tests conducted by Qualifying Laboratory of Institute of Building Science in 1952-53 (in Hungarian)

S. POPOVICS and J. UJHELYI, *Magyar Epitoipar*, V. 2, No. 12, 1953, pp. 389-394

HUNGARIAN TECHNICAL ABSTRACTS, V. 6, No. 3, 1954

Results of compression tests conducted on concrete block at various construction sites were treated by statistical methods. Distribution of strength of concrete samples of identical composition of average strength and dispersion are given. Strengths usually followed a normal dispersion; the dispersion ranged between 12 to 25 percent of the average values.

Structural research

Stresses in short beams. I: Experimental analysis. II: Theoretical analysis and conclusions

J. S. CASWELL. *Engineering* (London), V. 178, No. 4633-4634, Nov. 12, 1954, pp. 625-628; Nov. 19, 1954, pp. 656-658

Reviewed by ARON L. MIRSKY

Results of analytical investigation of the maximum shearing stresses in beams with relatively small span-depth ratios are compared with experimental results, for simply-supported beams with concentrated loads at midspan. Part I covers results of photoelastic investigations, with L/d ranging from 5.32 to 1.06. Part II discusses the Stokes-Wilson theory of stress distribution in short beams. Poor correlation of calculated and experimental values was found at certain points in the beams.

Tests on prestressed concrete beams (in Japanese)

SHUNJI INOMATA, *Transactions*, Japan Society of Civil Engineers (Tokyo), No. 17, Aug. 1953, 90 pp.

AUTHOR'S SUMMARY

Results are reported of (1) static tests on 17 post-tensioned beams of seven different kinds, (2) fatigue tests on 44 pre-tensioned beams of six kinds, (3) investigation of stress relaxation of high tensile steel wire under constant stress, and (4) creep tests on prestressed concrete beams.

Large size water pipes in steel-concrete (Les grosses conduites de distribution d' eau en sidero cement)

F. CAMPUS, *Bulletin du Centre Belge d'Etude et de Documentation des eaux*, No. 22, 1953, pp. 205-211

Reviewed by PHILLIP L. MELVILLE

A pipe 1 m in diameter and 1.73 m long was tested to destruction by application of 15 metric tons per m. The pipe was made of reinforced concrete with a watertight sheet metal inner lining. The combination of materials is claimed to be particularly efficient to resist corrosion, weathering, transverse and longitudinal bending, and bursting. An analytical study completes the investigation of the pipe.

Stresses and failure loads for statically indeterminate reinforced concrete frames

W. S. HANNA, MICHEL BAKHOUM, and ROUSHDY TOSSON, *Bulletin of the Faculty of Engineering*, Cairo University, Cairo, 1954, pp. 75-104

Presents the results of testing to destruction of 15 reinforced concrete frames, identica in dimensions but with varying reinforce

ment. The frames were rectangular closed rings, approximately 6 x 9 ft, with members of uniform cross section approximately 8 x 10 in. The tests show an average 30 percent larger ultimate capacity after yielding occurs at the first critical section. Analytical methods for predicting ultimate load are compared. Those of most interest are the familiar trapezoidal approximation of the stress-strain curve for concrete and steel, and a simplified rectangular approximation (assumes both materials incompressible in elastic range). The predicted ultimate loads on the basis of the trapezoidal distribution average 108 percent of the actual. Using the simpler rectangular approximation the predicted ultimate strengths average 91 percent of the actual. An interesting conception is the "critical failure load" which is defined as that load at which all critical sections reach the yield stress of steel or the crushing strength of concrete. The calculated critical failure loads following this definition averaged 96 percent of the ultimate load. The results of the tests described should prove of interest to any student of the ultimate load or plastic design theory. However, the development of analytic methods contains too many unproved assumptions and is too dependent upon test results for "corrections" to be used for direct application to design problems.

Combined strain and curvature gage for use in testing concrete beams

J. M. Prentis, *Journal of Scientific Instruments* (London), V. 32, No. 1, Jan. 1955, pp. 19-21
Reviewed by Aron L. Mirsky

Describes rugged, inexpensive apparatus for determining the strains in the concrete and the position of the neutral axis, by measuring just one strain and the chord offset (hence, radius of curvature). Using a 12-in. gage length, maximum possible errors are shown to be quite low. Apparatus has further advantage that it need not be removed before failure of test beam, since there is only part (the dial gage) which is relatively delicate and it is easily removed after each reading.

Frictional difficulty in concrete testing

A. G. Tarrant, *The Engineer* (London), V. 198, No. 5159, Dec. 10, 1954, pp. 801-802
Reviewed by Aron L. Mirsky

Compression tests on concrete cubes were conducted on a 60,000-lb machine whose characteristics had previously been studied. Significant differences in crushing strength were found, using two types of lubrication in the mating parts of the spherical head, one yielding a mean coefficient of friction of 0.48 and the other 0.04. Effect was, however, found to differ with cubes of different mixes, and author presents an interesting discussion of why results differ not only with freedom of testing-machine head to tilt but with characteristics of specimens.

General

Lift-slab engineering manual

W. Clark Craig, Fred N. Severud, and Oliver G. Bowen, United States Lift Slab Corp., Austin, Texas, 1955, 100 pp., $5

Presents design problems of the lift-slab construction method. It is the first collection of reference material on the subject, the need for which has been indicated by the growing popularity of the method. A revolutionary construction method such as lift-slab requires exceptionally close coordination with structural design. Much more than in ordinary structures the structural engineer must make provision for construction conditions, erection stresses, and load conditions intermediate between beginning and completed construction. Many brief descriptions of the method, architectural treatments, and design problems have appeared in engineering periodical literature. Since each structure is a separate problem, perhaps unique, none of these brief articles have been satisfactory to provide sufficient background material for a structural engineer's purpose. Typical problems encountered in extending interpretation of the flat slab section in the ACI Building Code and in preparing details, adequate structurally and satisfactory from the standpoint of construction economy, have been collected. It is the intent of the publishers to supplement this manual from time to time with new material based on continuing developments anticipated in the use of the method. To facilitate such additions to the loose leaf manual, only the section pages have been numbered and the new material may be easily incorporated to keep each manual up-to-date.

Numerous sketches, suggested details, and numerical examples have been used to provide a measure for comparison with

proposed design problems. Structural engineers will agree that most assumptions made in extending the chapter on flat slabs of the ACI Building Code are conservative except possibly the assumption of stiffness for a cast steel collar equivalent to a cast-in-place column capital monolithic with the reinforced concrete column.

Architectural engineers, considering the possibility for the first time of using the lift-slab method, should find this manual an excellent reference. For structural engineers engaged in design of a lift-slab the manual will serve principally as a guide and check list to avoid omitting consideration of any important detail or load condition. It is by no means a handbook of design since it merely indicates general methods and assumptions which have proved valid in practice to date. For designs outside the range of present practice, the extension of the concepts illustrated in the manual will require completely original work.

Design of acid-resisting flooring for industrial buildings

C. N. Nagaraj, *The Indian Builder* (Bombay), V. 2, No. 1, Jan. 1954, pp. 7, 30

Describes use of acid-resistant tiles (6 or 8 in. square, 1½ in. thick) to protect concrete floors. Jointing material is also acid-resistant; it is composed of finely powdered fused stoneware mixed with sodium silicate (soda glass). Built-up floor consists of tile, 1:4 cement mortar layer, layer of bituminous material, and concrete base.

Conversion factors and tables

O. T. Zimmerman and Irvin Lavine, Industrial Research Service, Inc., Dover, N. H., 2nd Edition, 1955, 526 pp., $5

A collection of more than 12,000 conversion factors and 122 pp. of conversion tables. Among the new features of the second edition are: an expanded conversion factor section, a section on foreign conversion factors, a table of physical constants, and an expanded conversion table section.

An early history of the construction and design of reinforced concrete

Benjamin A. Wasil, *Midwest Engineer*, V. 7, No. 6, Nov. 1954, pp. 3-4, 13-15

Reviewed by Aron L. Mirsky

Brief outline of concrete's illustrious history. Excellent as an appetite-whetter.

Comparative tests of railroad wood and asbestos-cement ties on elastic soil (Sollecitazioni e tensioni interne nelle traversine ferroviarie in legno e amiante-cemento (Eternit) posate su suolo elastico (ballast))

E. Casato, *Il Cemento* (Milan), V. 50, No. 2-10, Feb.-Oct. 1953, pp. 58-68

Reviewed by G. Mianulli

A report of laboratory tests made on timber and asbestos-cement (Eternit) railroad ties placed totally or partially on ballast considered as elastic soil. Wood ties were first tested to determine their behavior in the laboratory under simulated actual conditions; later a series of experiments followed on asbestos-cement ties of various sizes and shapes. The stresses and strains of the two materials, developed under loading, were compared after the modulus of elasticity, the flexural strength, shear, and resistance to compression were determined for the Eternit material used as ties. Computations, tables listing the measurement readings of distortions, and diagrams are included in the report.

Thermal properties of composite concrete floors

A. E. Moore, *Magazine of Concrete Research* (London), V. 6, No. 18, Dec. 1954, pp. 133-138

An investigation of the relative comfort of various types of concrete floors on ground is reported. Measurements were made comparing the heat loss from a living body on different types of floor. The conclusions drawn are: (1) any form of insulating layer containing air spaces is an improvement upon solid concrete; (2) the thinnest practicable solid topping layer should be used; (3) surface of the floor should be kept dry; (4) for a 1-in. topping, the best insulating base tested was a no-fines lightweight aggregate concrete, next, hollow clay tiles, and last, no-fines gravel concrete, although the three composite constructions were all superior to solid concrete; and (5) the suggested thickness for the insulating base is a minimum of 4 in.

Rail clamp for concrete sleepers

The Engineer (London), V. 198, No. 5144, Aug. 27, 1954, p. 305

Reviewed by Aron L. Mirsky

Brief description of new rubber-cushioned clamps for securing flat-bottom rails to concrete ties. Advantages of new clamps, now undergoing test, are smoother riding, improved tie life, and reduced rail creep.